New astrophysical frontiers from the binary black holes with LIGO and Virgo's observations

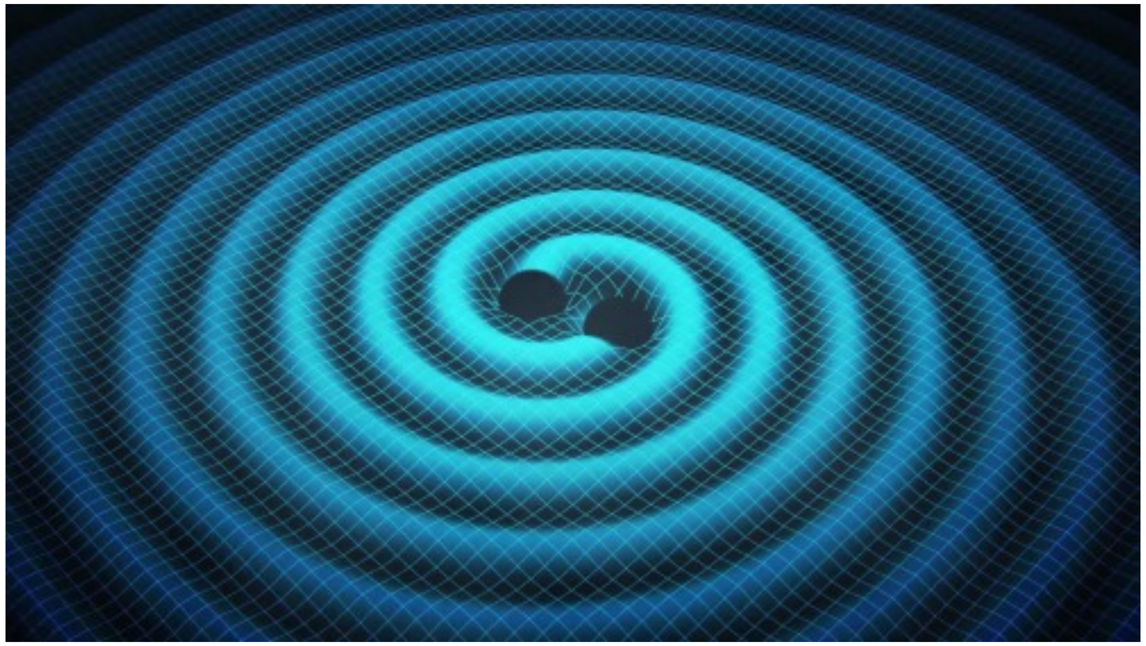

Samaya Nissanke

GRAPPA, University of Amsterdam, the Netherlands

Lecture 1: July 5th, NBIA and DARK summer school
Copenhagen

A few words of background about myself

Education: BSci & MSci in Physics, Cambridge UK

(Summer research: got hooked on GWs & Exoplanets)

PhD in 2007 at the IAP, Paris: Gravitational Waveforms
using the post-Newtonian approximation
in General Relativity (with Luc Blanchet)

Postdocs: CITA fellow, Caltech/JPL, Radboud University, NL

Faculty since 2016: Radboud University, NL
-> (GRAPPA) University of Amsterdam, NL

GW @ GRAPPA, Amsterdam

(+ great collabs. in Nijmegen)

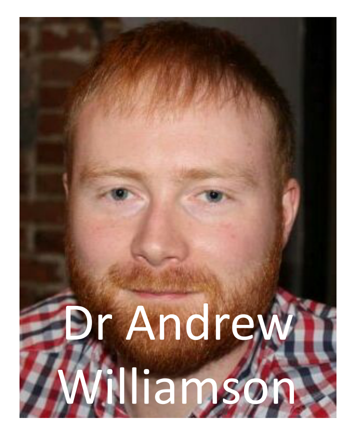

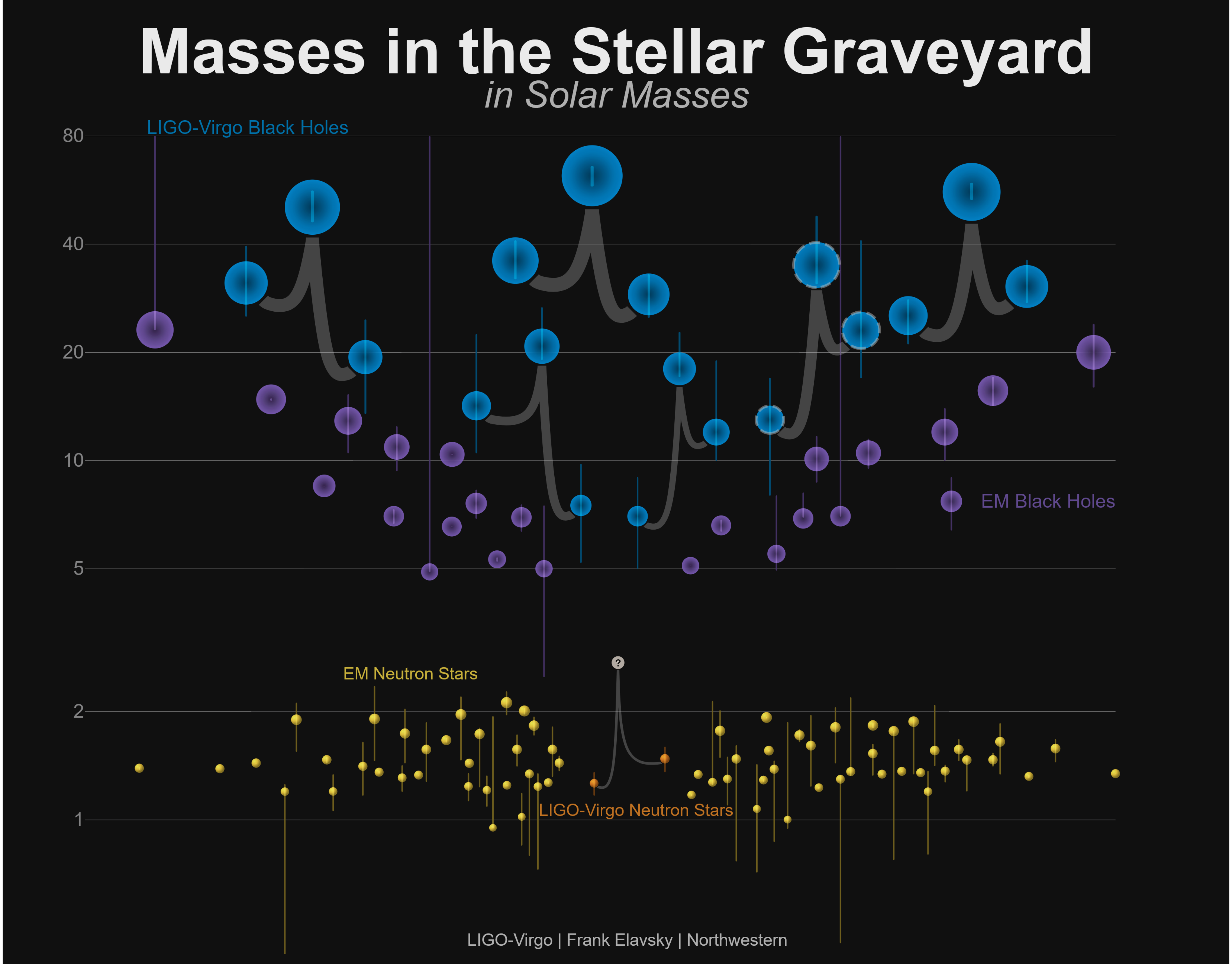

Masses in the Stellar Graveyard
in Solar Masses
LIGO-Virgo Black Holes
80
40
20
10
5
2
1
EM Black Holes
EM Neutron Stars
?
LIGO-Virgo Neutron Stars
LIGO-Virgo | Frank Elavsky | Northwestern

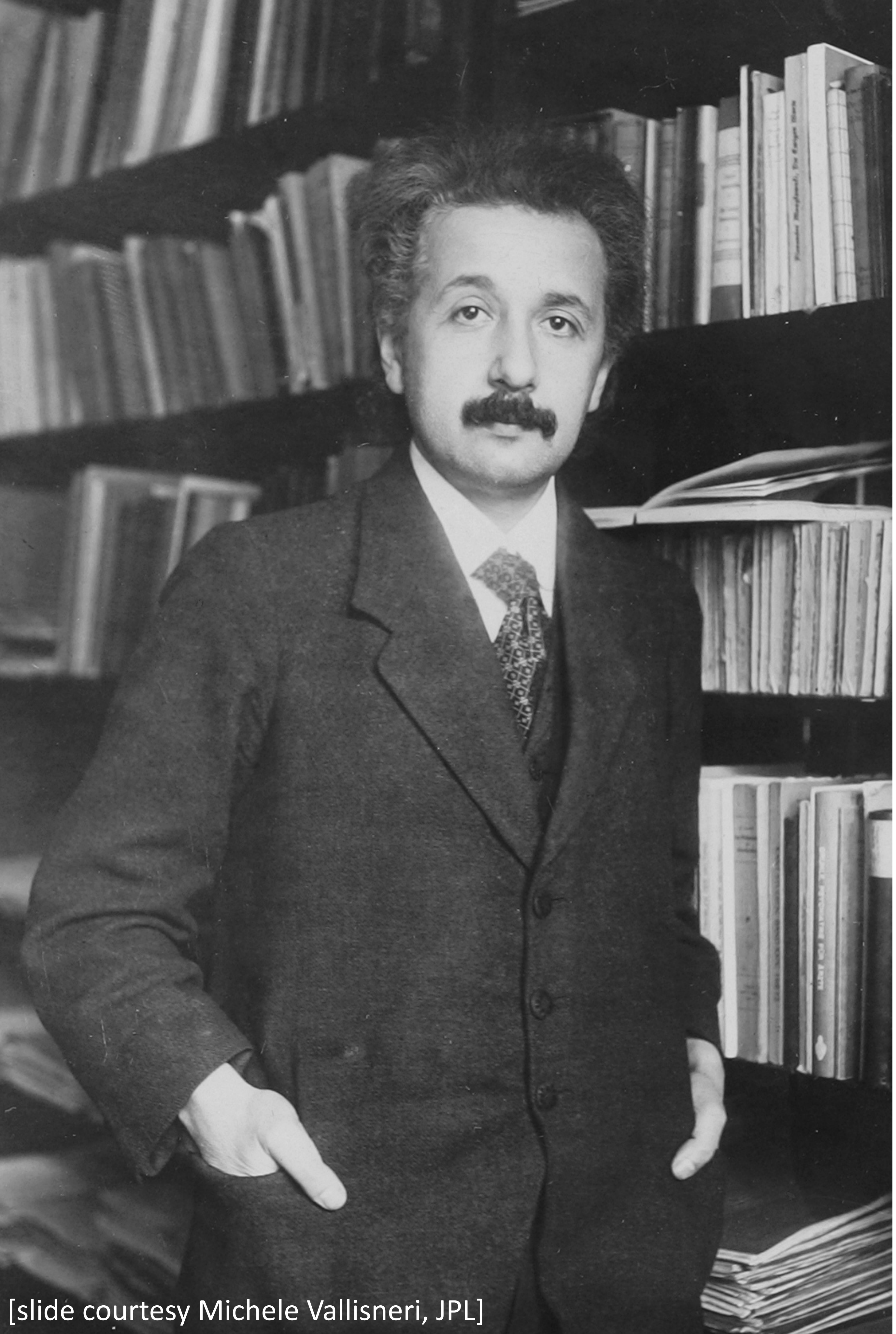

[slide courtesy Michele Vallisneri, JPL]

1915: GR
1916: GWs; Schwarzschild metric
1919: Eddington's expedition

1939: gravitational collapse

1957: Chapel Hill conference
1960: Weber bars

1967: "black hole", no-hair theorem
1971: Cygnus X-1
1972: GW interferometer design
1974: PSR B1913+16

1990, 1999: LIGO approved, inaugurated
2002: Sgr A* as black hole
2002–2010: initial LIGO runs

2015: aLIGO; GW150914

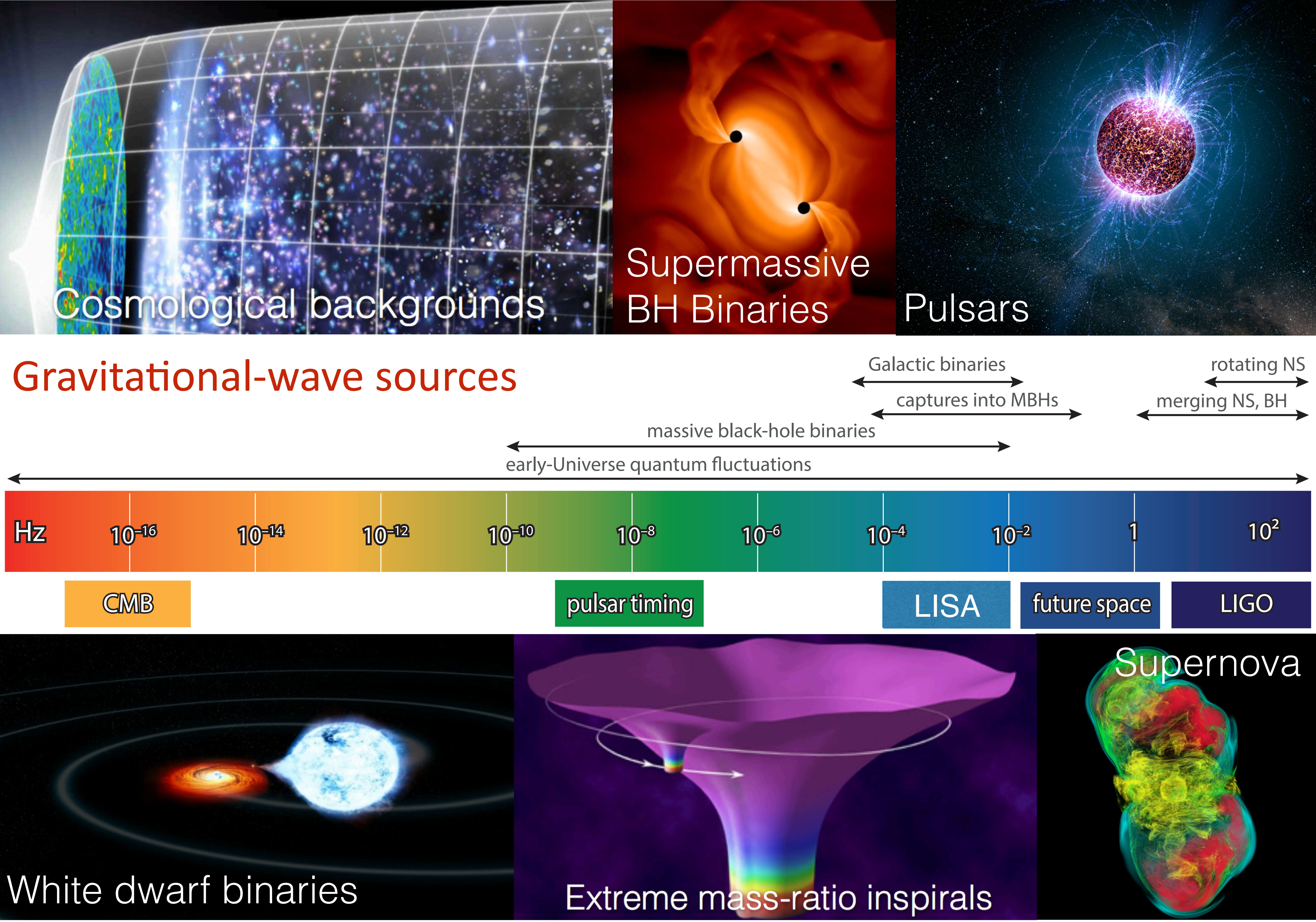

First-order phase transitions, superstring kink & cusps, inflationary signature, new sources!

GW sources

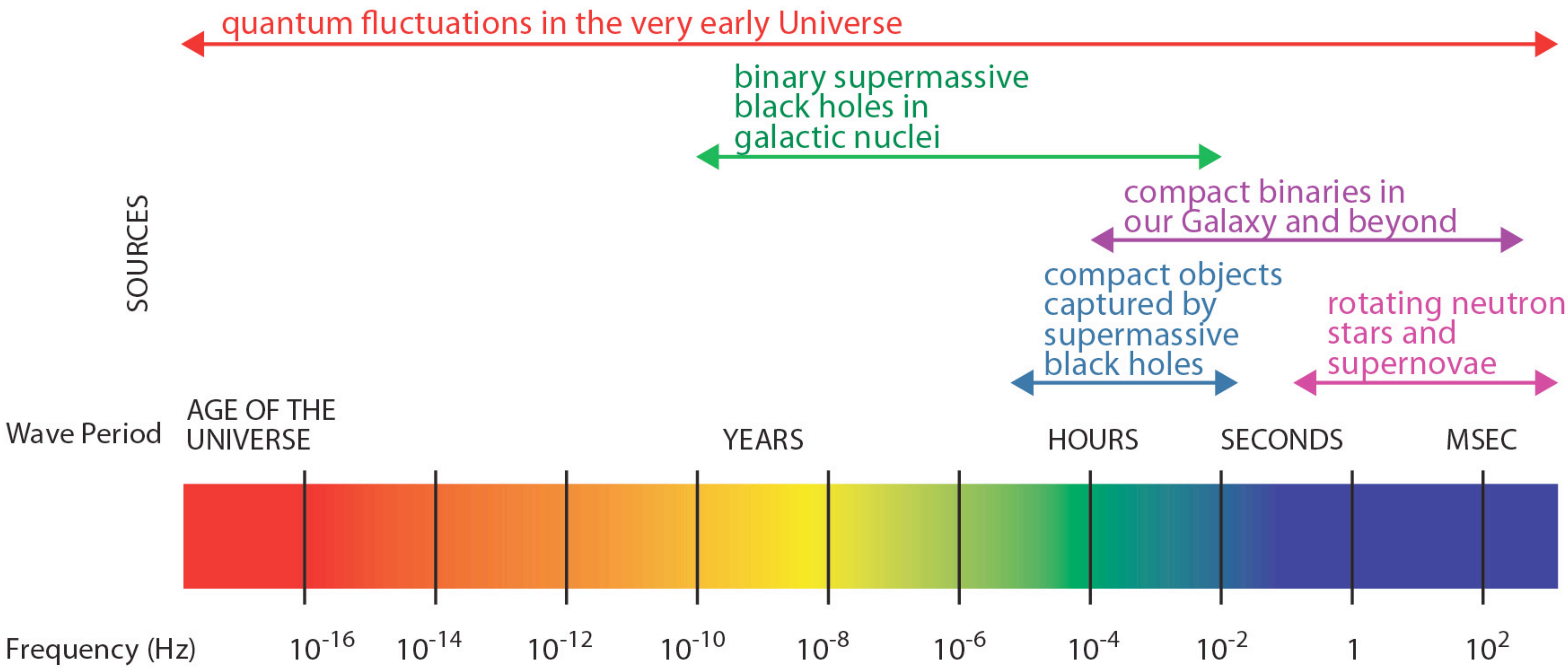

$$f_{\rm GW} \sim 2 f_{\rm orb} \sim \frac{1}{\pi}\sqrt{\frac{GM}{r_{12}^3}}$$

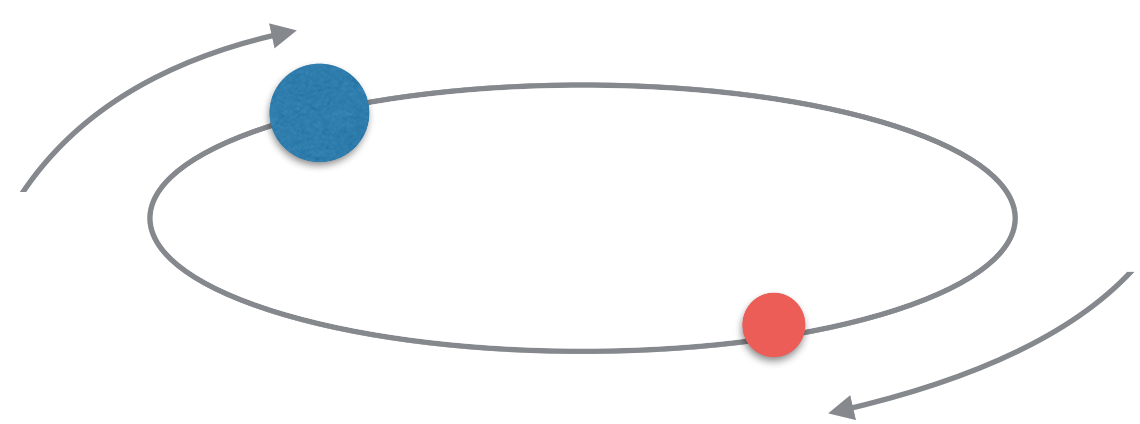

GW detectors

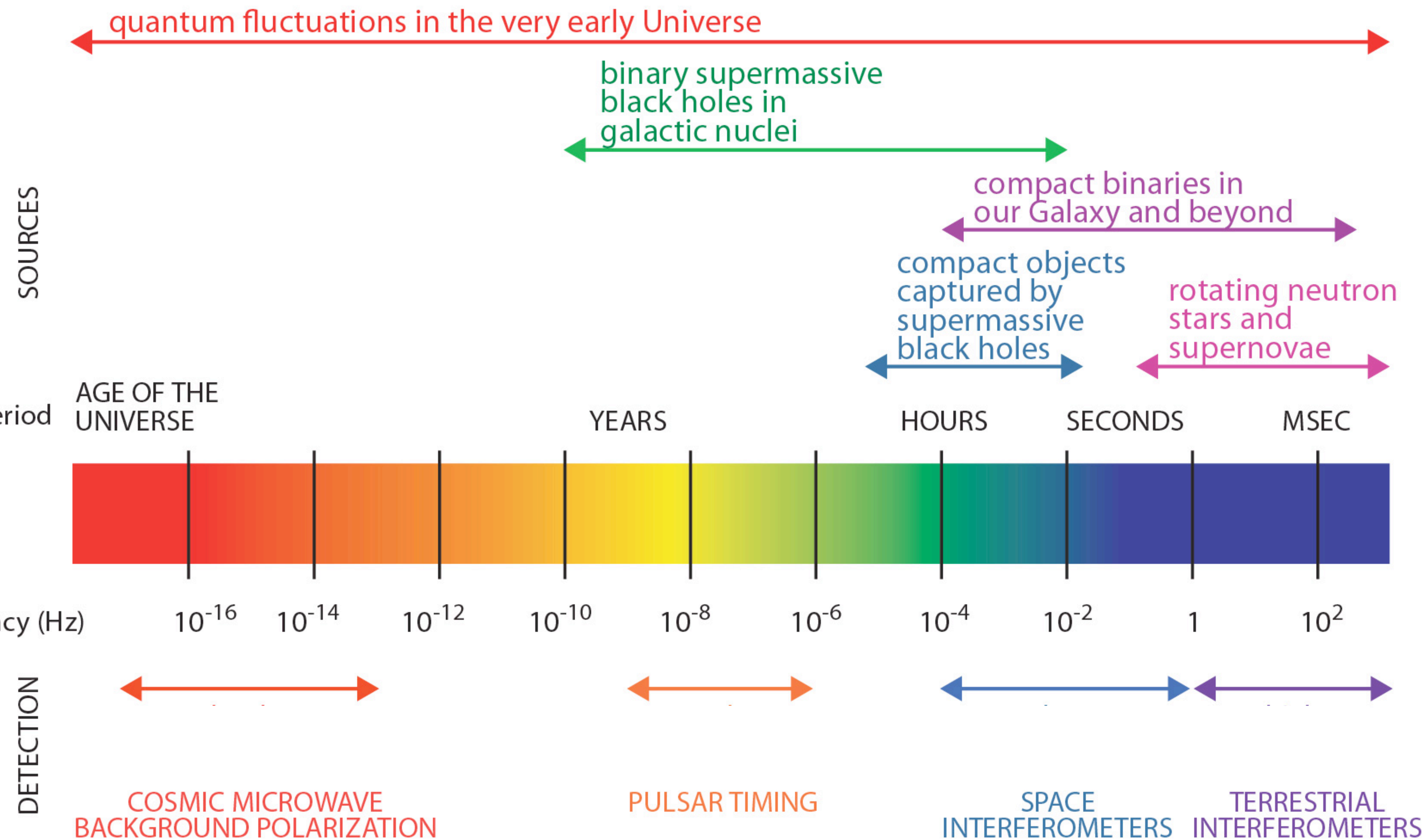

GW detectors

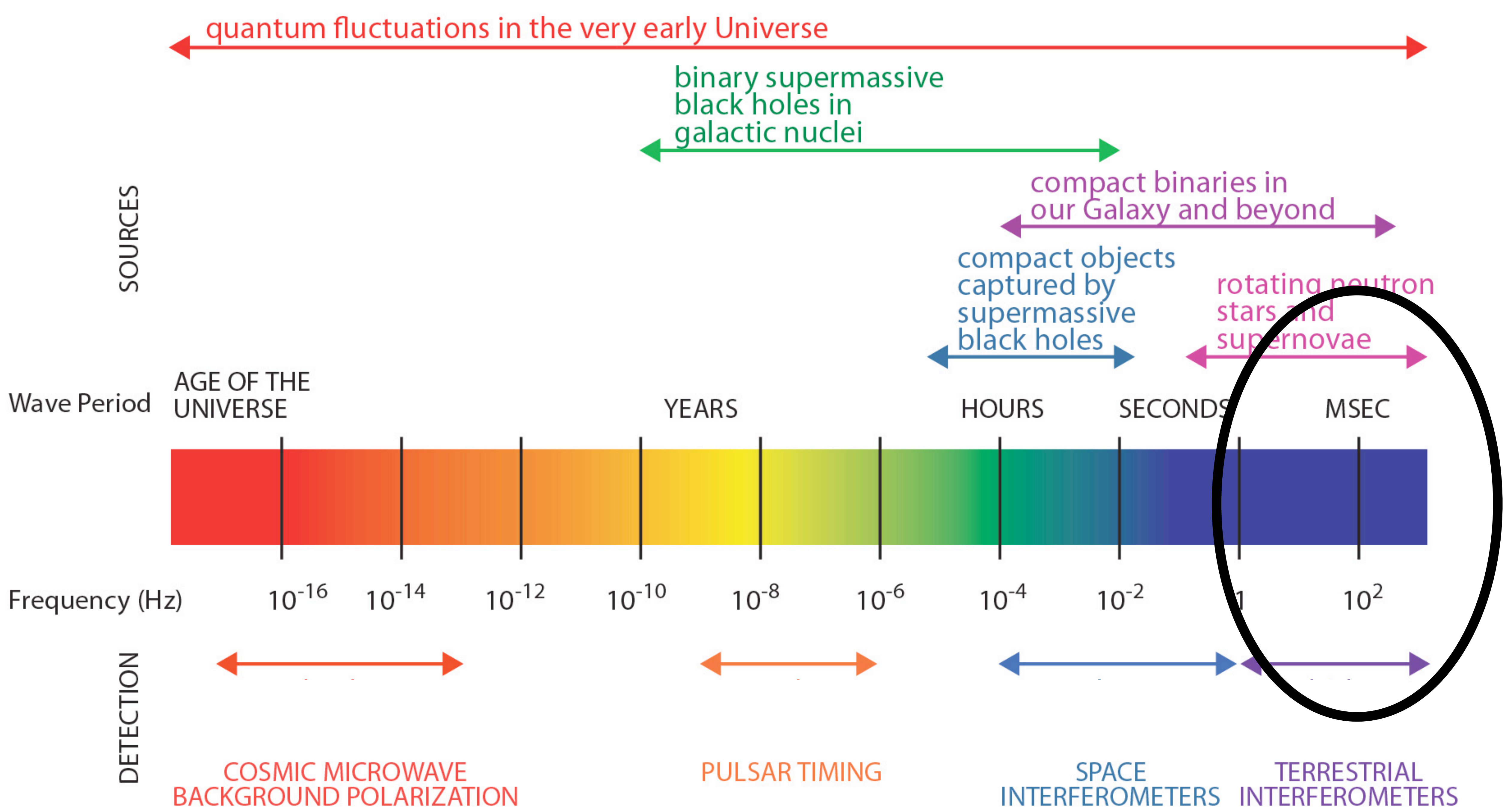

Gravitational and Electromagnetic Radiation: different probes for our universe

Oscillations of spacetime itself	Electric and magnetic fields propagating through spacetime
Coherent: dynamical state	Incoherent superposition of many emitters: thermodynamic state
Weakly interacting	Strongly interacting
$h \sim 1/r$	Energy flux $\sim 1/r^2$
wavelength ~/> size of source: analogous to sound	wavelength </<< size of emitting source: image
all sky sensitivity; poor angular resolution	deep imaging on small area; high angular resolution

Main papers referenced in this lecture

Discovery Paper: "Observation of Gravitational Waves from a Binary Black Hole Merger," arXiv:1602.03837, Physics Review Letters 116, 061102 (2016).

Astrophysical paper: "Astrophysical Implications of the Binary Black-Hole Merger GW150914," Astrophys. J. Lett. 818, L22 (2016).

Testing General Relativity: "Tests of general relativity with GW150914," arXiv: 1602.03841, Physics Review Letters 116, 221101 (2016).

Parameter Estimation: "Properties of the binary black hole merger GW150914," arXiv: 1602.03840, Physics Review Letters 116, 241102 (2016).

Stochastic Paper: "GW150914: Implications for the stochastic gravitational wave background from binary black holes", arXiv: 1602.03847, Physics Review Letters 116, 131102 (2016).

GW151226 discovery: "GW151226: Observation of Gravitational Waves from a 22 Solar-mass Binary Black Hole Coalescence," arXiv:1606.04755, Physics Review Letters 116, 241103 (2016)

O1 BBH paper: "Binary Black Hole Mergers in the first Advanced LIGO Observing Run," arXiv:1606.09619

Part I:
Retrieving BH parameters
[if General Relativity is correct]

First Observation of GWs

September 14 2015, 09:50:45.39 UTC

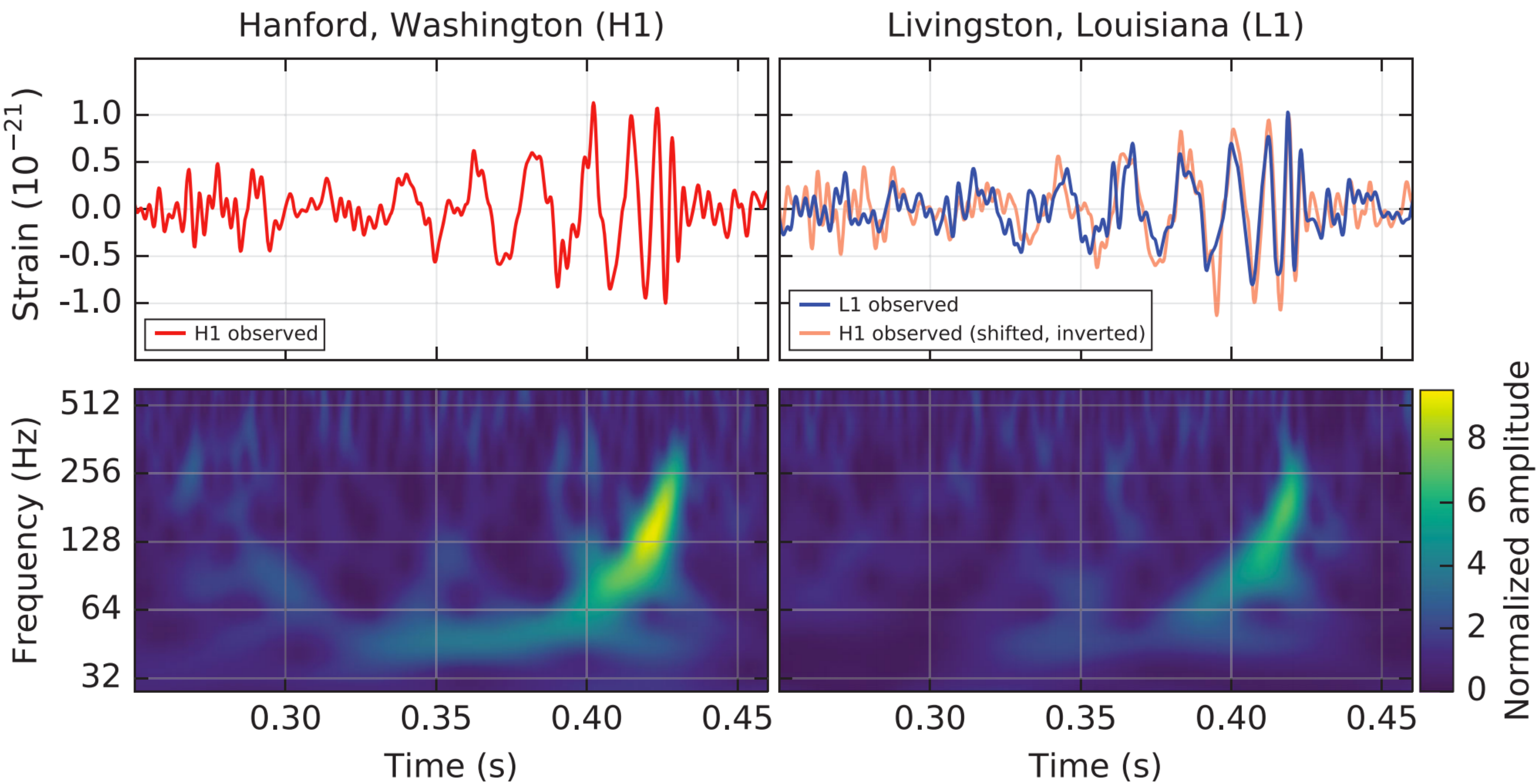

⇒ fundamental properties of BHs, astrophysics (how and where?) & tests of General Relativity

2. Simplest "Newtonian" model explains frequency chirp

i) Newtonian Orbital Dynamics:

$$E_{\rm orb} = -\frac{GM\mu}{2r} \qquad \Omega = \sqrt{\frac{GM}{r^3}}$$

ii) Quadrupole formula:

$$L = \frac{dE_{\rm rad}}{dt} = \frac{32G}{5c^5}\Omega^6\mu^2 r^4$$

iii) Enforce energy balance:

$$\left(\frac{dE}{dt}\right)_{\rm rad} + \left(\frac{dE}{dt}\right)_{\rm orb} = 0$$

iv) Orbital shrinkage:

$$\frac{dr}{dt} = -\frac{64G^2}{5c^5}\mu M\Omega^2$$

iv) Frequency chirp:

$$\frac{d\Omega}{dt} = \frac{96G^{5/3}}{5c^5}\mu M^{2/3}\Omega^{11/3} = \frac{96}{5}\left(\frac{G\mathcal{M}}{c^3}\right)^{5/3}\Omega^{11/3}$$

Simplest "Newtonian" model explains frequency chirp

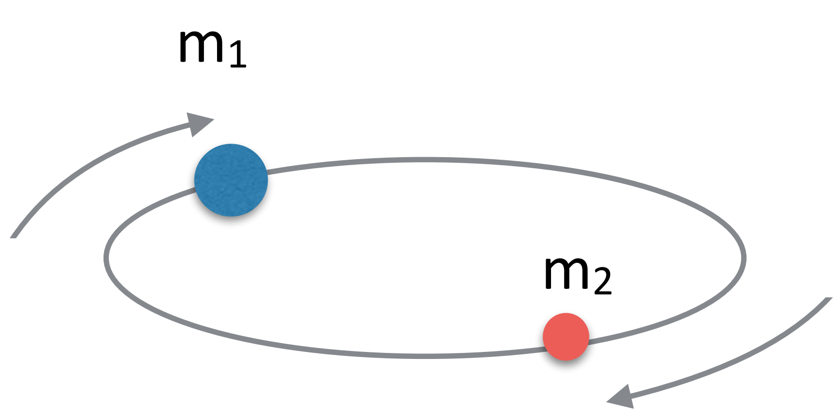

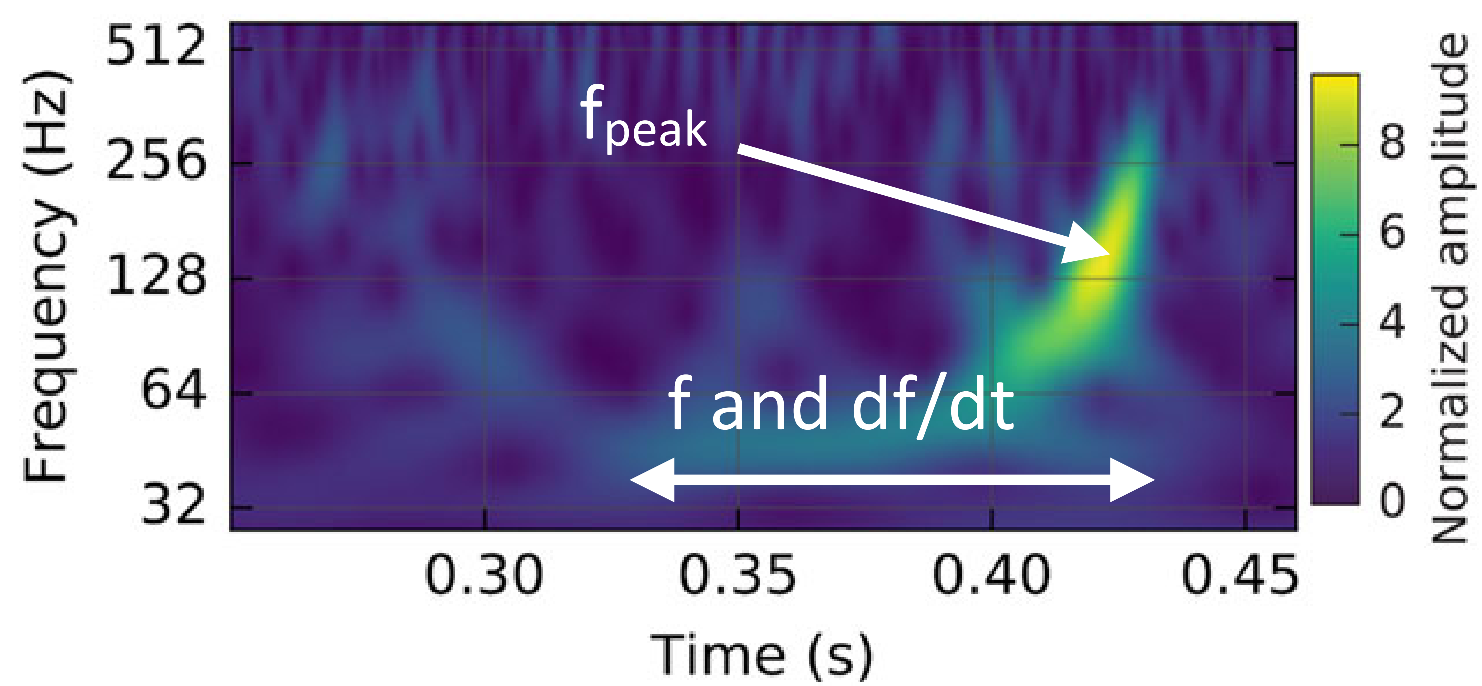

$$\left(\frac{dE}{dt}\right)_{\rm rad} + \left(\frac{dE}{dt}\right)_{\rm orb} = 0$$

⇒ Frequency chirp: $$\boxed{\frac{df}{dt} = \frac{96\,\pi}{5}\left(\frac{\pi\,G\mathcal{M}}{c^3}\right)^{5/3} f^{11/3}}$$

Chirp mass: $$\boxed{\mathcal{M} = \frac{(m_1 m_2)^{3/5}}{(m_1+m_2)^{1/5}}}$$

The GW waveform encapsulates Binary Black Hole Evolution

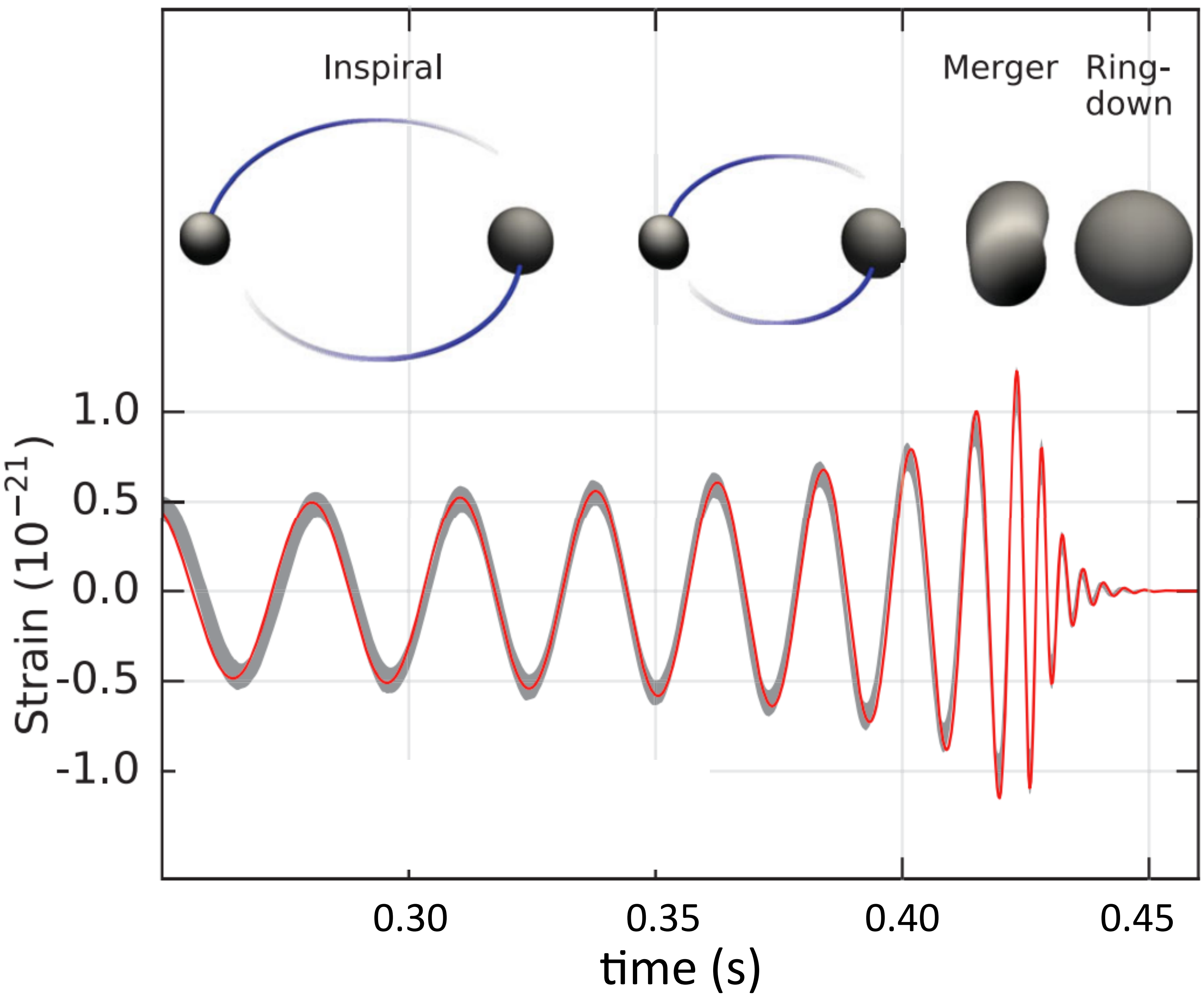

[LVC, arXiv:1602.03837, PRL 116, 061102, 2016]

Chirp mass drives inspiral waveform

[LVC, arXiv:1602.03837, PRL 116, 061102, 2016]

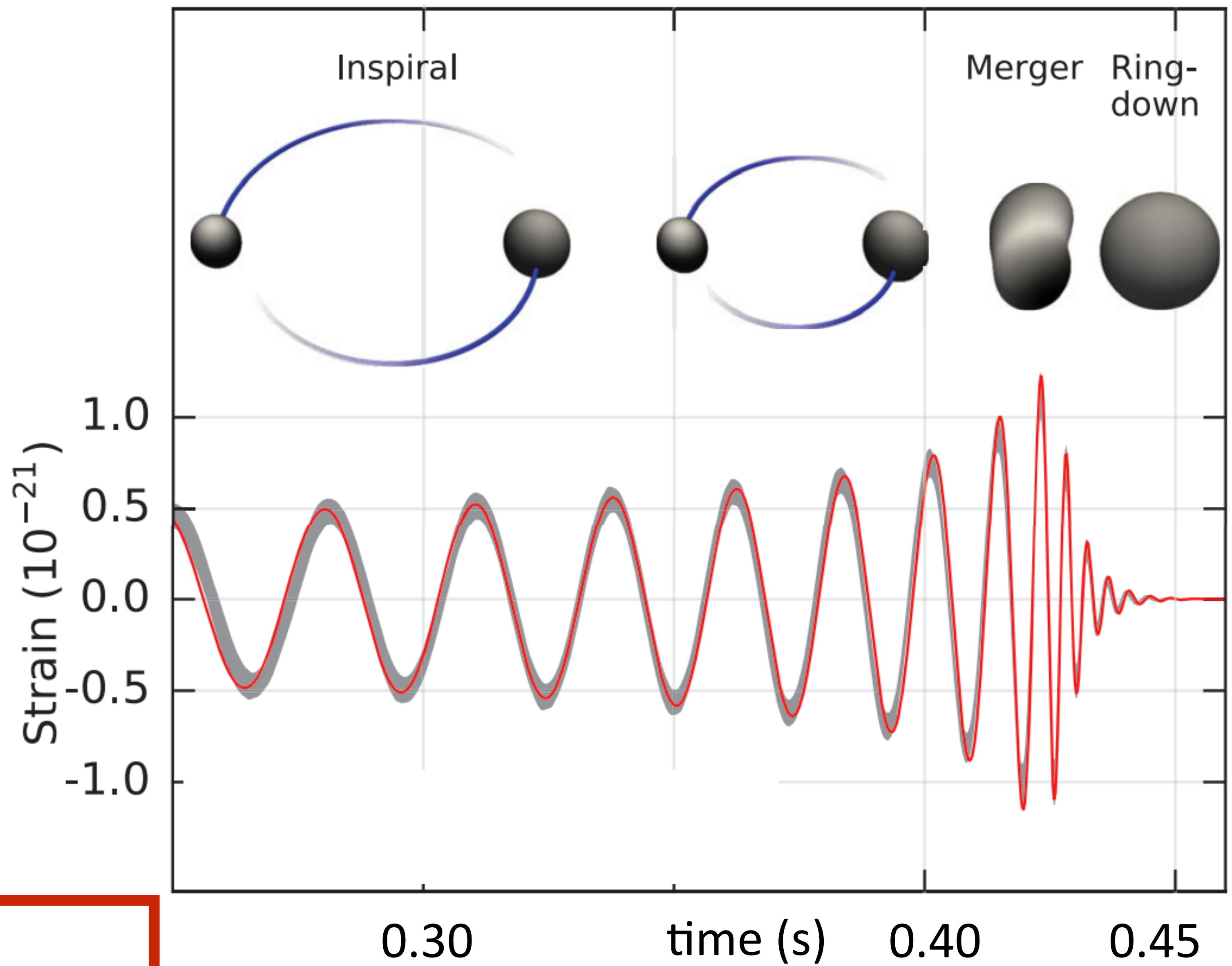

chirp mass:

$$\mathcal{M} = \frac{(m_1 m_2)^{3/5}}{(m_1+m_2)^{1/5}} = \frac{c^3}{G}\left[\frac{5}{96}\pi^{-8/3} f^{-11/3} \dot{f}\right]^{3/5}$$

Inspiral ~ Chirp

<u>driven</u> by the chirp mass

Ringdown

… remnant mass & spin

Decades of theoretical effort in source modelling

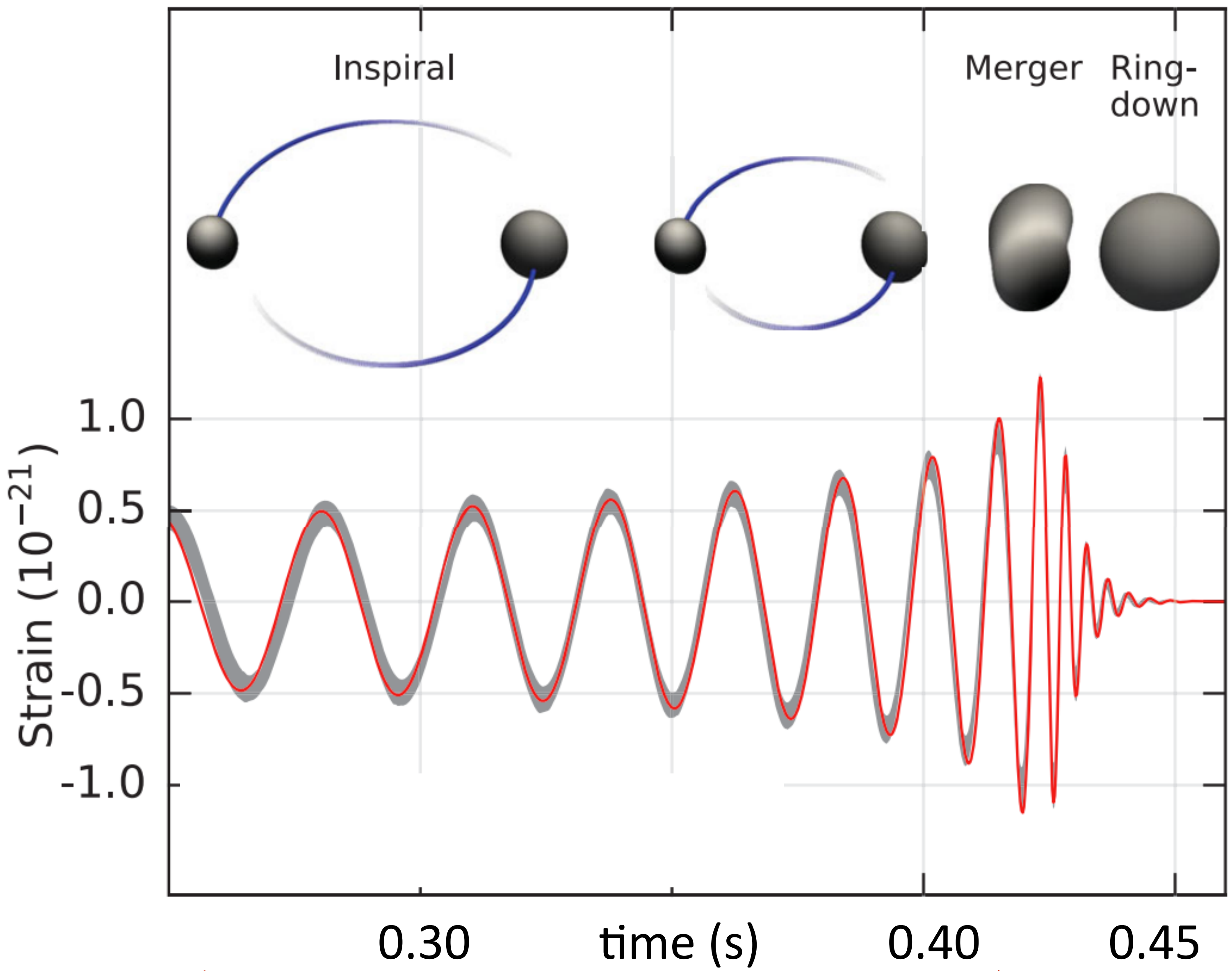

post-Newtonian

numerical relativity

quasi-normal modes

$$\boxed{1\mathrm{PN} \sim \frac{v^2}{c^2} \sim \frac{Gm}{rc^2} << 1}$$

[LVC, arXiv:1602.03837, PRL 116, 061102, 2016]

The GW waveform encodes source parameters

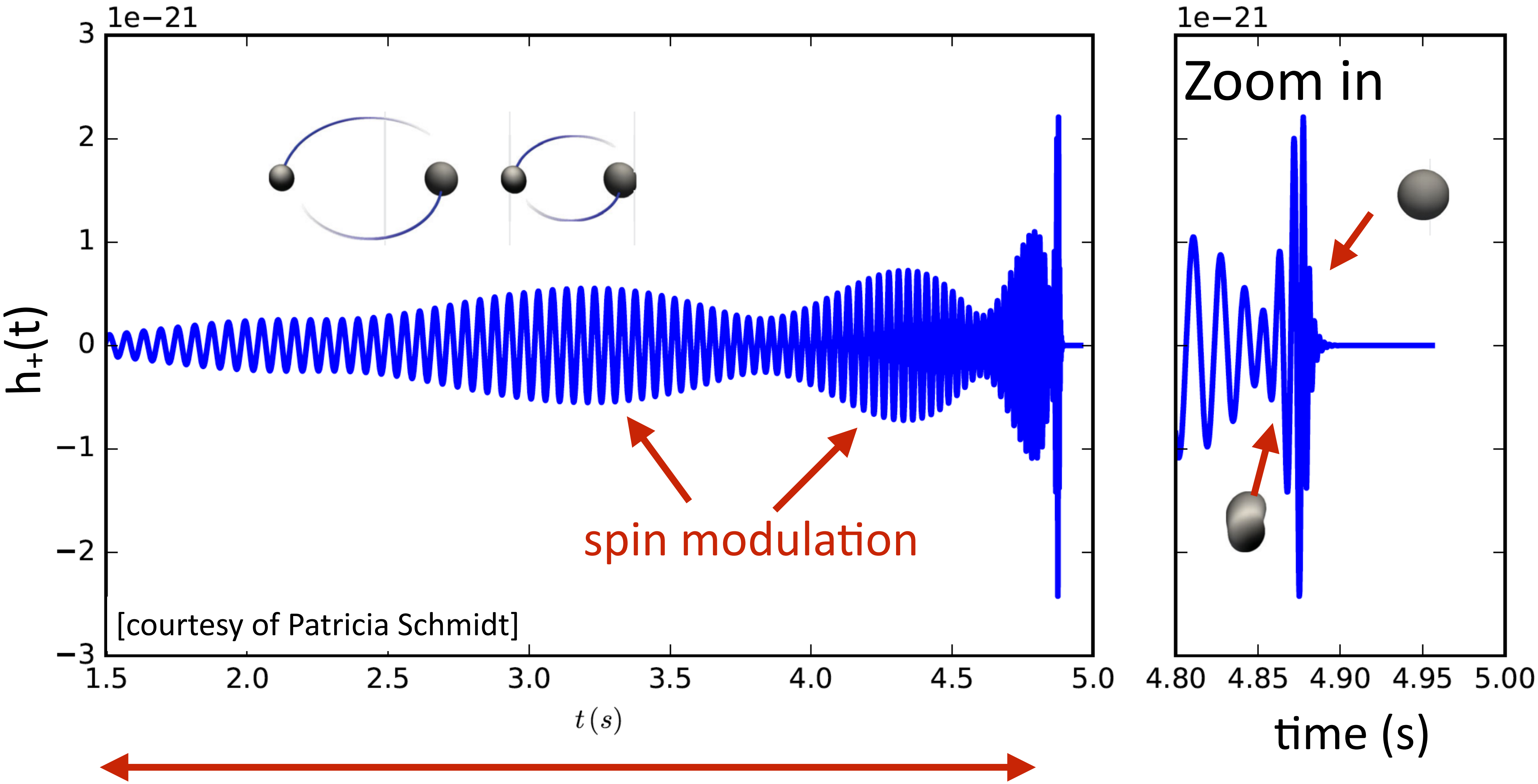

$\Phi_{\rm GW}(t)$ ⇒ chirp mass, reduced mass (1PN), spin-orbit (1.5PN), …

The GW chirp gives the progenitor masses and spins

$$a_1^i = -\frac{Gm_2 n_{12}^i}{r_{12}^2}$$
$$+\frac{1}{c^2}\Bigg\{ \Bigg[\frac{5G^2m_1m_2}{r_{12}^3} + \frac{4G^2m_2^2}{r_{12}^3} + \frac{Gm_2}{r_{12}^2}\Big(\frac{3}{2}(n_{12}v_2)^2 - v_1^2 + 4(v_1v_2) - 2v_2^2\Big)\Bigg] n_{12}^i$$
$$+\frac{Gm_2}{r_{12}^2}\left(4(n_{12}v_1) - 3(n_{12}v_2)\right) v_{12}^i \Bigg\}$$
$$+\frac{1}{c^4}\Bigg\{ \Bigg[-\frac{57G^3m_1^2m_2}{4r_{12}^4} - \frac{69G^3m_1m_2^2}{2r_{12}^4} - \frac{9G^3m_2^3}{r_{12}^4}$$
$$+\frac{Gm_2}{r_{12}^2}\Big(-\frac{15}{8}(n_{12}v_2)^4 + \frac{3}{2}(n_{12}v_2)^2v_1^2 - 6(n_{12}v_2)^2(v_1v_2) - 2(v_1v_2)^2 + \frac{9}{2}(n_{12}$$
$$+4(v_1v_2)v_2^2 - 2v_2^4\Big)$$
$$+\frac{G^2m_1m_2}{r_{12}^3}\Big(\frac{39}{2}(n_{12}v_1)^2 - 39(n_{12}v_1)(n_{12}v_2) + \frac{17}{2}(n_{12}v_2)^2 - \frac{15}{4}v_1^2 - \frac{5}{2}(v_1v_2) +$$
$$+\frac{G^2m_2^2}{r_{12}^3}\left(2(n_{12}v_1)^2 - 4(n_{12}v_1)(n_{12}v_2) - 6(n_{12}v_2)^2 - 8(v_1v_2) + 4v_2^2\right)\Bigg] n_{12}^i$$
$$+\Bigg[\frac{G^2m_2^2}{r_{12}^3}\left(-2(n_{12}v_1) - 2(n_{12}v_2)\right) + \frac{G^2m_1m_2}{r_{12}^3}\Big(-\frac{63}{4}(n_{12}v_1) + \frac{55}{4}(n_{12}v_2)\Big)$$
$$+\frac{Gm_2}{r_{12}^2}\Big(-6(n_{12}v_1)(n_{12}v_2)^2 + \frac{9}{2}(n_{12}v_2)^3 + (n_{12}v_2)v_1^2 - 4(n_{12}v_1)(v_1v_2)$$
$$+4(n_{12}v_2)(v_1v_2) + 4(n_{12}v_1)v_2^2 - 5(n_{12}v_2)v_2^2\Big)\Bigg] v_{12}^i \Bigg\}$$
$$+\frac{1}{c^5}\Bigg\{ \Bigg[\frac{208G^3m_1m_2^2}{15r_{12}^4}(n_{12}v_{12}) - \frac{24G^3m_1^2m_2}{5r_{12}^4}(n_{12}v_{12}) + \frac{12G^2m_1m_2}{5r_{12}^3}(n_{12}v_{12})v_{12}^2\Bigg] n_{12}^i$$
$$+\Bigg[\frac{8G^3m_1^2m_2}{5r_{12}^4} - \frac{32G^3m_1m_2^2}{5r_{12}^4} - \frac{4G^2m_1m_2}{5r_{12}^3}v_{12}^2\Bigg] v_{12}^i \Bigg\}$$
$$+\frac{1}{c^6}\Bigg\{ \Bigg[\frac{Gm_2}{r_{12}^2}\Big(\frac{35}{16}(n_{12}v_2)^6 - \frac{15}{8}(n_{12}v_2)^4v_1^2 + \frac{15}{2}(n_{12}v_2)^4(v_1v_2) + 3(n_{12}v_2)^2(v_1v_2)^2$$
$$-\frac{15}{2}(n_{12}v_2)^4v_2^2 + \frac{3}{2}(n_{12}v_2)^2v_1^2v_2^2 - 12(n_{12}v_2)^2(v_1v_2)v_2^2 - 2(v_1v_2)^2v_2^2$$
$$+\frac{15}{2}(n_{12}v_2)^2v_2^4 + 4(v_1v_2)v_2^4 - 2v_2^6\Big)$$
$$+\frac{G^2m_1m_2}{r_{12}^3}\Big(-\frac{171}{8}(n_{12}v_1)^4 + \frac{171}{2}(n_{12}v_1)^3(n_{12}v_2) - \frac{723}{4}(n_{12}v_1)^2(n_{12}v_2)^2$$
$$+\frac{383}{2}(n_{12}v_1)(n_{12}v_2)^3 - \frac{455}{8}(n_{12}v_2)^4 + \frac{229}{4}(n_{12}v_1)^2v_1^2$$
$$-\frac{205}{2}(n_{12}v_1)(n_{12}v_2)v_1^2 + \frac{191}{4}(n_{12}v_2)^2v_1^2 - \frac{91}{8}v_1^4 - \frac{229}{2}(n_{12}v_1)^2 v_1$$
$$+244(n_{12}v_1)(n_{12}v_2)(v_1v_2) - \frac{225}{2}(n_{12}v_2)^2(v_1v_2) + \frac{91}{2}v_1^2(v_1v_2)$$
$$-\frac{177}{4}(v_1v_2)^2 + \frac{229}{4}(n_{12}v_1)^2v_2^2 - \frac{283}{2}(n_{12}v_1)(n_{12}v_2)v_2^2$$
$$+\frac{259}{4}(n_{12}v_2)^2v_2^2 - \frac{91}{4}v_1^2v_2^2 + 43(v_1v_2)v_2^2 - \frac{81}{8}v_2^4\Big)$$
$$+\frac{G^2m_2^2}{r_{12}^3}\Big(-6(n_{12}v_1)^2(n_{12}v_2)^2 + 12(n_{12}v_1)(n_{12}v_2)^3 + 6(n_{12}v_2)^4$$
$$+4(n_{12}v_1)(n_{12}v_2)(v_1v_2) + 12(n_{12}v_2)^2(v_1v_2) + 4(v_1v_2)^2$$
$$-4(n_{12}v_1)(n_{12}v_2)v_2^2 - 12(n_{12}v_2)^2v_2^2 - 8(v_1v_2)v_2^2 + 4v_2^4\Big)$$
$$+\frac{G^3m_2^3}{r_{12}^4}\Big(-(n_{12}v_1)^2 + 2(n_{12}v_1)(n_{12}v_2) + \frac{43}{2}(n_{12}v_2)^2 + 18(v_1v_2) - 9v_2^2\Big)$$
$$+\frac{G^3m_1m_2^2}{r_{12}^4}\Big(\frac{415}{8}(n_{12}v_1)^2 - \frac{375}{4}(n_{12}v_1)(n_{12}v_2) + \frac{1113}{8}(n_{12}v_2)^2 - \frac{615}{64}(n_{12}v_{12})^2\pi^2$$
$$+18v_1^2 + \frac{123}{64}\pi^2v_{12}^2 + 33(v_1v_2) - \frac{33}{2}v_2^2\Big)$$
$$+\frac{G^3m_1^2m_2}{r_{12}^4}\Big(-\frac{45887}{168}(n_{12}v_1)^2 + \frac{24025}{42}(n_{12}v_1)(n_{12}v_2) - \frac{10469}{42}(n_{12}v_2)^2 + \frac{48197}{840}v_1^2$$
$$-\frac{36227}{420}(v_1v_2) + \frac{36227}{840}v_2^2 + 110(n_{12}v_{12})^2\ln\Big(\frac{r_{12}}{r'_1}\Big) - 22v_{12}^2\ln\Big(\frac{r_{12}}{r'_1}\Big)\Big)$$
$$+\frac{16G^4m_2^4}{r_{12}^5} + \frac{G^4m_1^2m_2^2}{r_{12}^5}\Big(175 - \frac{41}{16}\pi^2\Big) + \frac{G^4m_1^3m_2}{r_{12}^5}\Big(-\frac{3187}{1260} + \frac{44}{3}\ln\Big(\frac{r_{12}}{r'_1}\Big)\Big)$$
$$+\frac{G^4m_1m_2^3}{r_{12}^5}\Big(\frac{110741}{630} - \frac{41}{16}\pi^2 - \frac{44}{3}\ln\Big(\frac{r_{12}}{r'_2}\Big)\Big)\Bigg] n_{12}^i$$
$$+\Bigg[\frac{Gm_2}{r_{12}^2}\Big(\frac{15}{2}(n_{12}v_1)(n_{12}v_2)^4 - \frac{45}{8}(n_{12}v_2)^5 - \frac{3}{2}(n_{12}v_2)^3v_1^2 + 6(n_{12}v_1)(n_{12}v_2)^2(v_1v_2)$$
$$-6(n_{12}v_2)^3(v_1v_2) - 2(n_{12}v_2)(v_1v_2)^2 - 12(n_{12}v_1)(n_{12}v_2)^2v_2^2 + 12(n_{12}v_2)^3v_2^2$$
$$+(n_{12}v_2)v_1^2v_2^2 - 4(n_{12}v_1)(v_1v_2)v_2^2 + 8(n_{12}v_2)(v_1v_2)v_2^2 + 4(n_{12}v_1)v_2^4$$
$$-7(n_{12}v_2)v_2^4\Big)$$
$$+\frac{G^2m_2^2}{r_{12}^3}\Big(-2(n_{12}v_1)^2(n_{12}v_2) + 8(n_{12}v_1)(n_{12}v_2)^2 + 2(n_{12}v_2)^3 + 2(n_{12}v_1)(v_1v_2)$$
$$+4(n_{12}v_2)(v_1v_2) - 2(n_{12}v_1)v_2^2 - 4(n_{12}v_2)v_2^2\Big)$$
$$+\frac{G^2m_1m_2}{r_{12}^3}\Big(-\frac{243}{4}(n_{12}v_1)^3 + \frac{565}{4}(n_{12}v_1)^2(n_{12}v_2) - \frac{269}{4}(n_{12}v_1)(n_{12}v_2)^2$$
$$-\frac{95}{12}(n_{12}v_2)^3 + \frac{207}{8}(n_{12}v_1)v_1^2 - \frac{137}{8}(n_{12}v_2)v_1^2 - 36(n_{12}v_1)(v_1v_2)$$
$$+\frac{27}{4}(n_{12}v_2)(v_1v_2) + \frac{81}{8}(n_{12}v_1)v_2^2 + \frac{83}{8}(n_{12}v_2)v_2^2\Big)$$
$$+\frac{G^3m_2^3}{r_{12}^4}\left(4(n_{12}v_1) + 5(n_{12}v_2)\right)$$
$$+\frac{G^3m_1m_2^2}{r_{12}^4}\Big(-\frac{307}{8}(n_{12}v_1) + \frac{479}{8}(n_{12}v_2) + \frac{123}{32}(n_{12}v_{12})\pi^2\Big)$$
$$+\frac{G^3m_1^2m_2}{r_{12}^4}\Big(\frac{31397}{420}(n_{12}v_1) - \frac{36227}{420}(n_{12}v_2) - 44(n_{12}v_{12})\ln\Big(\frac{r_{12}}{r'_1}\Big)\Big)\Bigg] v_{12}^i \Bigg\}$$

$$+\frac{1}{c^7}\Bigg\{ \Bigg[\frac{G^4m_1^3m_2}{r_{12}^5}\Big(\frac{3992}{105}(n_{12}v_1) - \frac{4328}{105}(n_{12}v_2)\Big)$$
$$+\frac{G^4m_1^2m_2^2}{r_{12}^6}\Big(-\frac{13576}{105}(n_{12}v_1) + \frac{2872}{21}(n_{12}v_2)\Big) - \frac{3172}{21}\frac{G^4m_1m_2^3}{r_{12}^6}(n_{12}v_{12})$$
$$+\frac{G^3m_1^2m_2}{r_{12}^4}\Big(48(n_{12}v_1)^3 - \frac{696}{5}(n_{12}v_1)^2(n_{12}v_2) + \frac{744}{5}(n_{12}v_1)(n_{12}v_2)^2 - \frac{288}{5}(n_{12}v_2)^3$$
$$-\frac{4888}{105}(n_{12}v_1)v_1^2 + \frac{5056}{105}(n_{12}v_2)v_1^2 + \frac{2056}{21}(n_{12}v_1)(v_1v_2)$$
$$-\frac{2224}{21}(n_{12}v_2)(v_1v_2) - \frac{1028}{21}(n_{12}v_1)v_2^2 + \frac{5812}{105}(n_{12}v_2)v_2^2\Big)$$
$$+\frac{G^3m_1m_2^2}{r_{12}^4}\Big(-\frac{582}{5}(n_{12}v_1)^3 + \frac{1746}{5}(n_{12}v_1)^2(n_{12}v_2) - \frac{1954}{5}(n_{12}v_1)(n_{12}v_2)^2$$

$$+158(n_{12}v_2)^3 + \frac{3568}{105}(n_{12}v_{12})v_1^2 - \frac{2864}{35}(n_{12}v_1)(v_1v_2)$$
$$+\frac{10048}{105}(n_{12}v_2)(v_1v_2) + \frac{1432}{35}(n_{12}v_1)v_2^2 - \frac{5752}{105}(n_{12}v_2)v_2^2\Big)$$
$$+\frac{G^2m_1m_2}{r_{12}^3}\Big(-56(n_{12}v_{12})^5 + 60(n_{12}v_1)^3v_{12}^2 - 180(n_{12}v_1)^2(n_{12}v_2)v_{12}^2$$
$$+174(n_{12}v_1)(n_{12}v_2)^2v_{12}^2 - 54(n_{12}v_2)^3v_{12}^2 - \frac{246}{35}(n_{12}v_{12})v_1^4$$
$$+\frac{1068}{35}(n_{12}v_1)v_1^2(v_1v_2) - \frac{984}{35}(n_{12}v_2)v_1^2(v_1v_2) - \frac{1068}{35}(n_{12}v_1)(v_1v_2)^2$$
$$+\frac{180}{7}(n_{12}v_2)(v_1v_2)^2 - \frac{534}{35}(n_{12}v_1)v_1^2v_2^2 + \frac{90}{7}(n_{12}v_2)v_1^2v_2^2$$
$$+\frac{984}{35}(n_{12}v_1)(v_1v_2)v_2^2 - \frac{732}{35}(n_{12}v_2)(v_1v_2)v_2^2 - \frac{204}{35}(n_{12}v_1)v_2^4$$
$$+\frac{24}{7}(n_{12}v_2)v_2^4\Big)\Bigg] n_{12}^i$$
$$+\Bigg[-\frac{184}{21}\frac{G^4m_1^3m_2}{r_{12}^5} + \frac{6224}{105}\frac{G^4m_1^2m_2^2}{r_{12}^6} + \frac{6388}{105}\frac{G^4m_1m_2^3}{r_{12}^6}$$
$$+\frac{G^3m_1^2m_2}{r_{12}^4}\Big(\frac{52}{15}(n_{12}v_1)^2 - \frac{56}{15}(n_{12}v_1)(n_{12}v_2) - \frac{44}{15}(n_{12}v_2)^2 - \frac{132}{35}v_1^2 + \frac{152}{35}(v_1v_2)$$
$$-\frac{48}{35}v_2^2\Big)$$
$$+\frac{G^3m_1m_2^2}{r_{12}^4}\Big(\frac{454}{15}(n_{12}v_1)^2 - \frac{372}{5}(n_{12}v_1)(n_{12}v_2) + \frac{854}{15}(n_{12}v_2)^2 - \frac{152}{21}v_1^2$$
$$+\frac{2864}{105}(v_1v_2) - \frac{1768}{105}v_2^2\Big)$$
$$+\frac{G^2m_1m_2}{r_{12}^3}\Big(60(n_{12}v_{12})^4 - \frac{348}{5}(n_{12}v_1)^2v_{12}^2 + \frac{684}{5}(n_{12}v_1)(n_{12}v_2)v_{12}^2$$
$$-66(n_{12}v_2)^2v_{12}^2 + \frac{334}{35}v_1^4 - \frac{1336}{35}v_1^2(v_1v_2) + \frac{1308}{35}(v_1v_2)^2 + \frac{654}{35}v_1^2v_2^2$$
$$-\frac{1252}{35}(v_1v_2)v_2^2 + \frac{292}{35}v_2^4\Big)\Bigg] v_{12}^i \Bigg\}$$
$$+\mathcal{O}\Big(\frac{1}{c^8}\Big).$$

[Nissanke et al. 2005]

[Blanchet 2015; see also Nissanke et al. 2005, Nissanke 2006, Blanchet, Faye, Nissanke 2005, MacDonald, Nissanke, Pfeiffer 2011]

Necessity of Numerical Relativity

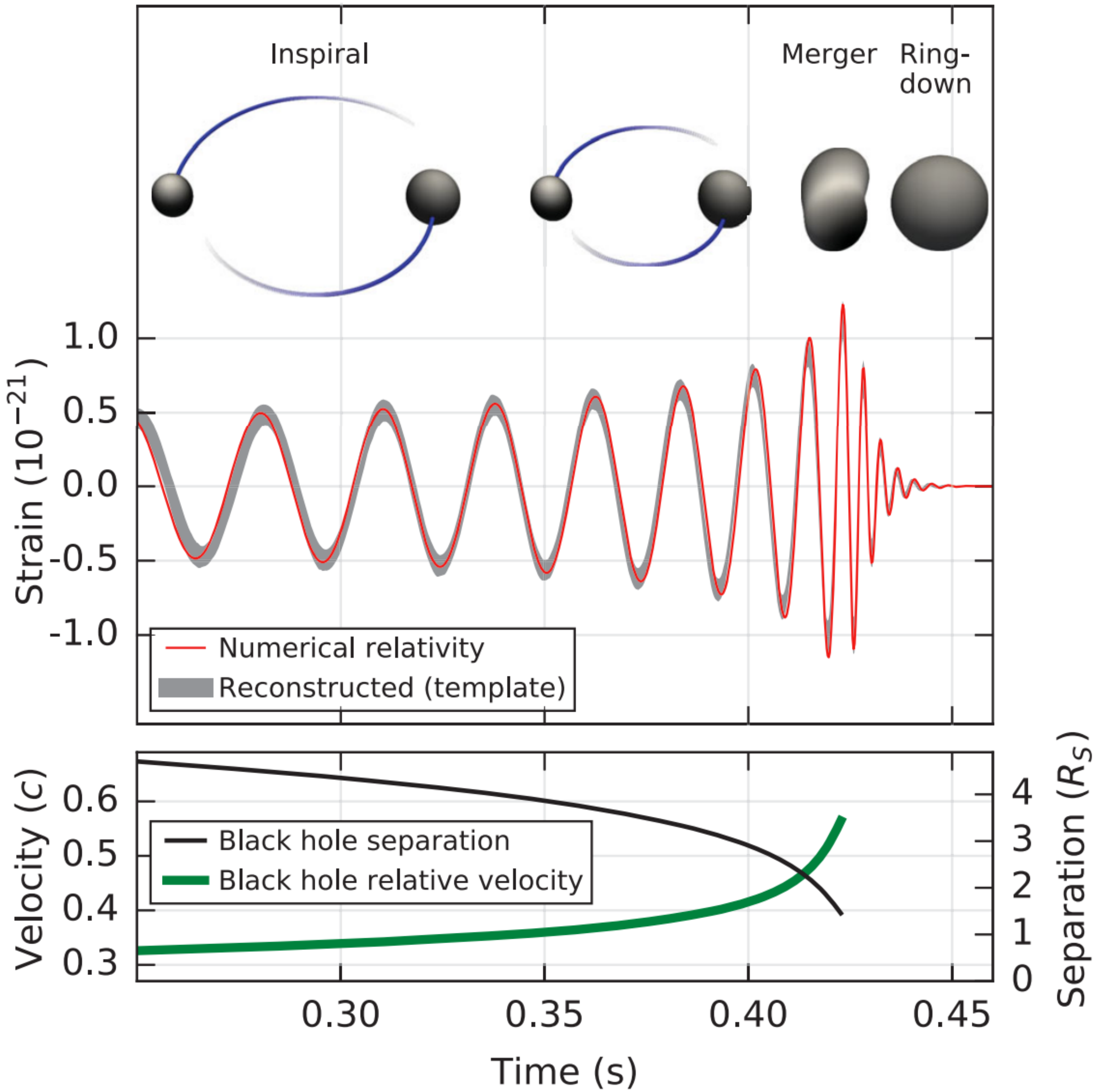

[LVC, arXiv:1602.03837, PRL 116, 061102, 2016]

Unprecendented high velocity, dynamic regime of strong-field gravity

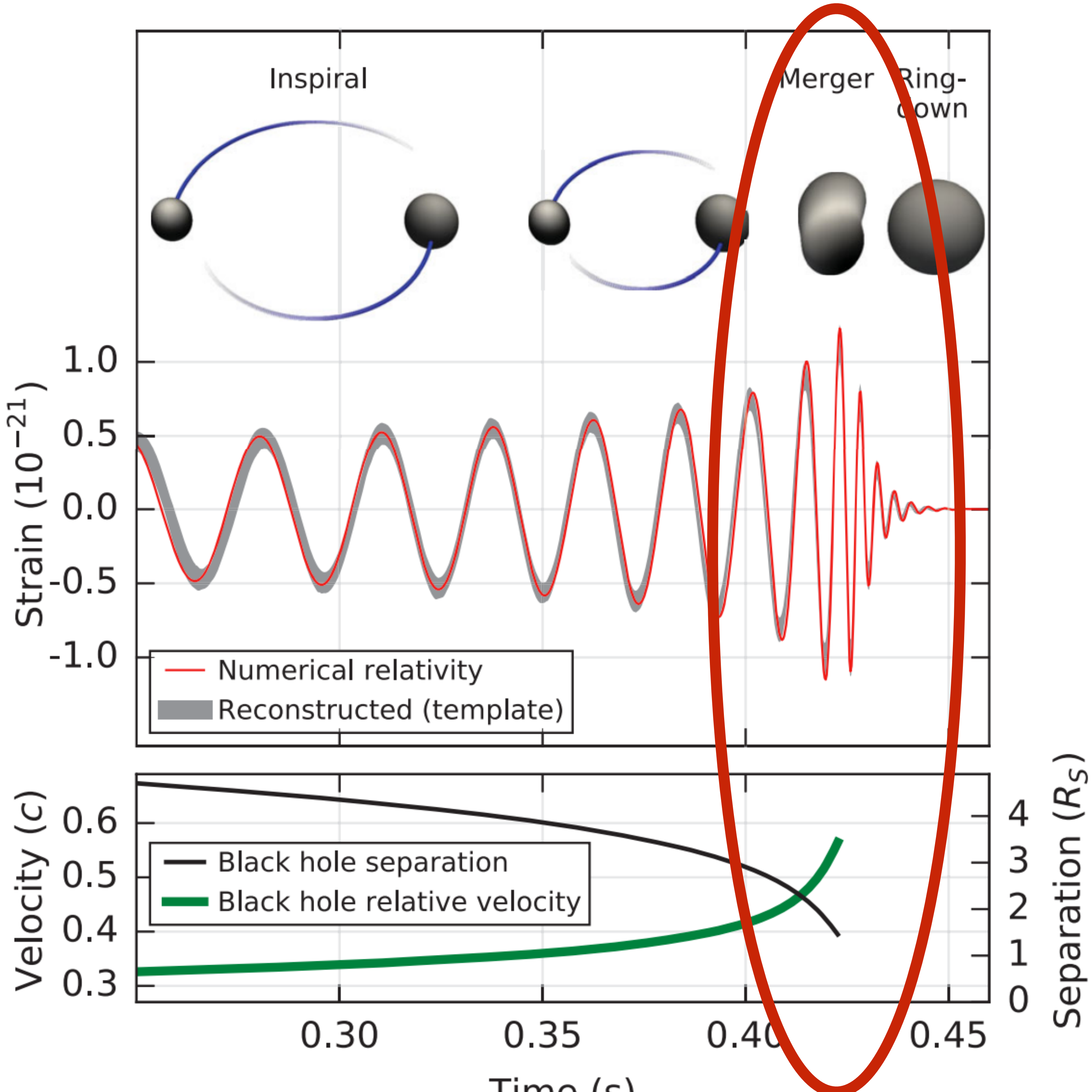

[LVC, arXiv:1602.03837, PRL 116, 061102, 2016]

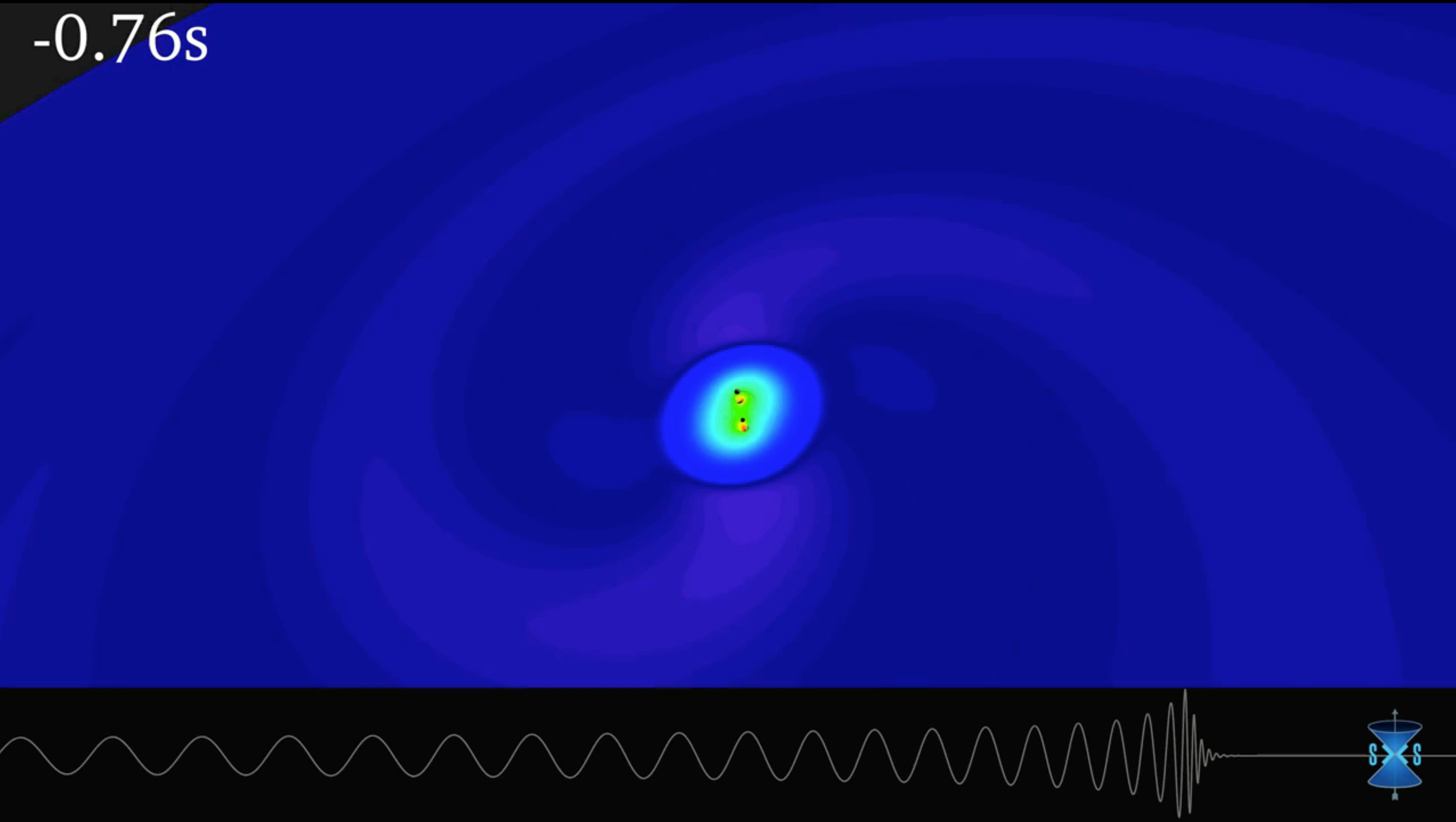

GW150914: numerical relativity simulation

[SXS collaboration 2016]

Different flavors of numerical relativity waveforms

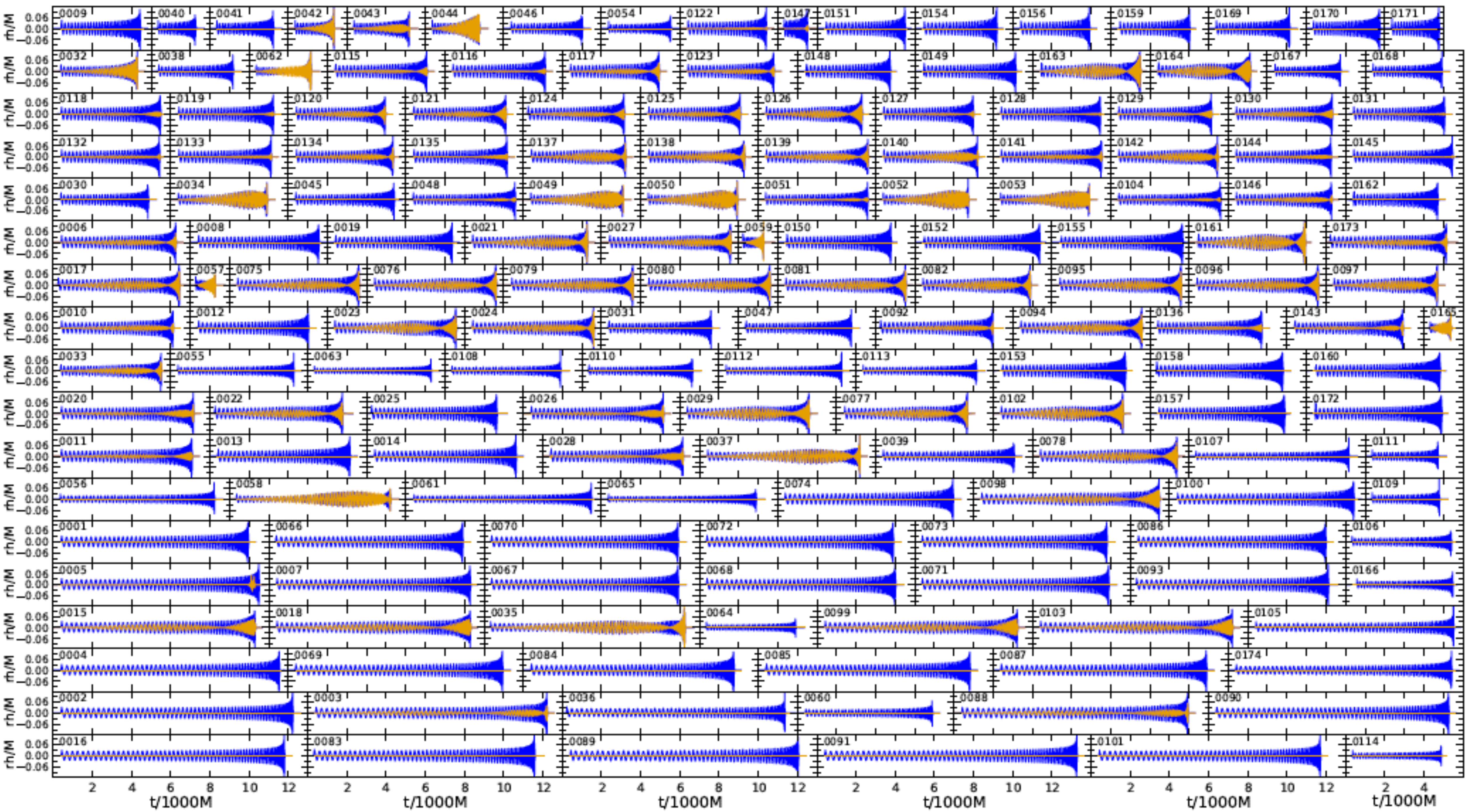

[e.g., SXS Collaboration 2014; see also simulations by Cardiff, UIB, RIT and GATech;
combined analysis with several hundred simulations from all groups for GW150914 detailed in arXiv: 1606.01262]

Measured GW encodes fundamental and geometric source parameters

$$h_M = \sum_{a=+,\times} \mathrm{Antenna\ \ function\,(source\,position,\ orientation)} \times h_a$$

$$h_{+,\times} \sim \frac{g_{+,\times}\,\mathrm{(inclination\,angle)}\,h(\,\mathrm{redshifted\,masses/spins,\ frequency\,chirp...})}{\mathrm{Luminosity\,distance}}$$

Polarisation gives inclination angle.

Triangulation and antenna response give sky localisation.

Strong degeneracy between amplitude parameters:
{source position, orientation and distance}

Measured GW encodes fundamental and geometric source parameters

$$h_M = \sum_{a=+,\times} \text{Antenna function (source position, orientation)} \times h_a$$

$$h_+(t) = 2\left(\frac{G\mathcal{M}_z}{c^3}\right)^{5/3} \frac{\Omega(t)^{2/3}}{D_L}\left(1+\cos^2(\hat{\mathbf{L}}.\hat{\mathbf{n}})\right)\left[2\int \Omega(t)dt\right]$$

Chirp mass has dimensions of time ⇒ masses are redshifted.

Phase of GWs can be measured to within a fraction of a radian ⇒ chirp mass with fractional accuracy ~ 1/total accumulated phase.

Amplitude with precision 1/SNR ⇒ need multiple detectors and polarization.

Extract source information from GWs

h(t): 9-15 dimensions

+ Masses
+ Spins
+ Geometric properties:
  - Inclination angle
  - Source Position
  - Luminosity distance

[see e.g. Cutler and Flanagan 1994, Poisson and Will 1996…]

Extract source information from GWs

h(t): 9-15 dimensions

+ Masses
+ Spins
+ Geometric properties:
  - Inclination angle
  - Source Position
  - Luminosity distance

Model h(t)

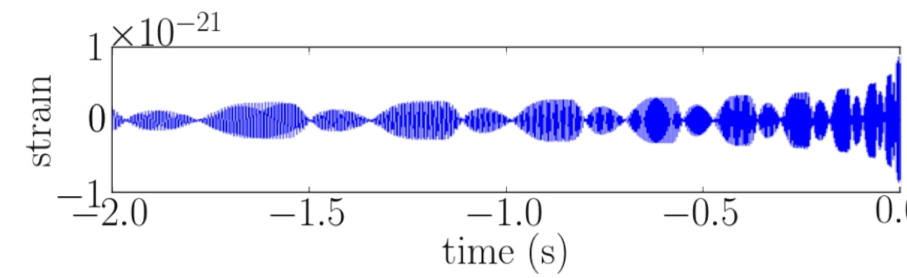

Detector output

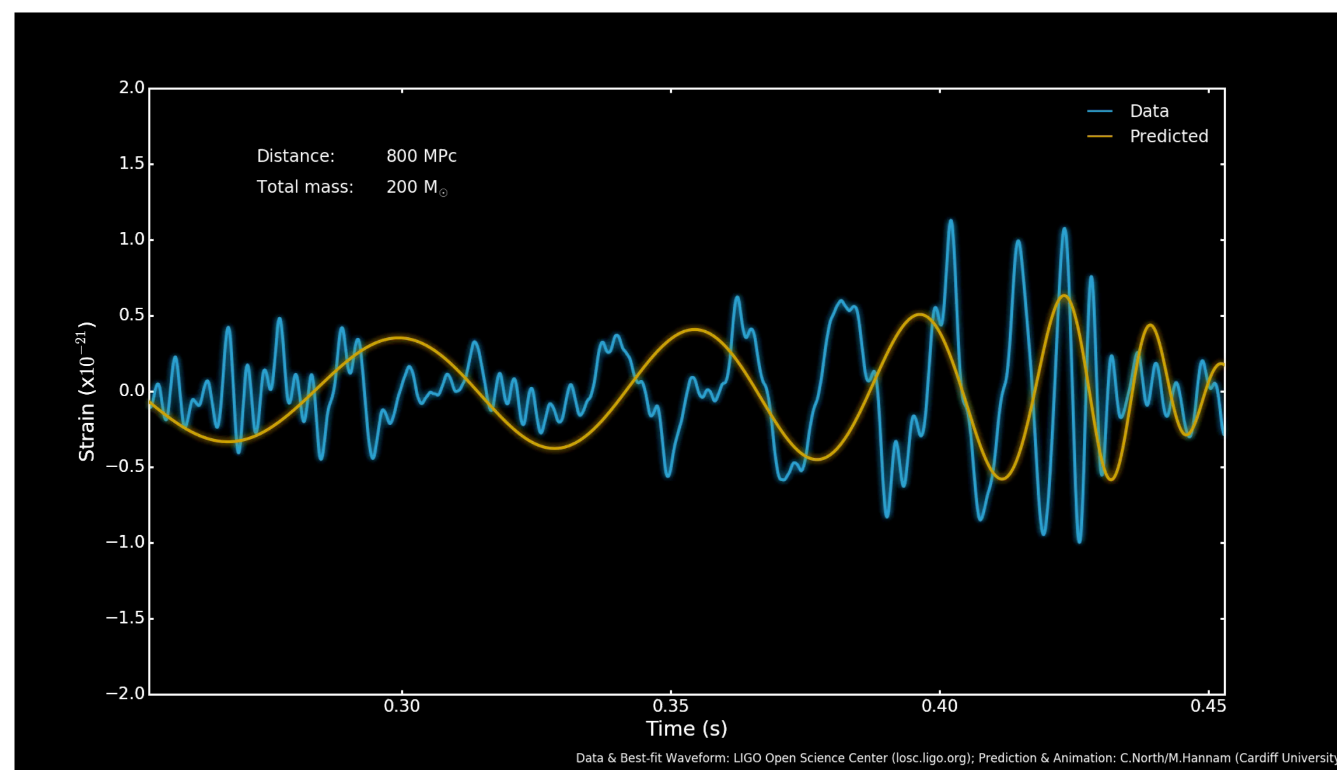

[figure courtesy of Chris North/Mark Hannam]

[see e.g. Veitch et al. 2015;
LVC, arXiv: 1602.03840, PRL 116, 241102, 2016]

Extract source information from GWs

frequency

$$h_+(t) = \frac{A[\mathcal{M}\, f(t)]}{D}(1+\cos^2 \iota)\cos\Phi_{\rm GW}(t)$$

distance inclination angle GW Phase

h(t): 9-15 parameters

+ Redshifted Masses
+ Redshifted Spins
+ Geometric properties:
  - Inclination angle
  - Source Position
  - Luminosity distance

Model h(t)

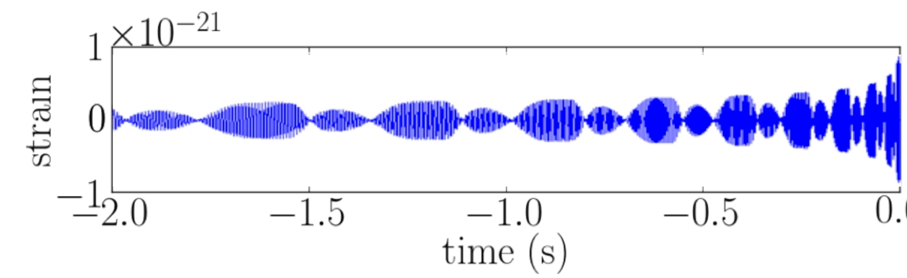

Detector output

Explicitly map out: $p(\boldsymbol{\theta}|s) \propto p(\boldsymbol{\theta})\mathcal{L}_{\rm total}(s|\boldsymbol{\theta})$

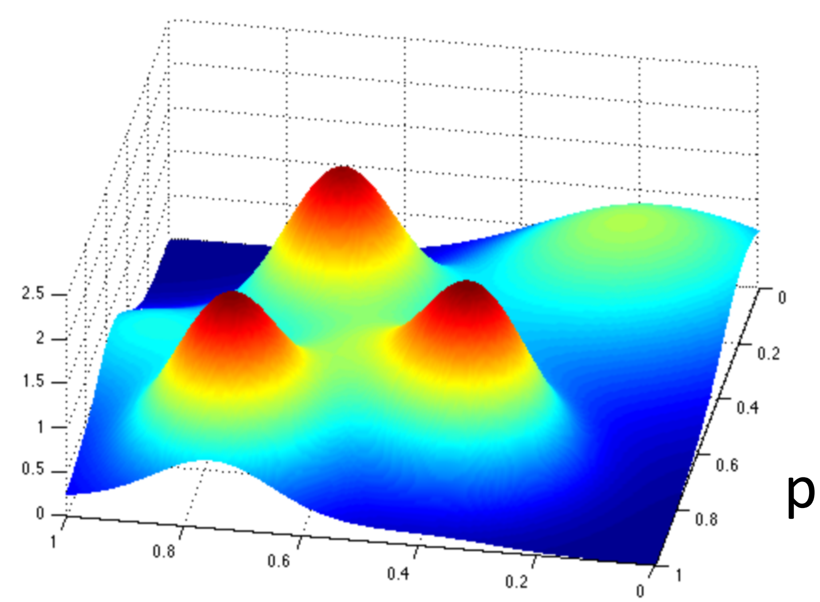

Likelihood

parameter 1

parameter 2

using Bayesian Markov Chain Monte Carlo and Nested Sampling Techniques

[see LVC, arXiv: 1602.03840, PRL 116, 241102, 2016]

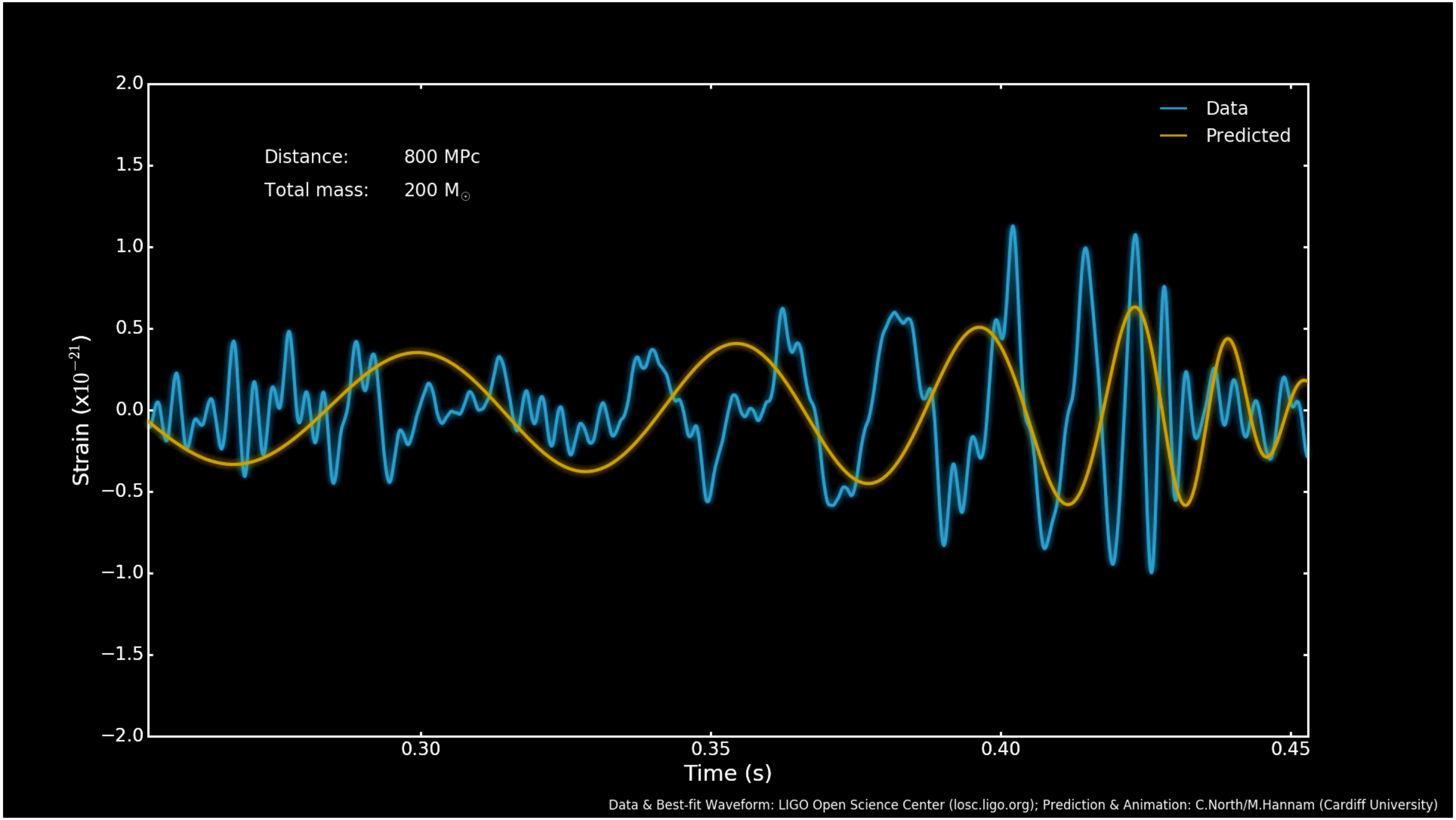
Data
Predicted
Distance: 800 MPc
Total mass: 200 $M_\odot$
Strain (x10^{-21})
2.0
1.5
1.0
0.5
0.0
−0.5
−1.0
−1.5
−2.0
0.30
0.35
0.40
0.45
Time (s)
Data & Best-fit Waveform: LIGO Open Science Center (losc.ligo.org); Prediction & Animation: C.North/M.Hannam (Cardiff University)

Large degeneracies when retrieving BH parameters: errors are several 10s of %

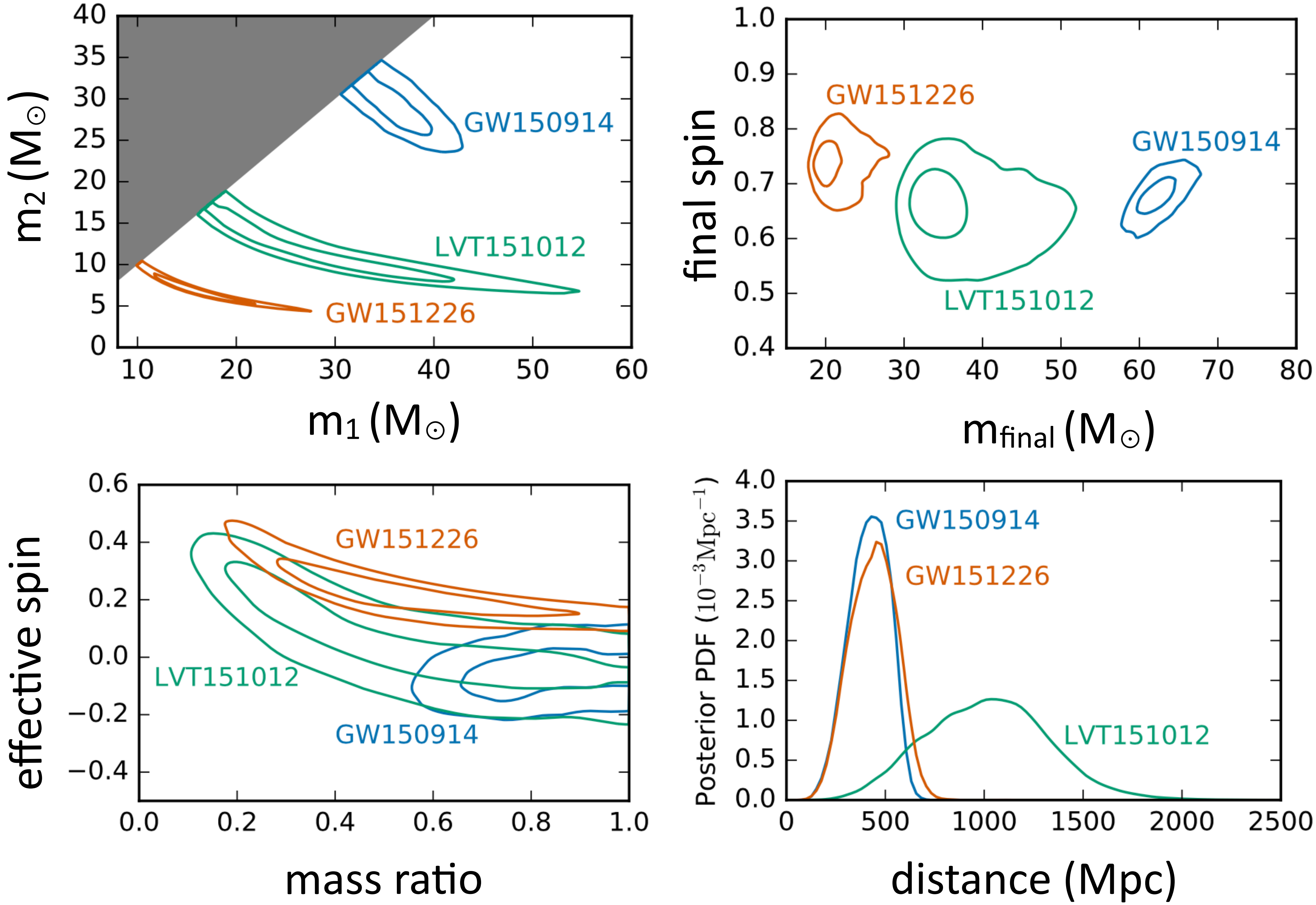

[LVC, arXiv:1606.04856, PRX 6, 041015, 2016]

[1 Mpc = 3.086e22 m]

… errors depend on what part of waveform is in the detector noise bucket!

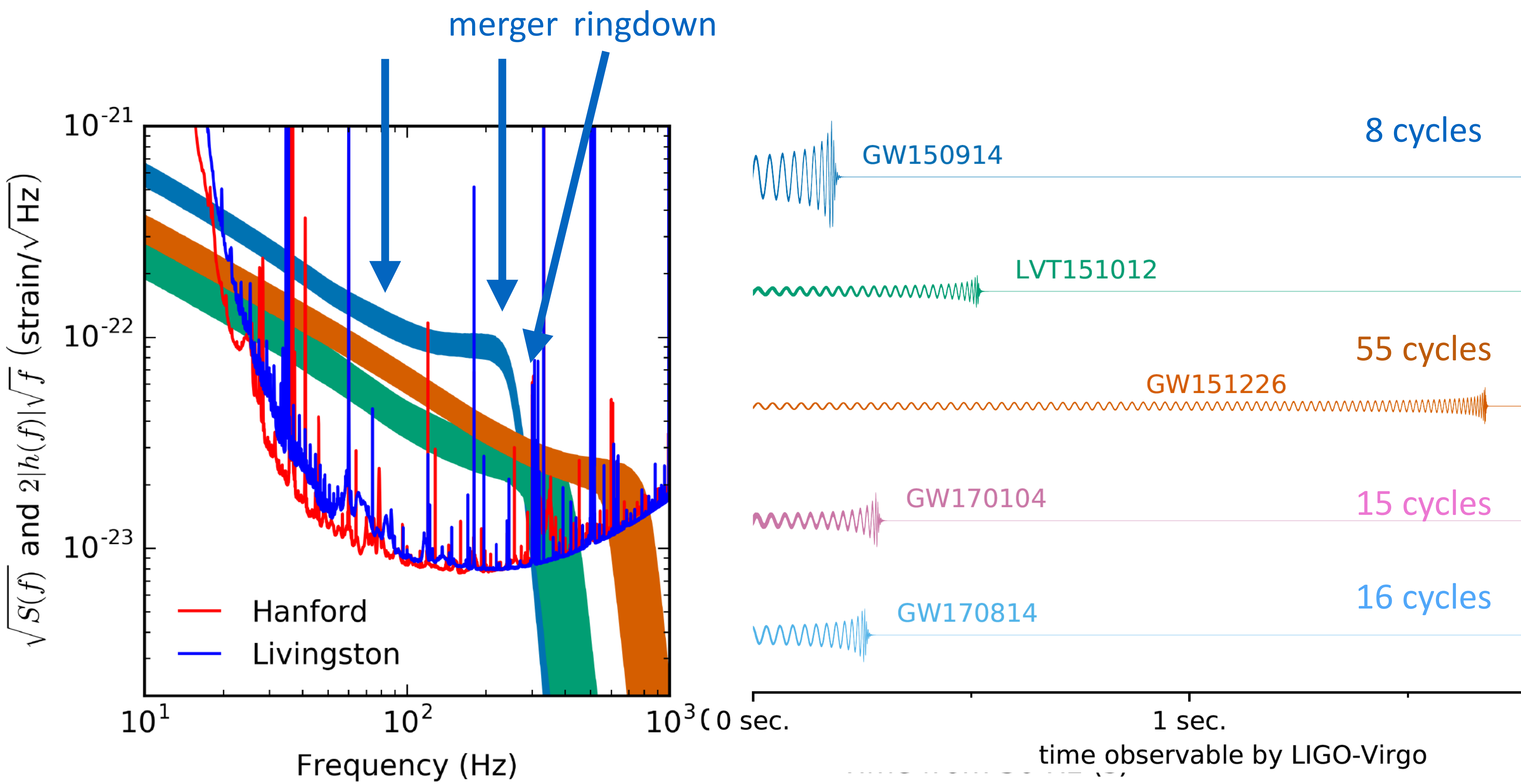

[LVC, arXiv:1606.04856, PRX 6, 041015, 2016]

How well can we localise the source on the sky?

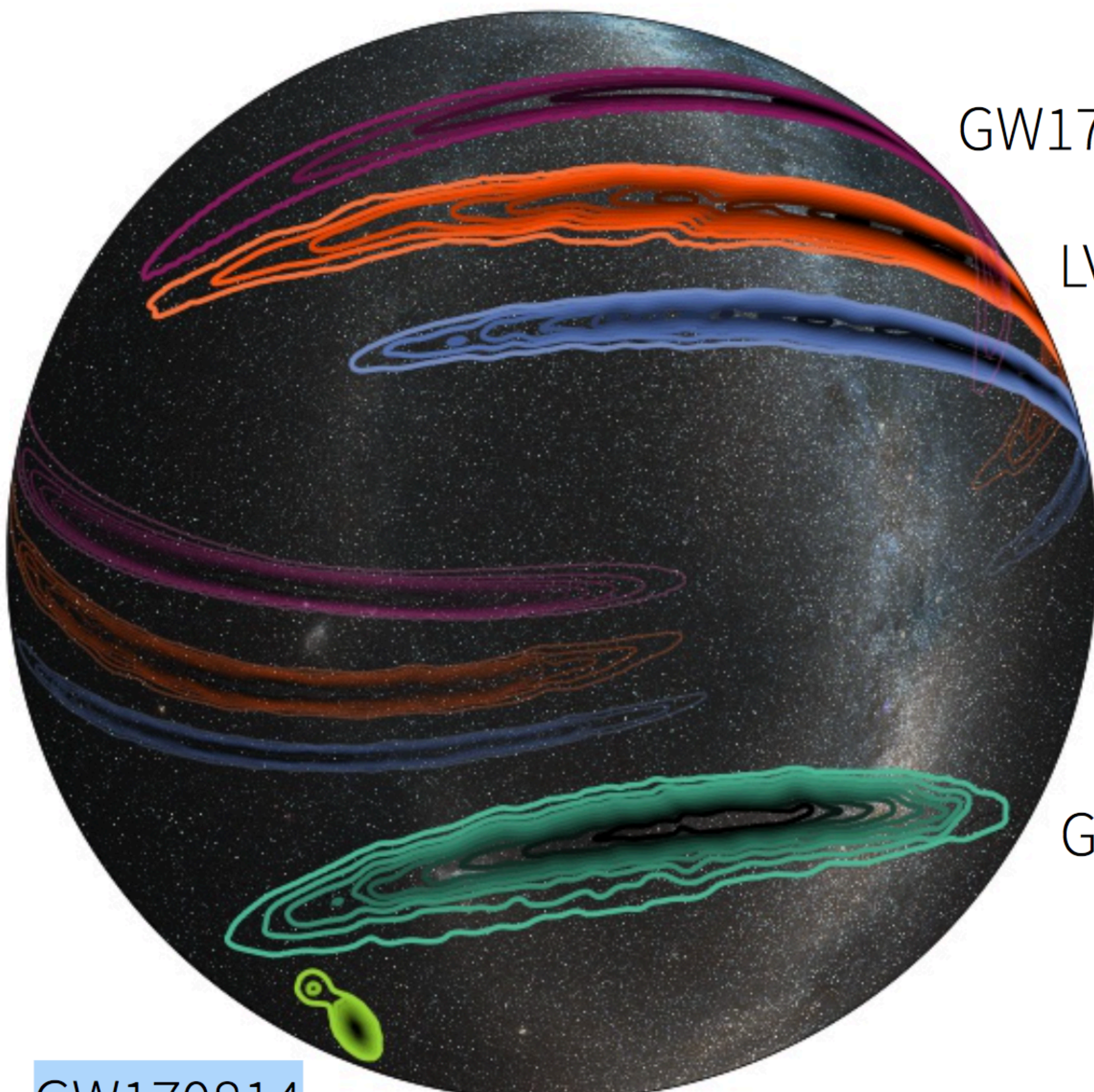

GW170104

1200 sq. deg. (90% c.r.)

LVT151012

1600 sq. deg. (90% c.r.)

GW151226

1000 [850] sq. deg.
(90% c.r.)

GW150914

590 [230] sq. deg. (90% c.r.)

GW170814

60 sq. deg. (90% c.r.)

10^5-10^7 galaxies in these volumes

[Image credit: LIGO/L. Singer/A. Messinger]

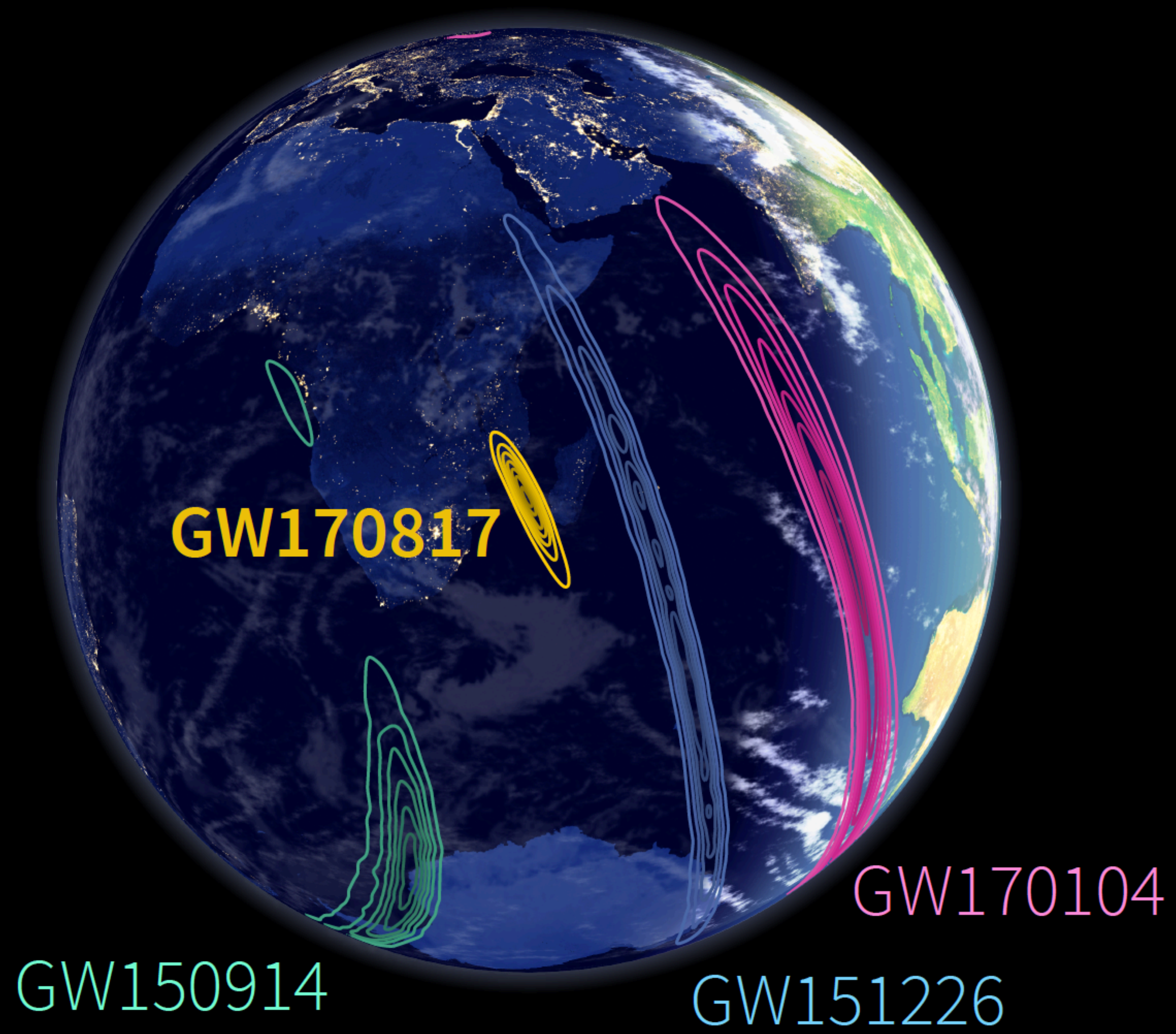

Credit: LIGO/Virgo/NASA/Leo Singer

Part II:
Tests of General Relativity in dynamical strong-field gravity

Deviations from GR Waveform Coefficients

Introduce parameterized violations of GR: $p_i \to p_i(1 + \delta\hat{p}_i)$

$$\Psi_{\rm GW}(f) = \sum_i [\psi_i + \psi_{il} \log f] f^{(i-5)/3} + \Phi^{\rm MR}[\beta_i, \alpha_i]$$

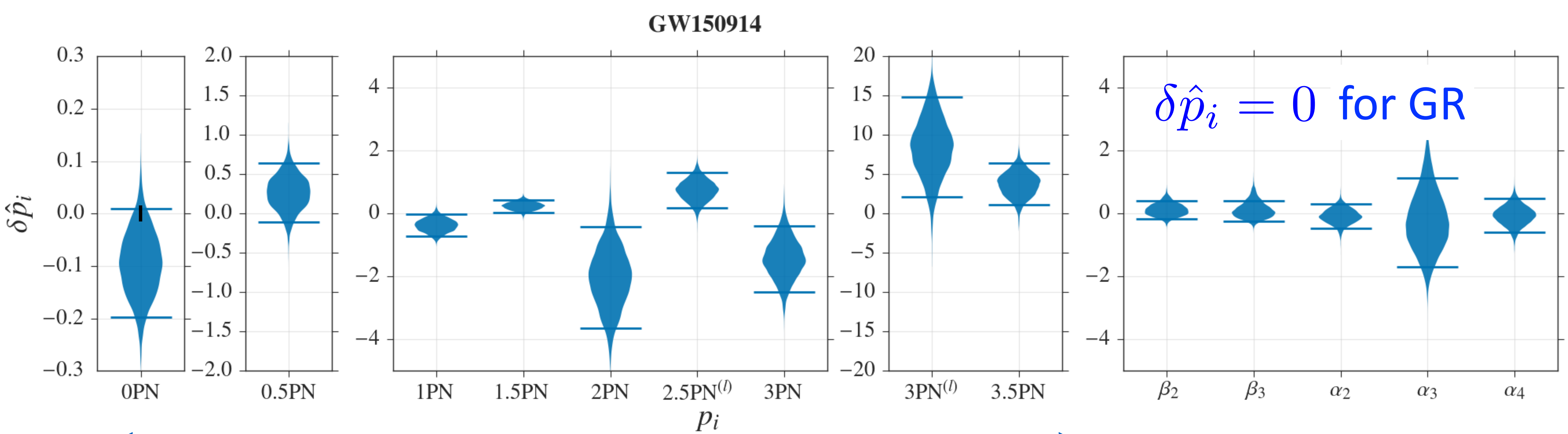

Inspiral

Merger Ringdown

[LVC, arXiv:1606.09619, 2016; arXiv: 1602.03841, PRL 116, 221101, 2016]

Deviations from GR Waveform Coefficients

Introduce parameterized violations of GR: $p_i \rightarrow p_i(1 + \delta\hat{p}_i)$

$$\Psi_{\rm GW}(f) = \sum_i [\psi_i + \psi_{il} \log f] f^{(i-5)/3} + \Phi^{\rm MR}[\beta_i, \alpha_i]$$

tail - backscattering of GWs by curved spacetime

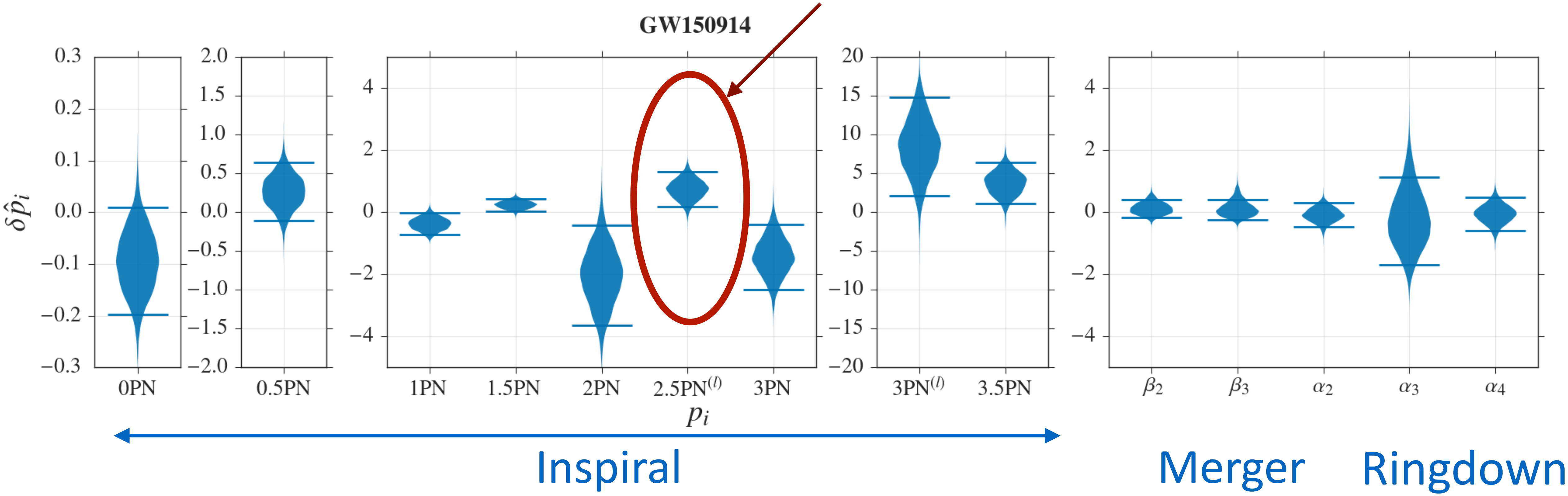

[LVC, arXiv:1606.09619, 2016; arXiv: 1602.03841, PRL 116, 221101, 2016]

… two events constrain different parts of waveform

[LVC, arXiv:1606.09619, 2016]

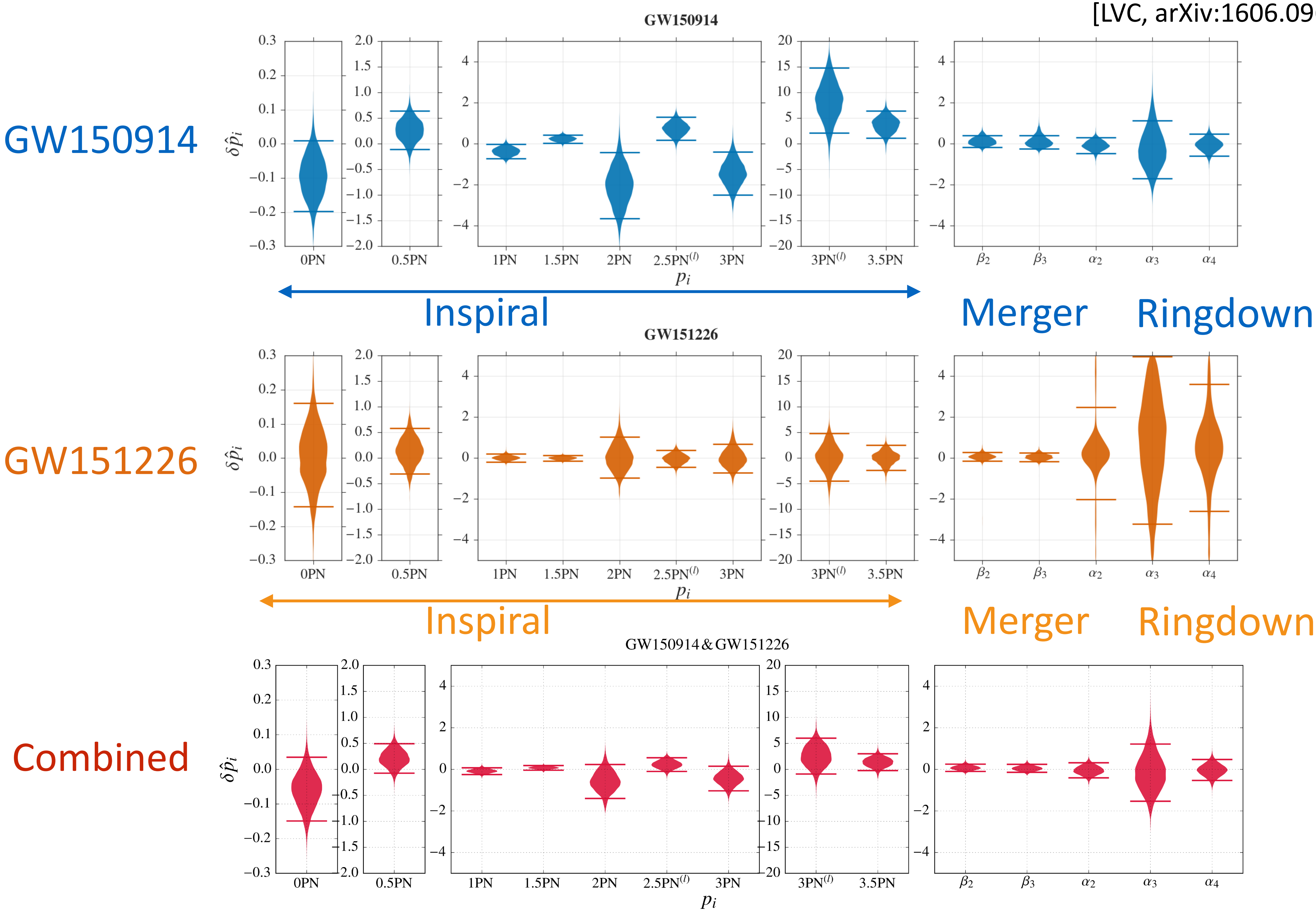

… GW150914 merger + ringdown in the detector noise bucket!

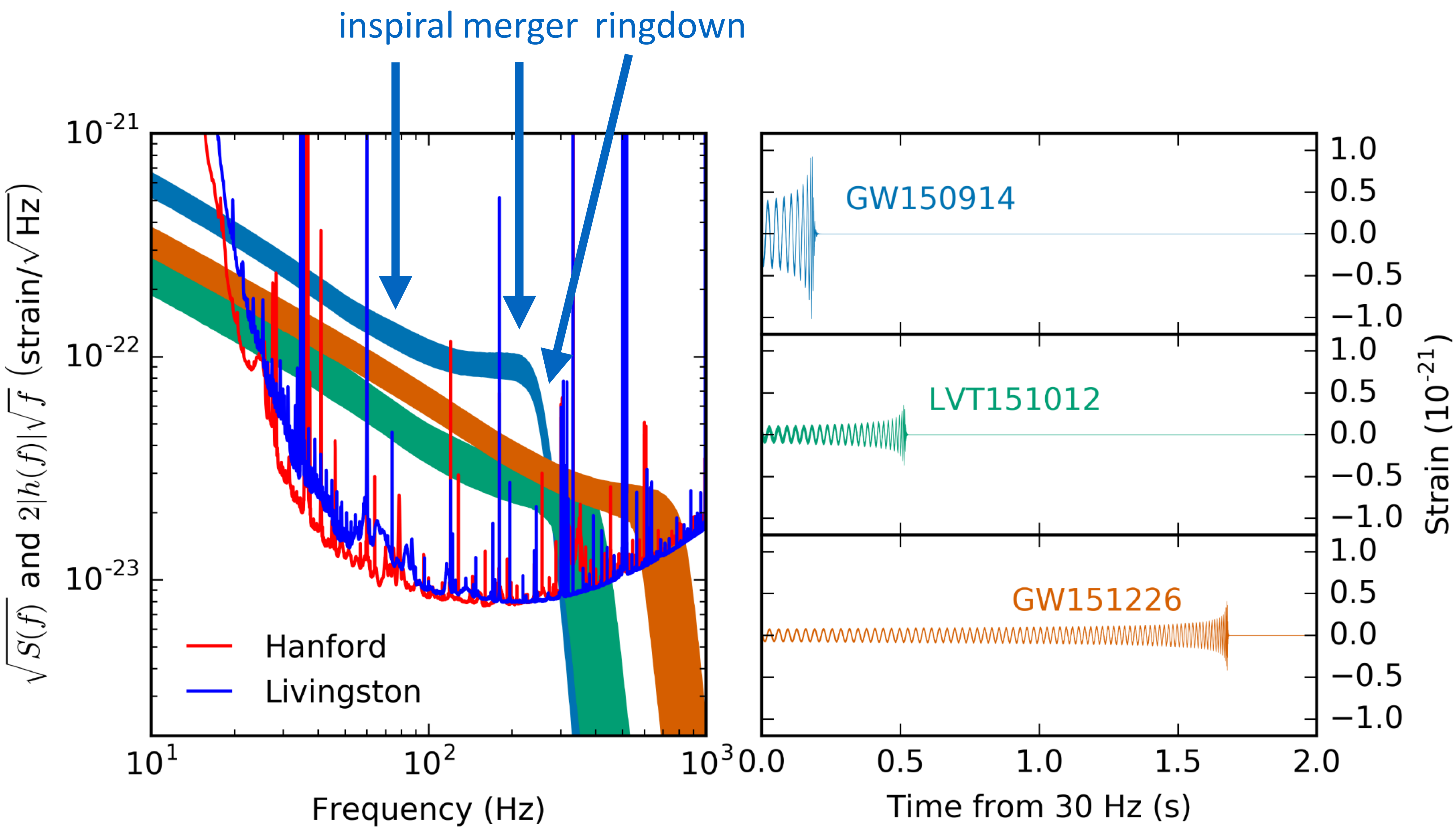

[LVC, arXiv:1606.09619, 2016]

GW150914: Inspiral vs. merger-ringdown consistency

[LVC, arXiv:1606.09619, PRL 116, 221101, 2016; see also Ghosh et al. 2016]

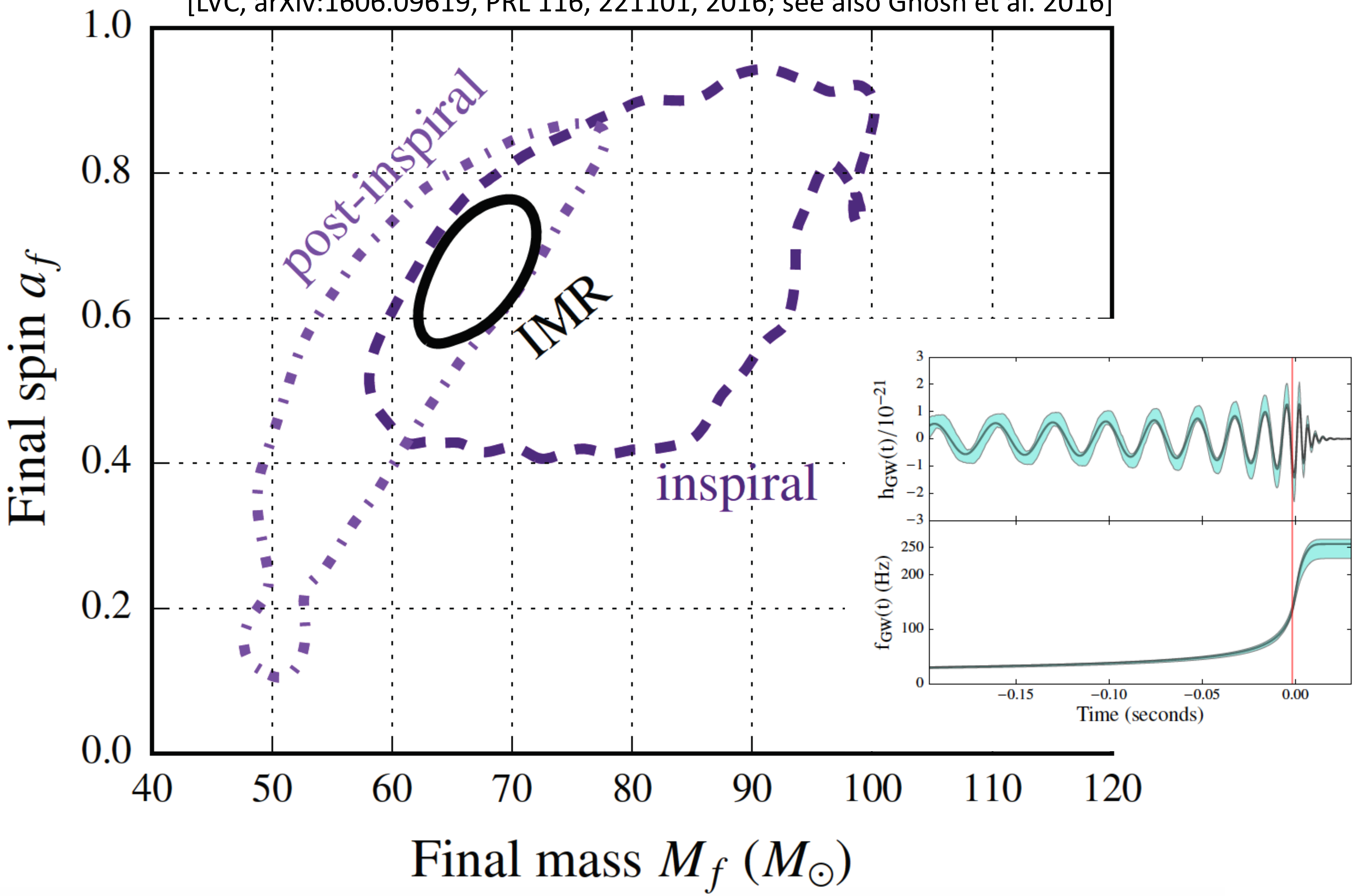

GW150914: Massive Graviton Bounds

- massive graviton dispersion relation:

$$E^2 = p^2c^2 + m_g^2c^4$$

where $\lambda_g = \dfrac{h}{m_g c}$

- higher frequencies arrive earlier:

$$\left(\frac{v_g}{c}\right)^2 = 1 - \frac{h^2c^2}{\lambda_g^2 E^2}$$

- waveform distortion:

$$\delta\Phi(f) = \frac{\pi D c}{\lambda_g^2(1+z)f}$$

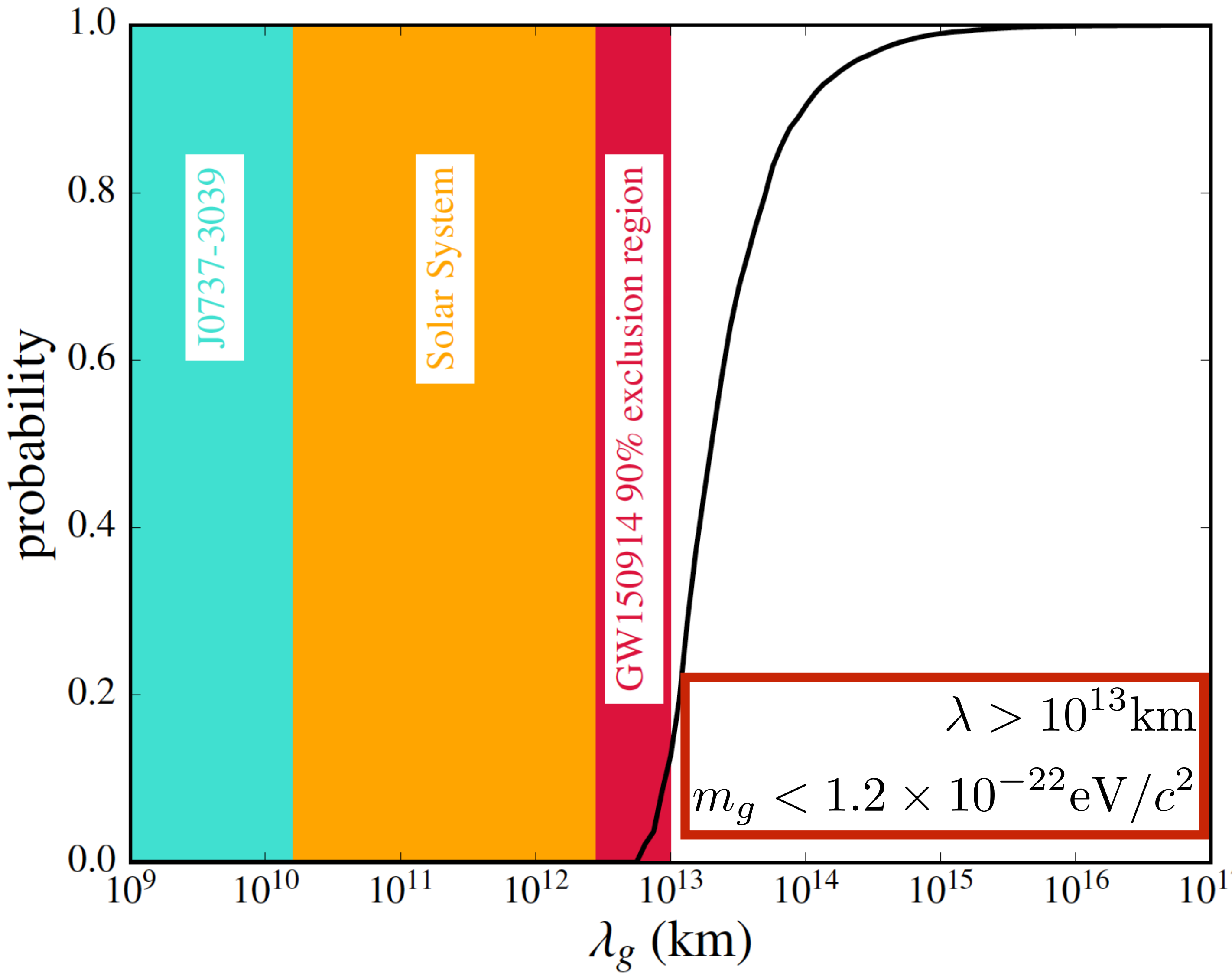

[LVC, PRL 116, 221101, 2016]

Part III: Implications for Astrophysics

i) how to form heavy BHs?
ii) how & where do binary black holes (BBH) form?
iii) astrophysical rates ?
iv) absence of an EM counterpart ?

Challenge: how, when and where do BBHs form?

Primordial BHs from density fluctuations in early Universe

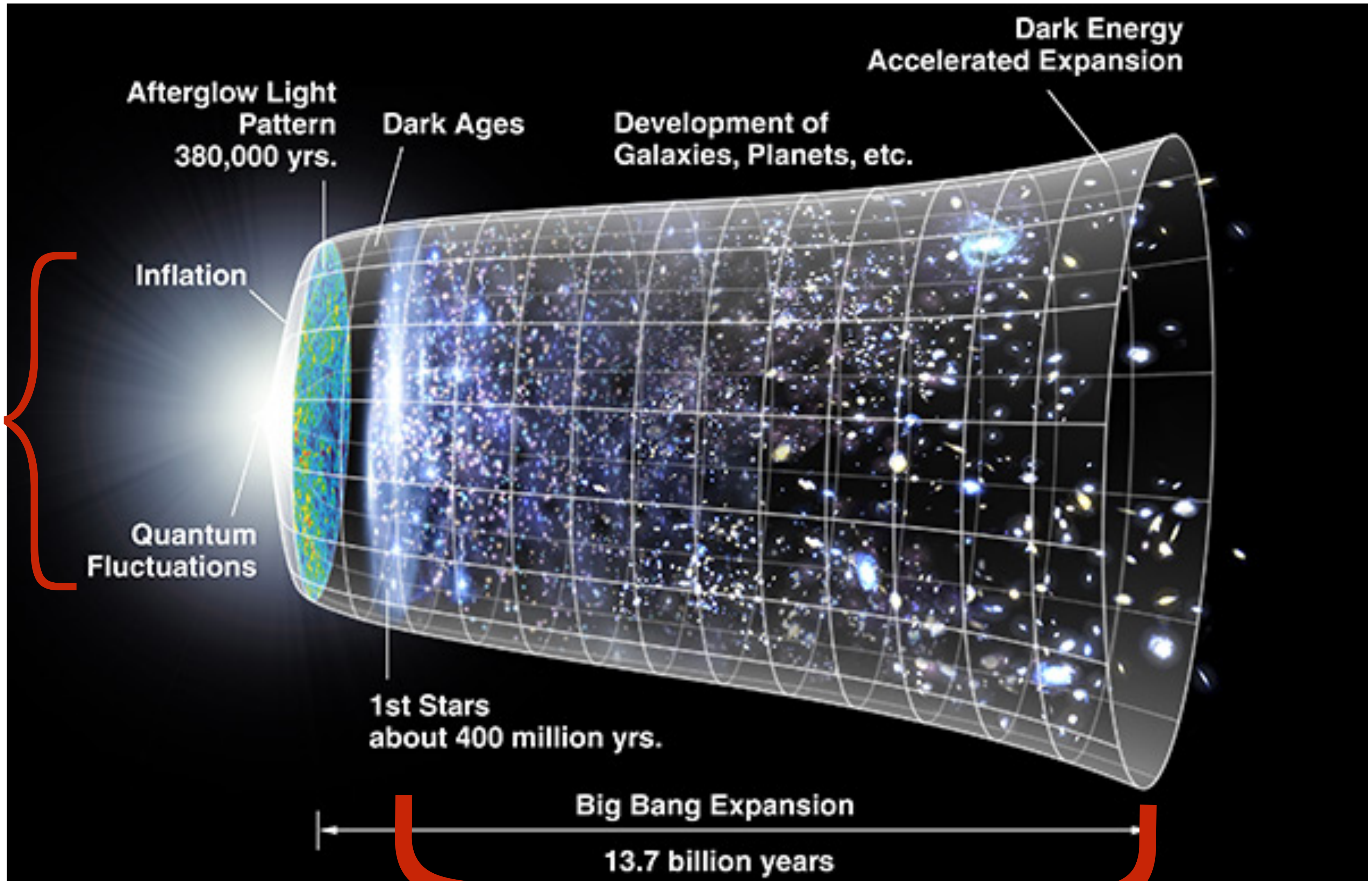

Pop III: first massive stars (1% of stars in Universe)
Pop II/I: classic field binary evolution (90%)
Pop II/I: rapid rotation (10%)
Pop II/I: dynamical formation in globular clusters (0.1%)
Exotic: e.g. single star core splitting

[LVC, ApJL 818, L22, 2016]

How to make a stellar-mass BH?

Stellar core collapse at end of lives of massive stars:
direct formation or fallback? first stars?

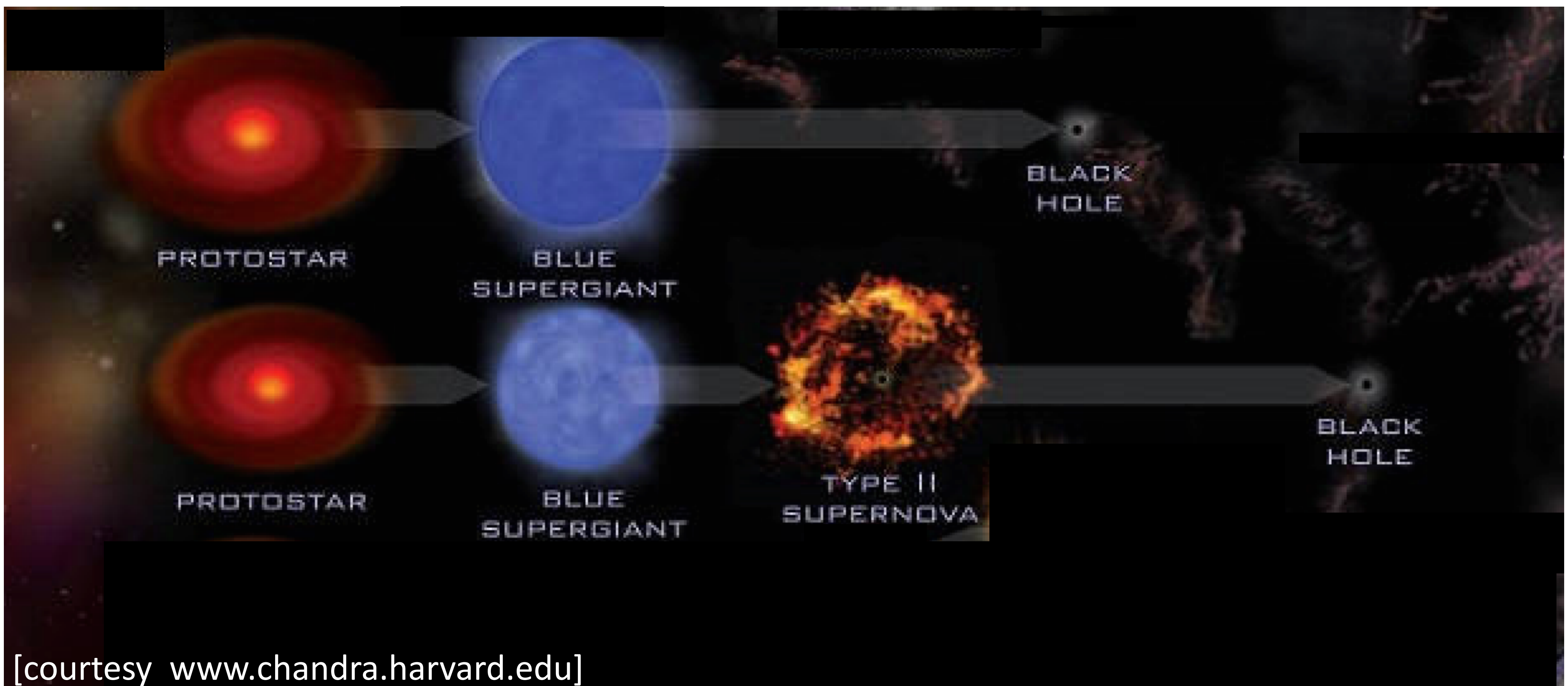

[courtesy www.chandra.harvard.edu]

Low metallicity with $Z < 0.5\ Z_\odot$ (solar) and weak massive stellar winds

Recipe for making heavy BHs

[LVC, ApJL 818, L22, 2016; adapted from Belczynski et al. 2010]

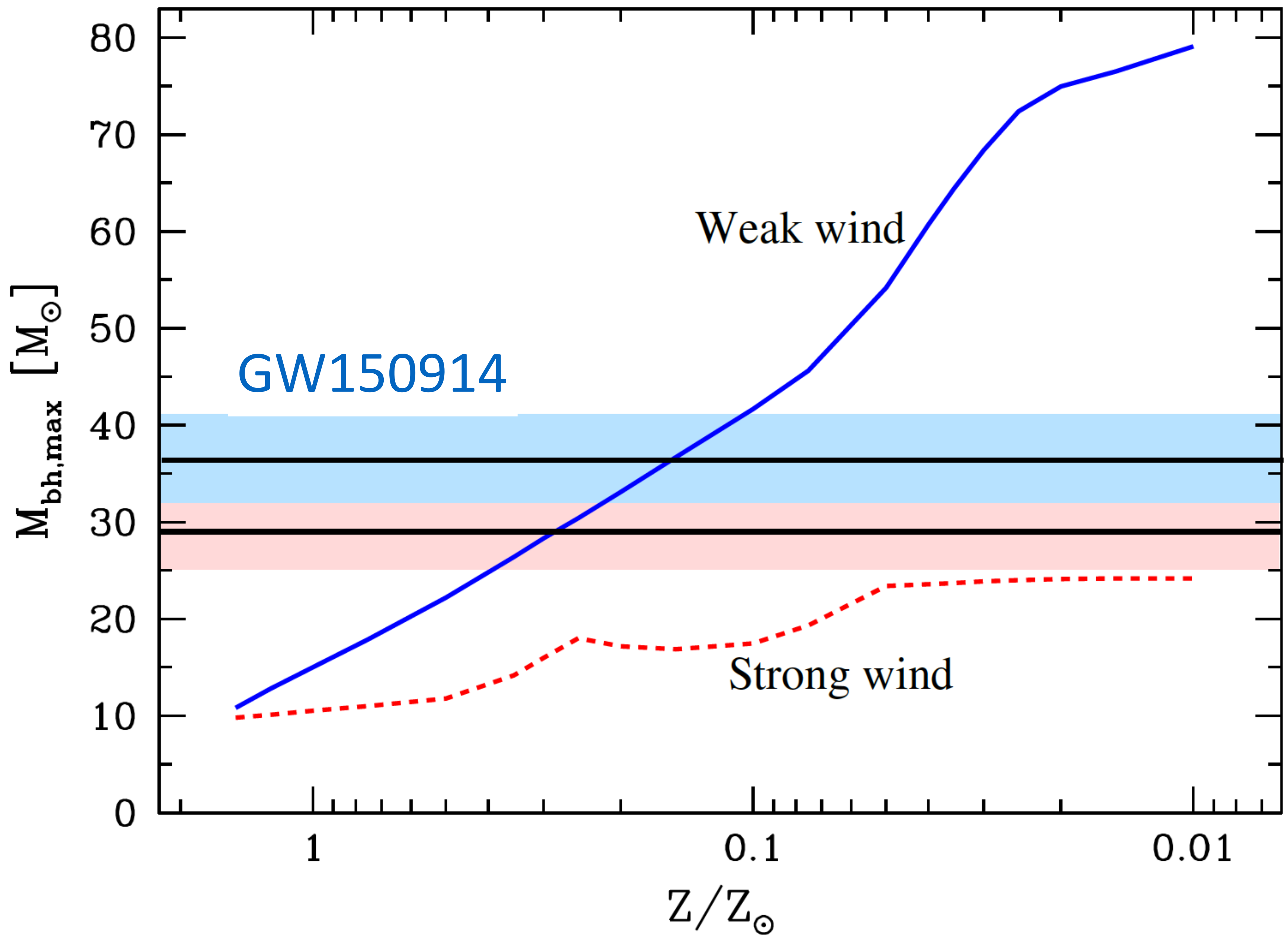

Low metallicity with $Z < 0.5\ Z_\odot$ (solar) and weak massive stellar winds

Tale of two binaries

[see review by Miller 2016;
LVC, ApJL 818, L22, 2016]

Isolated Binary in Field

[0.15 pc^{-3}]

range of binary interactions

low redshift to Pop III

rapidly rotating massive stars

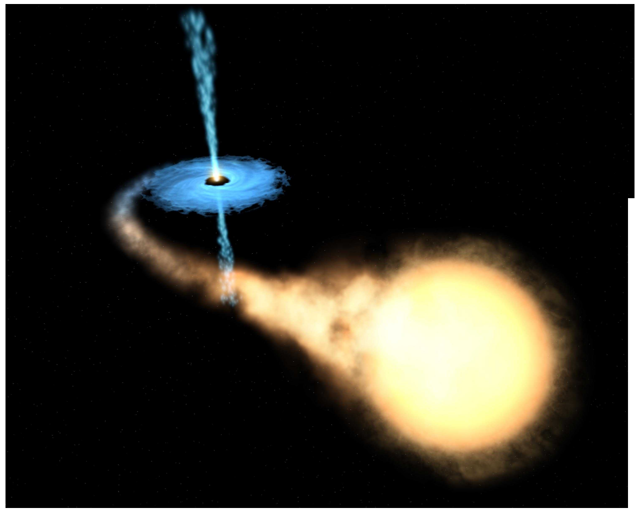

[e.g., Tutukov & Yungelson 1993, Lipunov+97, … Belczynski+10, Mandel+deMink 16, Marchant+16, Belczynski+04, Kinugawa+14]

Dense Environments (e.g., Clusters)

[10^5-10^9 pc^{-3}]

BHs sink towards cluster core

Dynamical interaction -> pairs

Binaries ejected with inspiral < Hubble time

[e.g., Portegies Zwart+00, O'Leary+06, Downing+10, Morscher+13, Ziosi+14.; NB Galactic Center: Miller+Lauburg+09, O'Leary+09, Koscis+12, Bartos+16, Stone+16]

Lifecycle of Isolated Binary Massive Stars

Rare but important (feedback, chemical enrichment)

Complex physics in multi-staged evolutionary process

Supernova, Common Envelope, Mass Transfer, BH natal kicks

~ 6 to 9 steps: survival is 0.01-10%

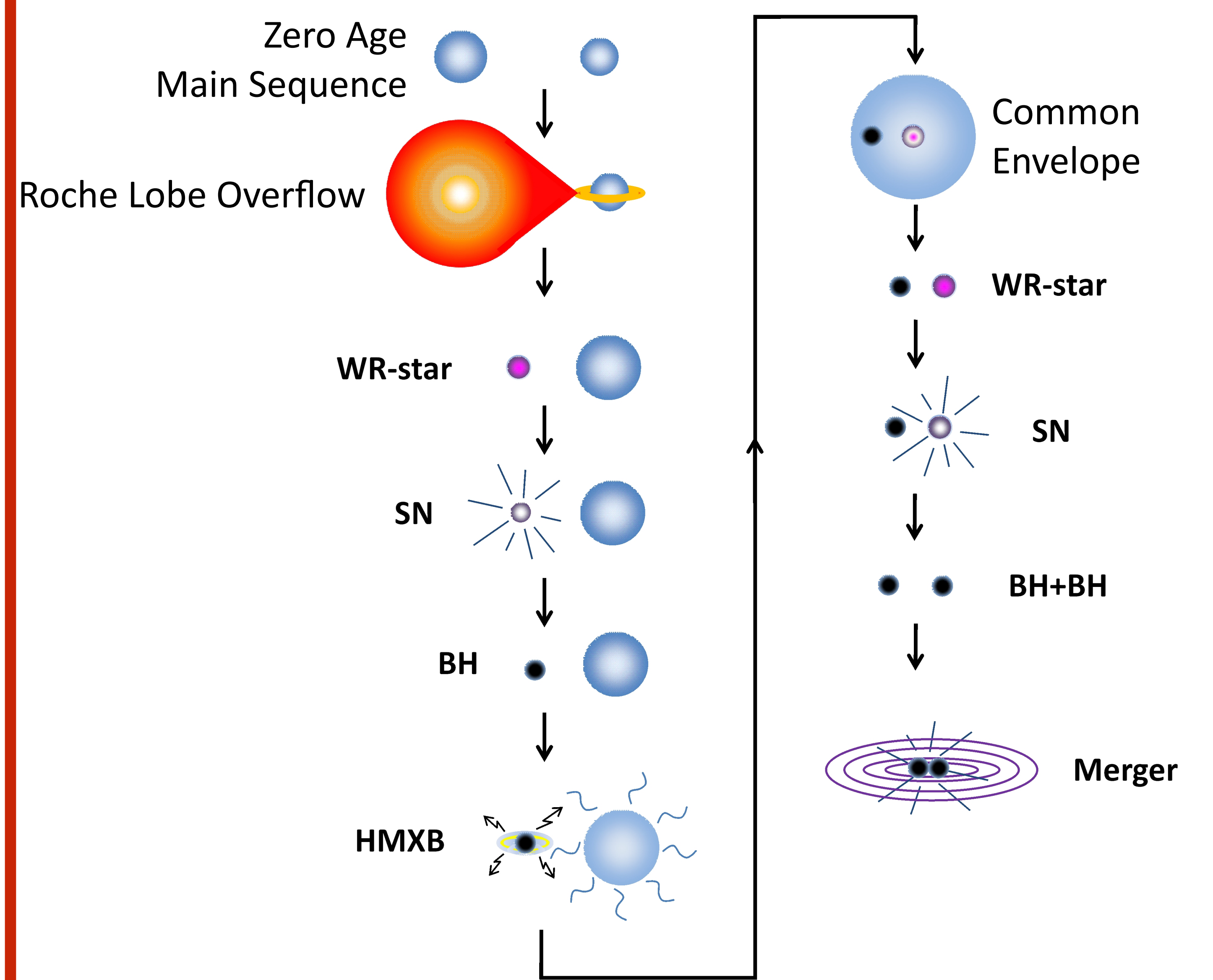

[figure from Marchant et al. 2016]

Astrophysical rates could soon probe formation scenarios

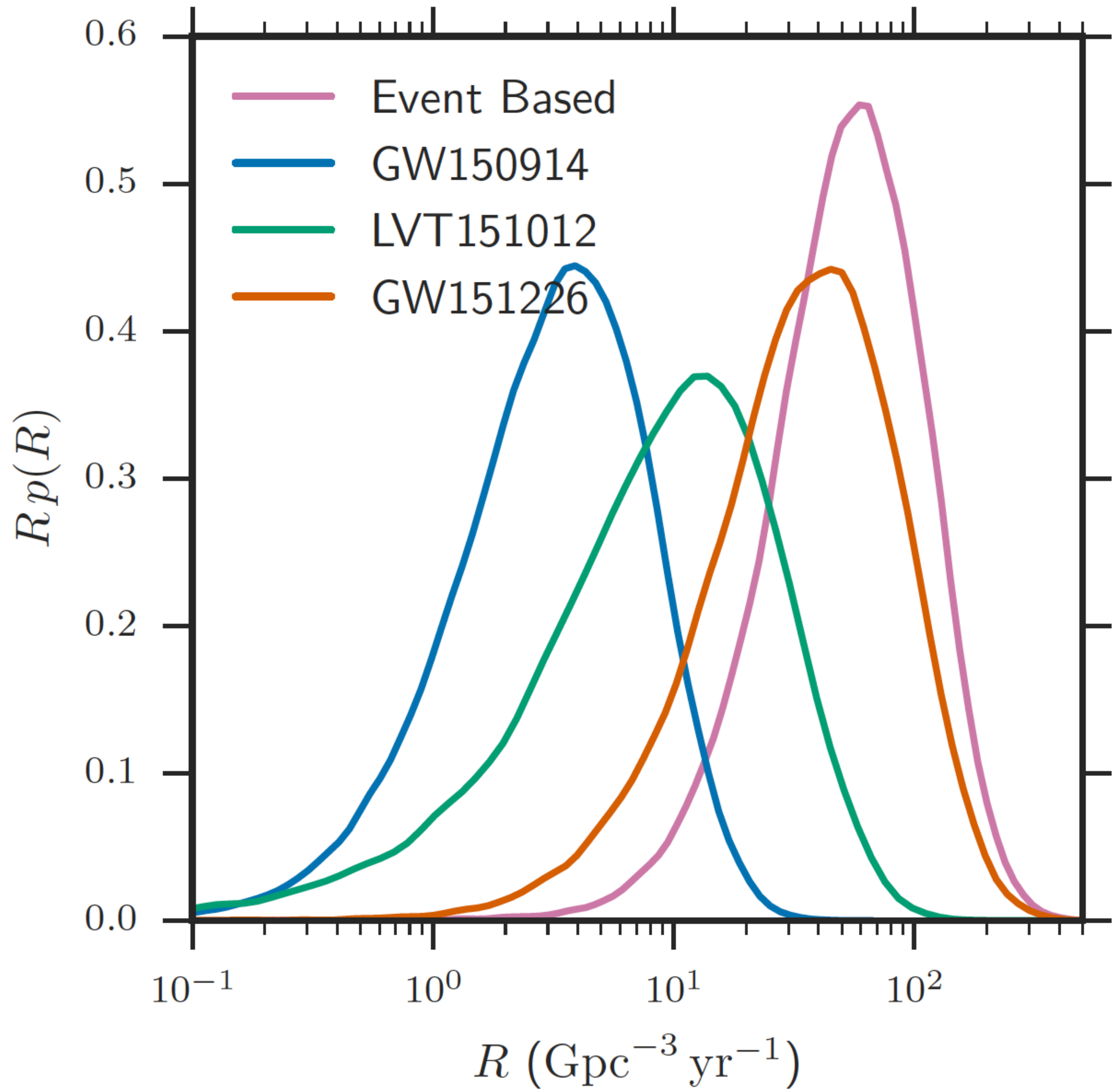

[LVC, arXiv:1606.09619, 2016]

12 - 240 Gpc^{-3} yr^{-1}

Excludes < 10 Gpc^{-3} yr^{-1} $\Rightarrow$

Isolated

Disfavours a v. low common envelope binding energy or v. high BH natal kicks (> several hundred km s^{-1})

Dynamical

Disfavours low-mass clusters

2030s: Einstein Telescope & Cosmic Explorer Concepts

Target sensitivity a factor of > 10 improvement to current advanced detectors

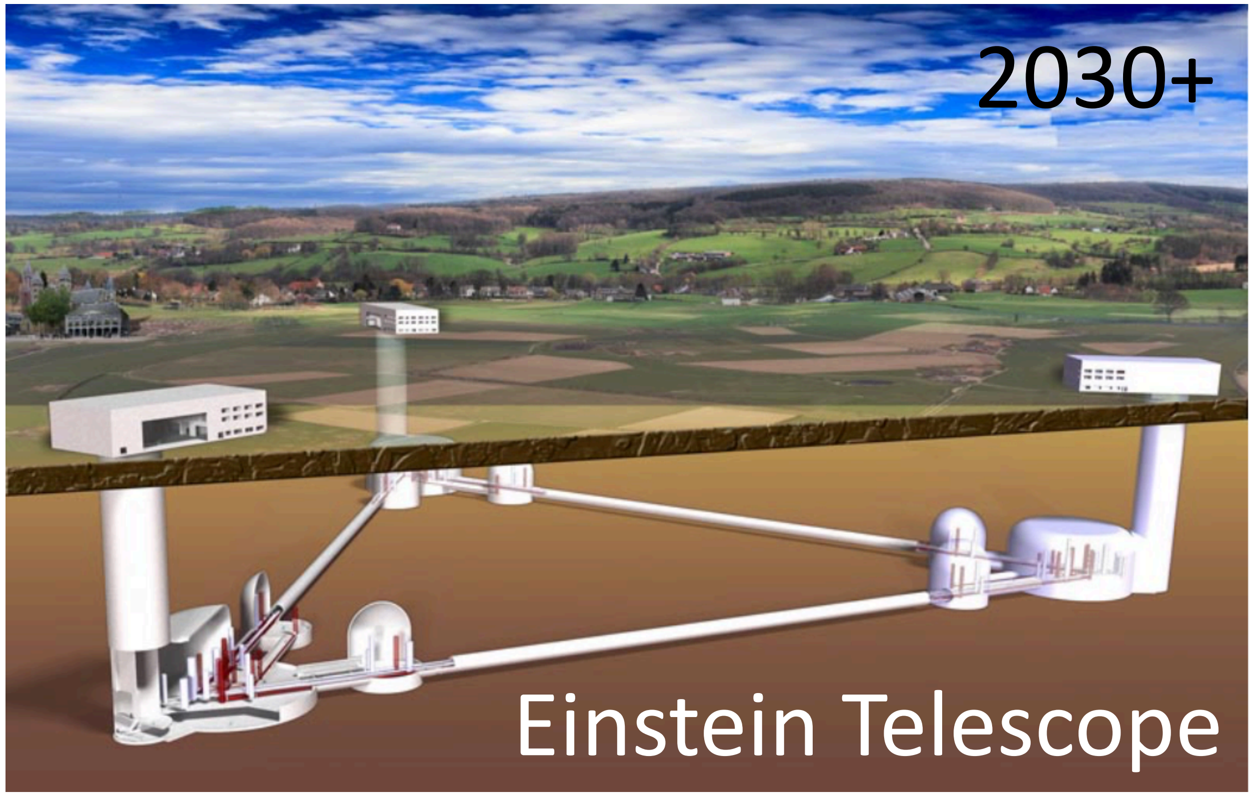

Cosmic Explorer

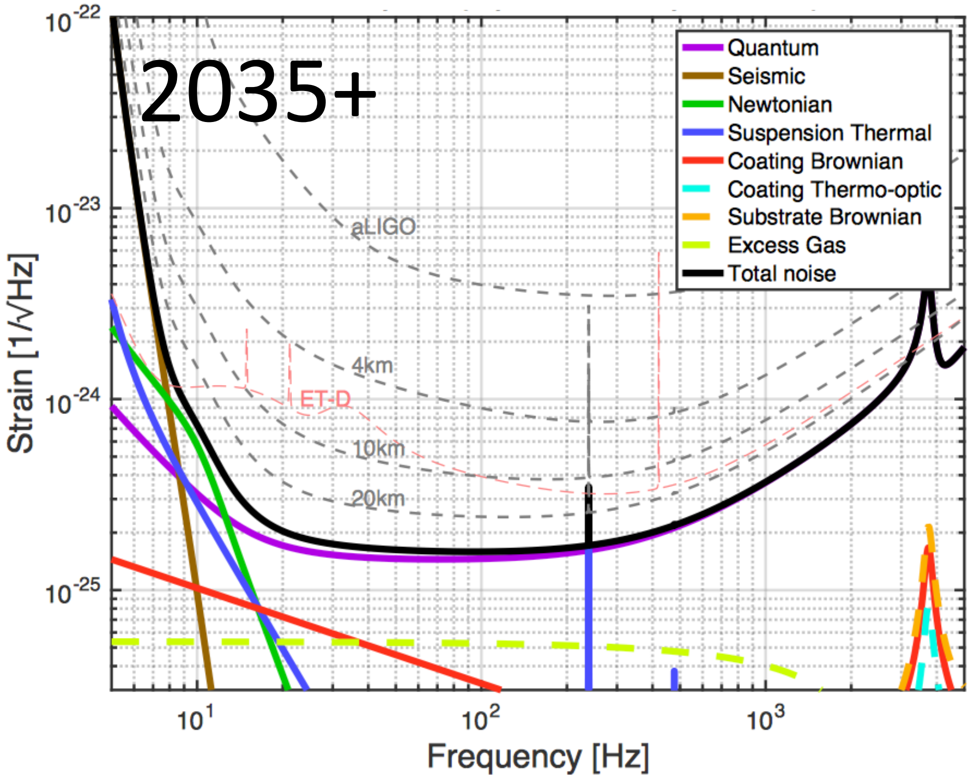

10 km long, Underground, cryogenic
Xylophone configuration, 6 interferometers

Formal Design Study completed in 2011:

http://www.et-gw.eu/etdsdocument

Above ground, 40 km arm length, L configuration, signal grows with length (not most noise sources), room temperature, modest laser improvements

No formal design study yet but in proposal

LSC, arXiv: 1607.08697

Einstein Telescope and Cosmic Explorer have cosmological reach

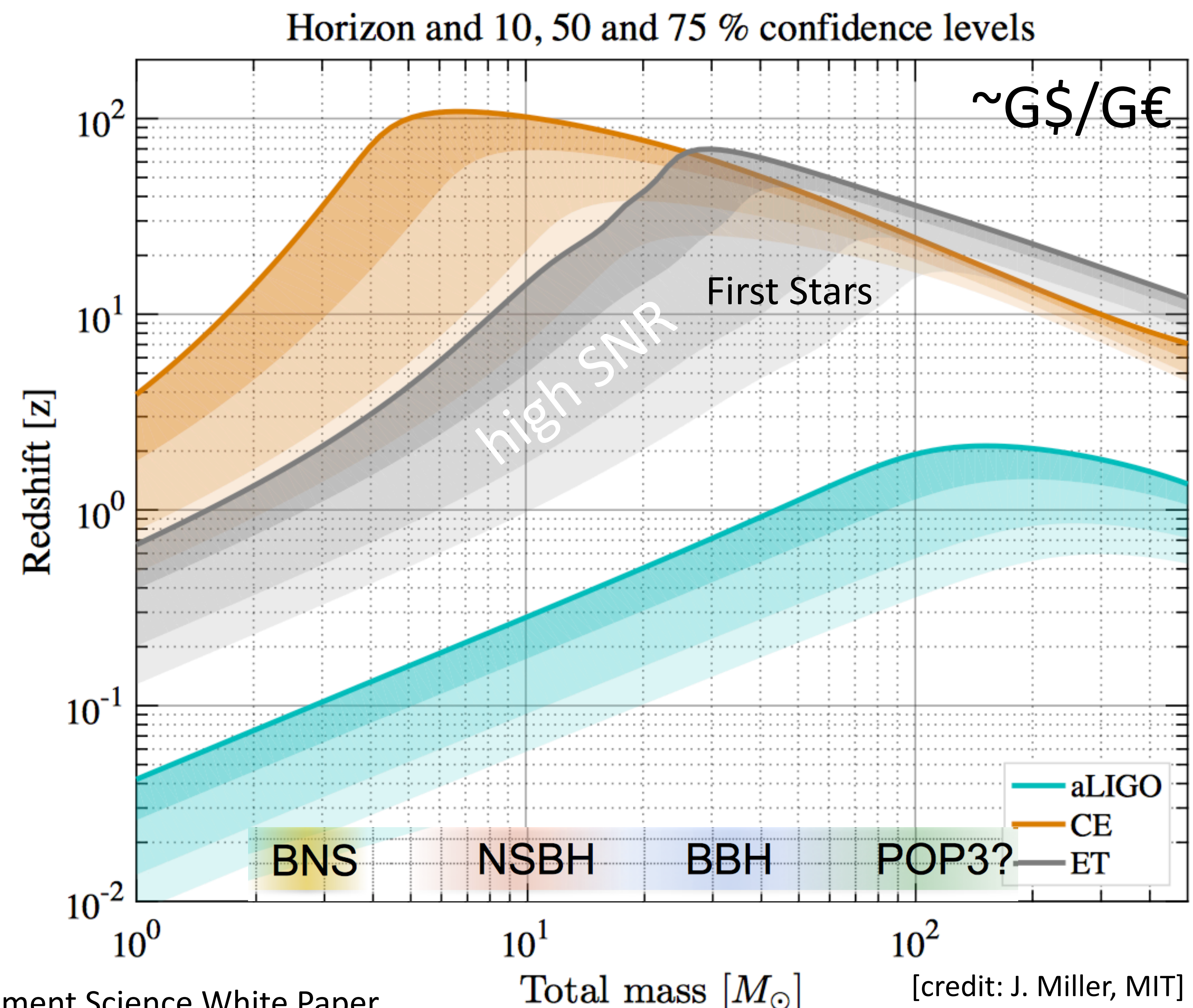

[credit: J. Miller, MIT]

See LSC Instrument Science White Paper
https://dcc.ligo.org/public/0125/T1600119/004/wp2016.pdf

Einstein Telescope and Cosmic Explorer have cosmological reach

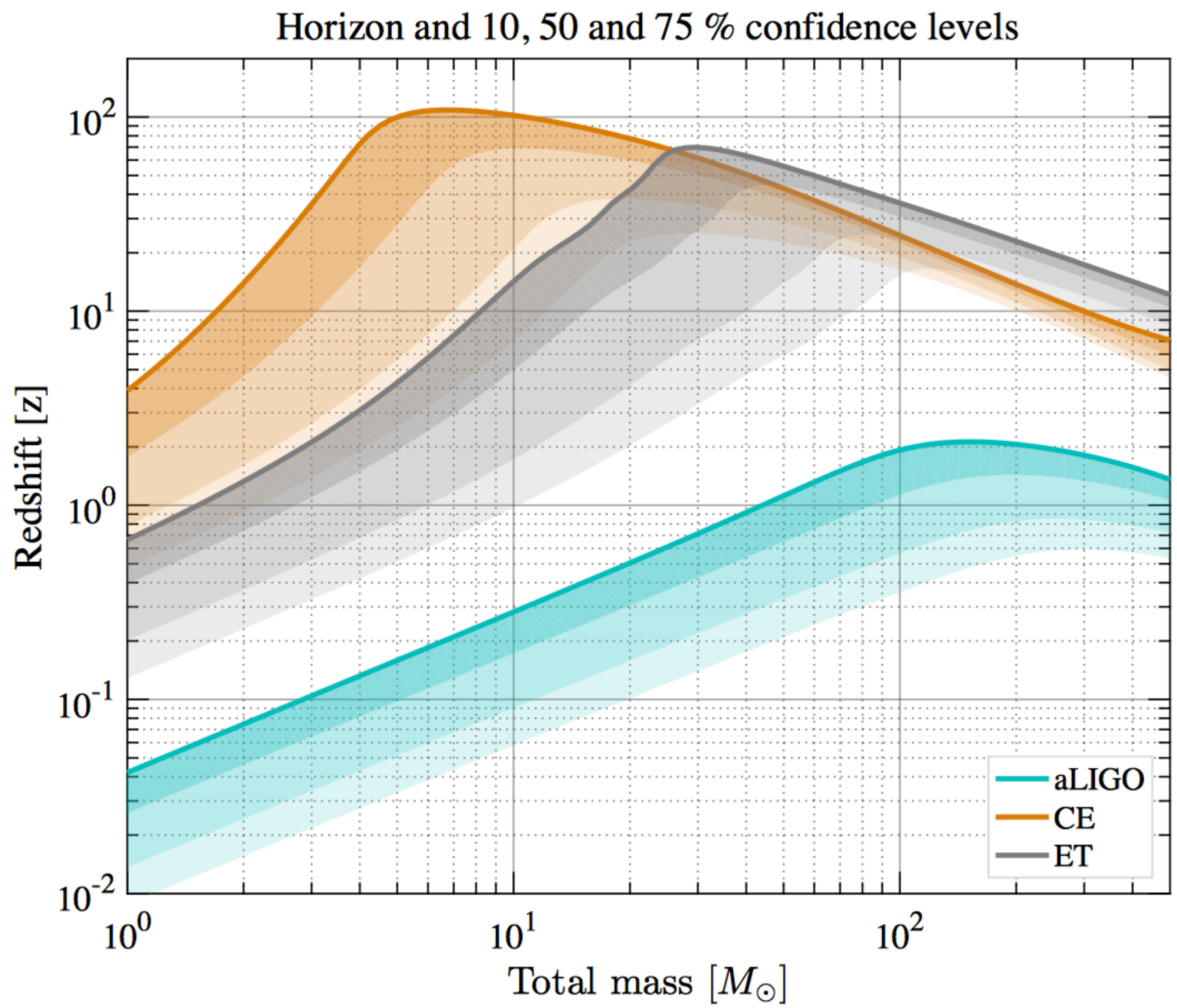

How well can we constrain SFR? Dependence on metallicity

Cosmic (redshift-dependent) Merger Rate?

Mass gaps: NS and BH, intermediate BH desert?

End of lecture 1

Stellar Remnants from Massive Stars

Table 16.4. *End products of stellar evolution as a function of initial mass*

		Final product
Initial mass	He-core mass	Single star
$< 2.3\,M_\odot$	$< 0.45\,M_\odot$	CO white dwarf
$2.3-6\,M_\odot$	$0.5-1.9\,M_\odot$	CO white dwarf
$6-8\,M_\odot$	$1.9-2.1\,M_\odot$	O-Ne-Mg white dwarf or C-deflagration SN?
$8-12\,M_\odot$	$2.1-2.8\,M_\odot$	neutron star
$12-25\,M_\odot$	$2.8-8\,M_\odot$	neutron star
$> 25\,M_\odot$	$> 8\,M_\odot$	black hole

[Tauris and van der Heuvel 2006]

Evolution: self-gravitating gas in hydrostatic equilibrium (virial theorem) — radiative loss of energy causes it to contract and hence, due to release of gravitational potential energy, T ↑ .

Negative heat capacity: while the star tries to cool itself by radiating away energy from its surface, it gets hotter instead of cooler.

Unstable virial theorem: the more it radiates to cool itself, contract ↑, T ↑ and the more it is forced to go on radiating.

Massive Star Evolution: three timescales

Dynamical timescale:

when the hydrostatic equilibrium of a star is disturbed

$$\tau_{\rm dyn} = \sqrt{R^3/GM} \simeq 50 \text{ min } (R/R_\odot)^{3/2}(M/M_\odot)^{-1/2}$$

Kelvin-Helmholtz timescale:

when the thermal equilibrium of a star is disturbed, time taken to emit all of its thermal energy content at its present luminosity

$$\tau_{\rm th} = GM^2/RL \simeq 30 \text{ Myr } (M/M_\odot)^{-2}$$

Nuclear timescale

time needed for the star to exhaust its nuclear fuel reserve ($\propto$ M), at its present fuel consumption rate ($\propto$ L)

$$\tau_{\rm nuc} \simeq 10 \text{ Gyr } (M/M_\odot)^{-2.5}$$

$$R \propto M^{0.5}$$

$$L \propto M^{3.5}$$

Massive Stellar Evolution: Hertzsprung Russell Diagram

Example	t_{dyn}	t_{KH}	t_{nuc}
main-sequence stars			
a) $M = 0.1\,M_\odot$, $L = 10^{-3}\,L_\odot$, $R = 0.15\,R_\odot$	4 min	10^9 yr	10^{12} yr
b) $M = 1\,M_\odot$, $L = 1\,L_\odot$, $R = 1\,R_\odot$	30 min	15×10^6 yr	10^{10} yr
c) $M = 30\,M_\odot$, $L = 2 \times 10^5\,L_\odot$, $R = 20\,R_\odot$	400 min	3×10^3 yr	2×10^6 yr
red giant ($M = 1\,M_\odot$, $L = 10^3\,L_\odot$, $R = 200\,R_\odot$)	50 d	75 yr	
white dwarf ($M = 1\,M_\odot$, $L = 5 \times 10^{-3}\,L_\odot$, $R = 2.6 \times 10^{-3}\,R_\odot$)	7 s	10^{11} yr	
neutron star ($M = 1.4\,M_\odot$, $L = 0.2\,L_\odot$, $R = 10$ km, $T_{eff} = 10^6$ K)	0.1 ms	10^{13} yr	

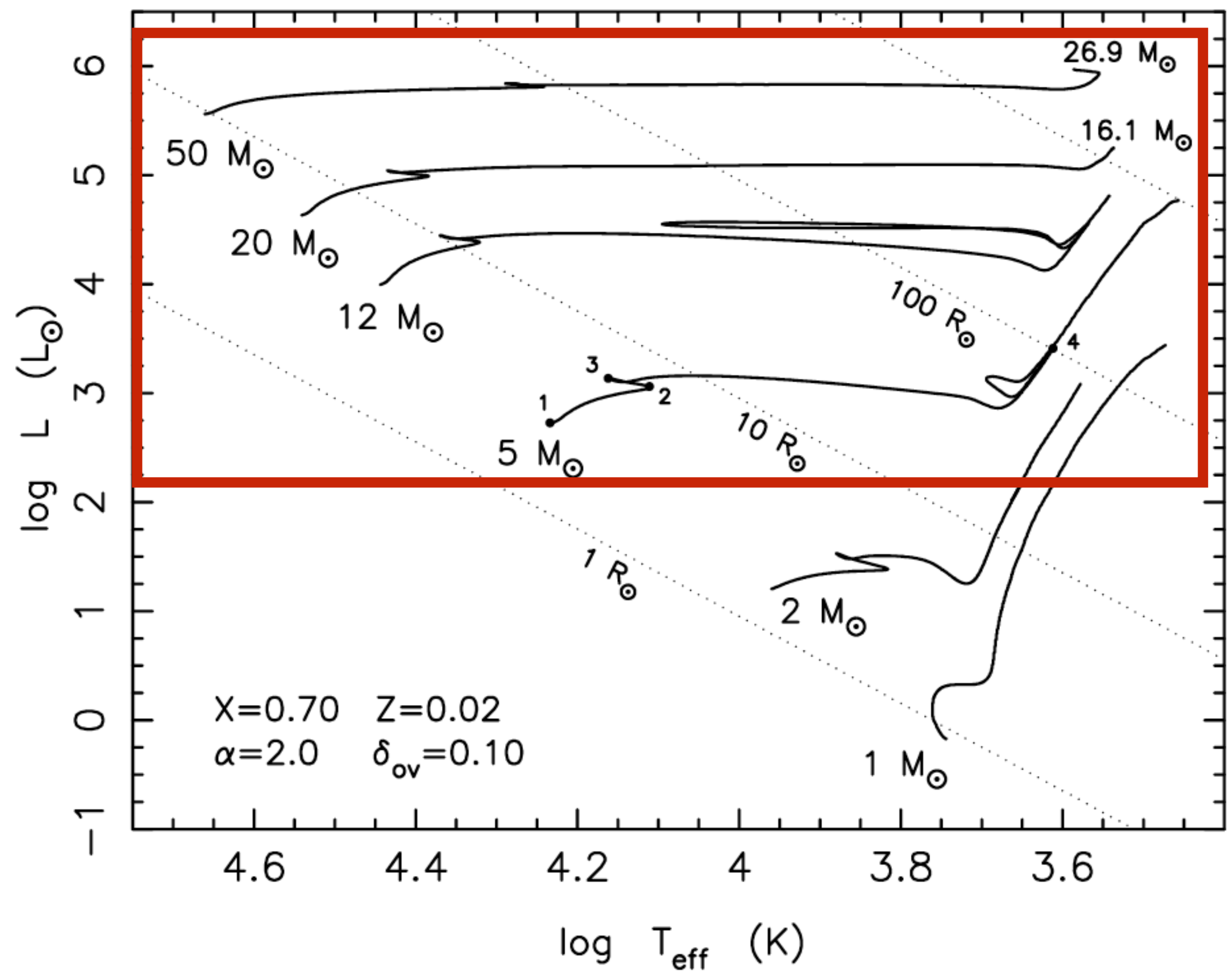

$$L = 4\pi R^2 \sigma T_{\mathrm{eff}}^4$$

Important Evolutionary Stages

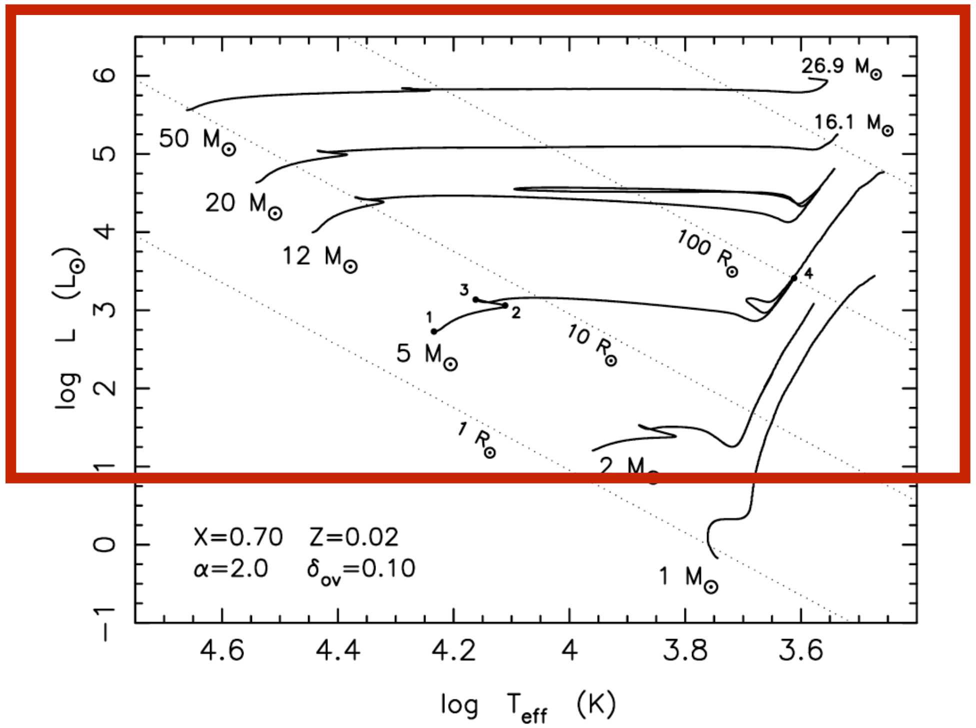

$5\ M_\odot$ ZAMS

1->2. long-lasting phase of core H burning (nuclear timescale).

3. H ignites in a shell around the He core. For massive stars, the entire star briefly contracts causing its central temperature to rise.

4. When the central temperature reaches ~ 10^8 K, core He ignites -> red giant, with a dense core and a very large radius. During He burning, we have a loop in the H-R diagram.

2->4. thermal timescale; helium-burning loop on a (helium) nuclear timescale.

5. During He shell burning, the outer radius expands again and at C ignition the star has become a red supergiant on the asymptotic giant branch (AGB) ⇒ e^- degenerate C core.

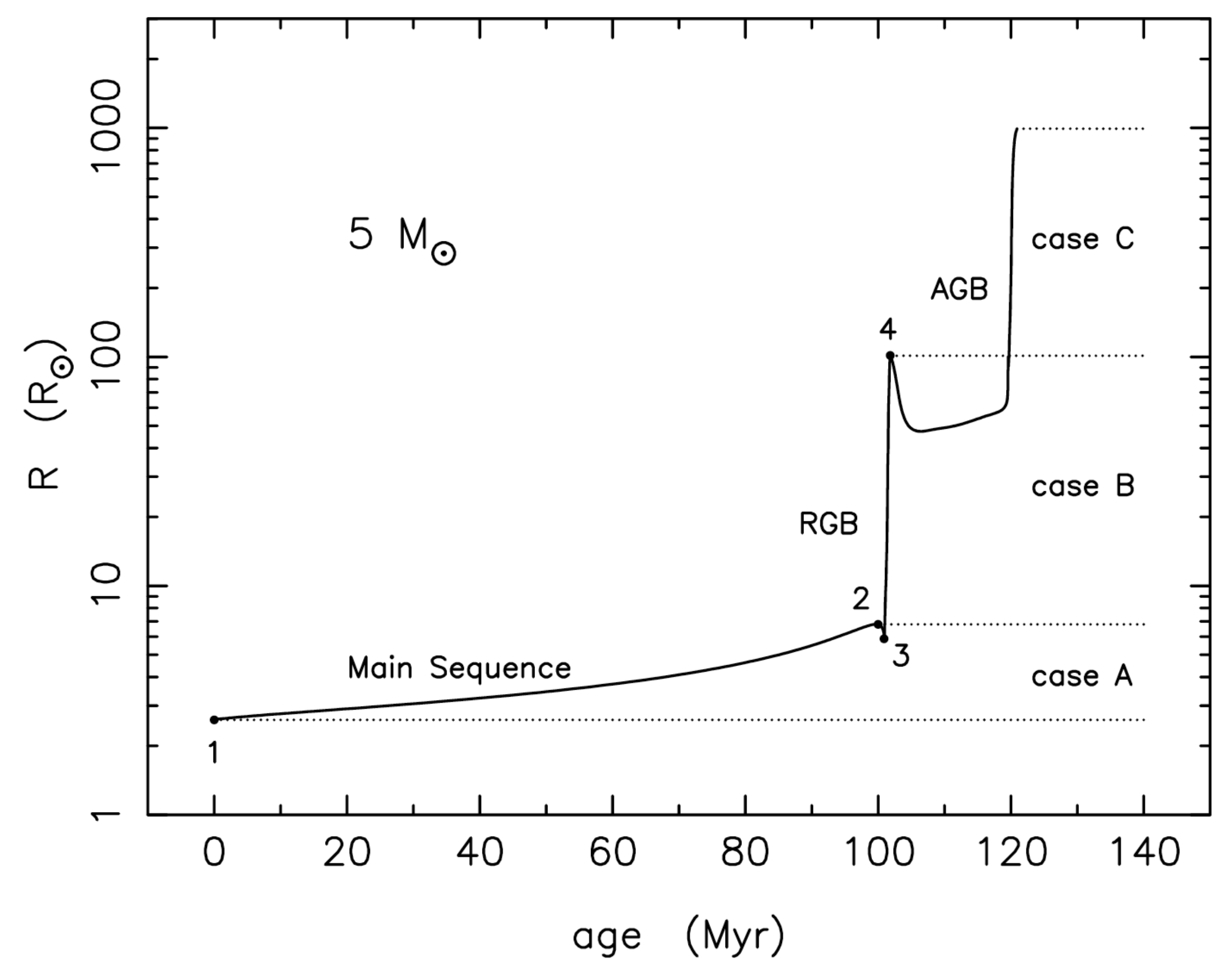

Important Evolutionary Stages

$>$ 10 $_{\odot}$ ZAMS

- Massive stars continue to burn nuclear fuel beyond H and He burning and ultimately form an Fe core.

- Alternation of nuclear burning and contraction phases.

  carbon burning ($T \sim 6 \times 10^8$ K)
  oxygen burning ($T \sim 10^9$ K)
  silicon burning: photodisintegration of complex nuclei, hundreds of reactions ⇒ iron

- form iron core

- iron is the most tightly bound nucleus ⇒ no further energy from nuclear fusion

- iron core surrounded by onion-like shell structure

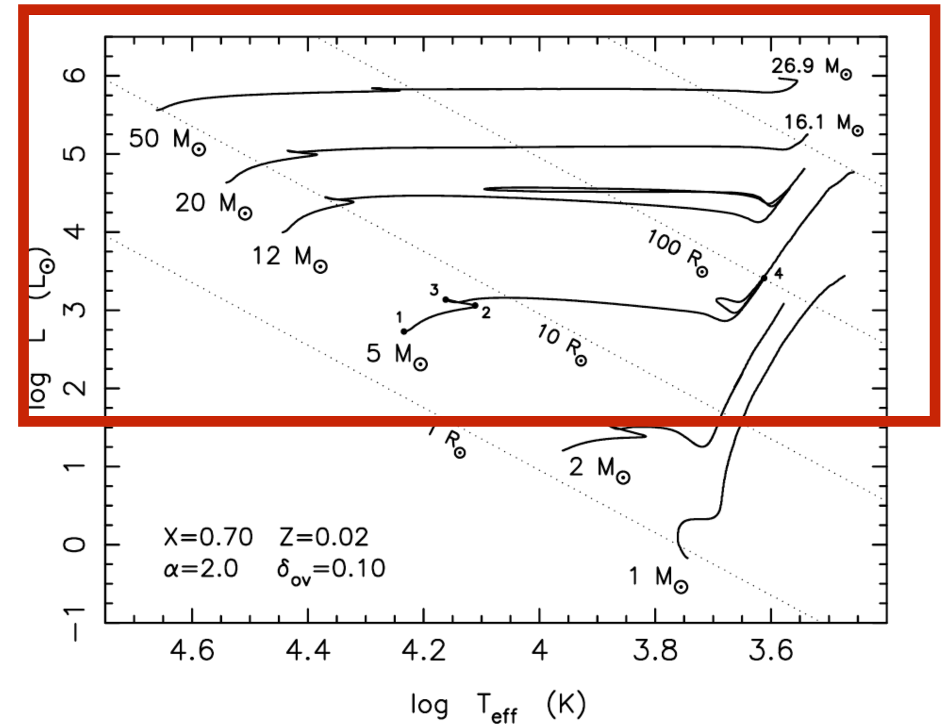

For a 25 solar mass star:

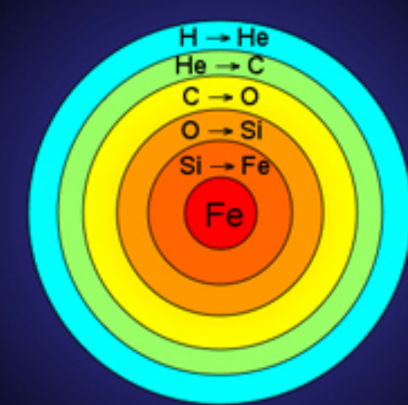

Stage	Duration
H → He	7×10^6 years
He → C	7×10^5 years
C → O	600 years
O → Si	6 months
Si → Fe	1 day
Core Collapse	1/4 second

$$\begin{aligned}
{}^{12}\mathrm{C} + {}^{12}\mathrm{C} &\rightarrow {}^{20}\mathrm{Ne} + {}^{4}\mathrm{He} \\
&\rightarrow {}^{23}\mathrm{Na} + {}^{1}\mathrm{H} \\
&\rightarrow {}^{23}\mathrm{Mg} + \mathrm{n}
\end{aligned}$$

$$\begin{aligned}
{}^{16}\mathrm{O} + {}^{16}\mathrm{O} &\rightarrow {}^{28}\mathrm{Si} + {}^{4}\mathrm{He} \\
&\rightarrow {}^{31}\mathrm{P} + {}^{1}\mathrm{H} \\
&\rightarrow {}^{31}\mathrm{S} + \mathrm{n} \\
&\rightarrow {}^{30}\mathrm{S} + 2\,{}^{1}\mathrm{H} \\
&\rightarrow {}^{24}\mathrm{Mg} + {}^{4}\mathrm{He} + {}^{4}\mathrm{He}
\end{aligned}$$

Step 1 — GW: how many? how far?

[LIGO Scientific and Virgo Collaborations (LVC), Living Reviews in Relativity 19, 1, 2016]

Epoch			2015 – 2016	2016 – 2017	2018 – 2019	2020+	2024+
Planned run duration			4 months	9 months	12 months	(per year)	(per year)
Expected burst range/Mpc		LIGO	40 – 60	60 – 75	75 – 90	105	105
		Virgo	—	20 – 40	40 – 50	40 – 70	80
		KAGRA	—	—	—	—	100
Expected BNS range/Mpc		LIGO	40 – 80	80 – 120	120 – 170	190	190
		Virgo	—	20 – 65	65 – 85	65 – 115	125
		KAGRA	—	—	—	—	140
Achieved BNS range/Mpc		LIGO	60 – 80	*60 – 100*	—	—	—
		Virgo	—	*25 – 30*	—	—	—
		KAGRA	—	—	—	—	—
Estimated BNS detections			0.002 – 2	0.007 – 30	0.04 – 100	0.1 – 200	0.4 – 400
Actual BNS detections			0	—	—	—	—
90% CR	% within	5 deg^2	< 1	1 – 5	1 – 4	3 – 7	23 – 30
		20 deg^2	< 1	7 – 14	12 – 21	14 – 22	65 – 73
	median/deg^2		460 – 530	230 – 320	120 – 180	110 – 180	9 – 12
Searched area	% within	5 deg^2	4 – 6	15 – 21	20 – 26	23 – 29	62 – 67
		20 deg^2	14 – 17	33 – 41	42 – 50	44 – 52	87 – 90

Part 2 — GW mHz regime (entirely new in 2030s!): Laser Interferometer Space Antenna

ESA L3 selected (06/17), joint with NASA, 2034+

Three spacecraft in △, earth-trailing,
2.5 Mkm arms, 6 laser links
4 year mission (10 yr goal),
Timing measurement between masses in space

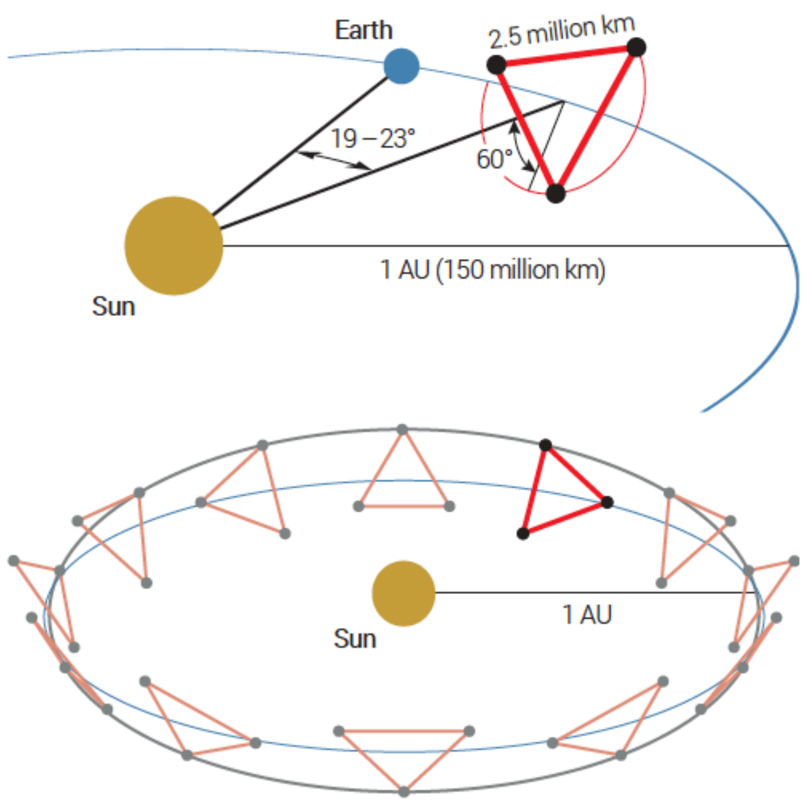

see https://www.elisascience.org/files/publications/LISA_L3_20170120.pdf, arXiv: 1702.00786

Rich diversity of mHz GW sources with LISA

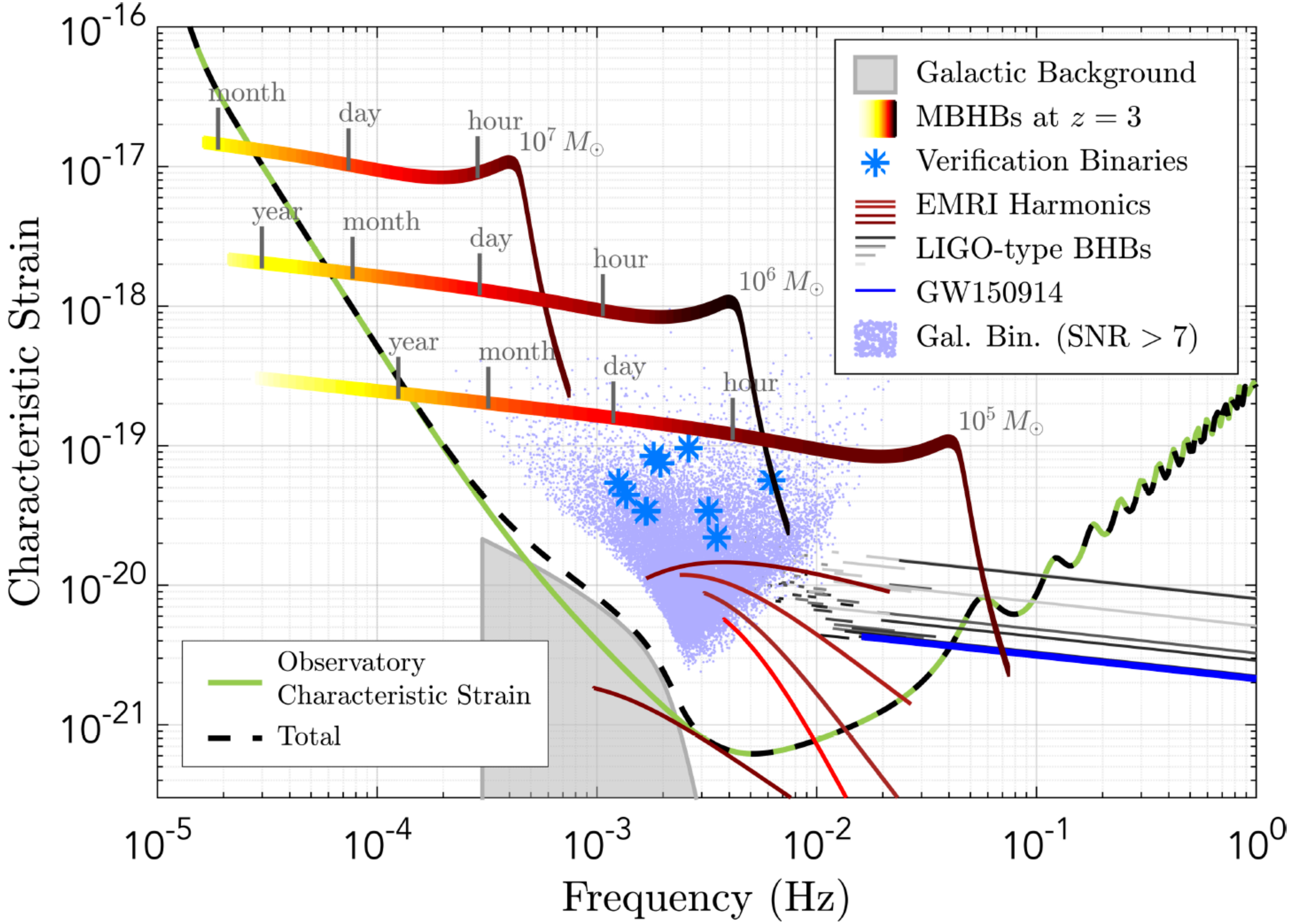

1. Trace the origin, growth & merger history of massive BH (MBH) mergers

Seed Formation
for 10^4 - 10^5 $M_\odot$ BH

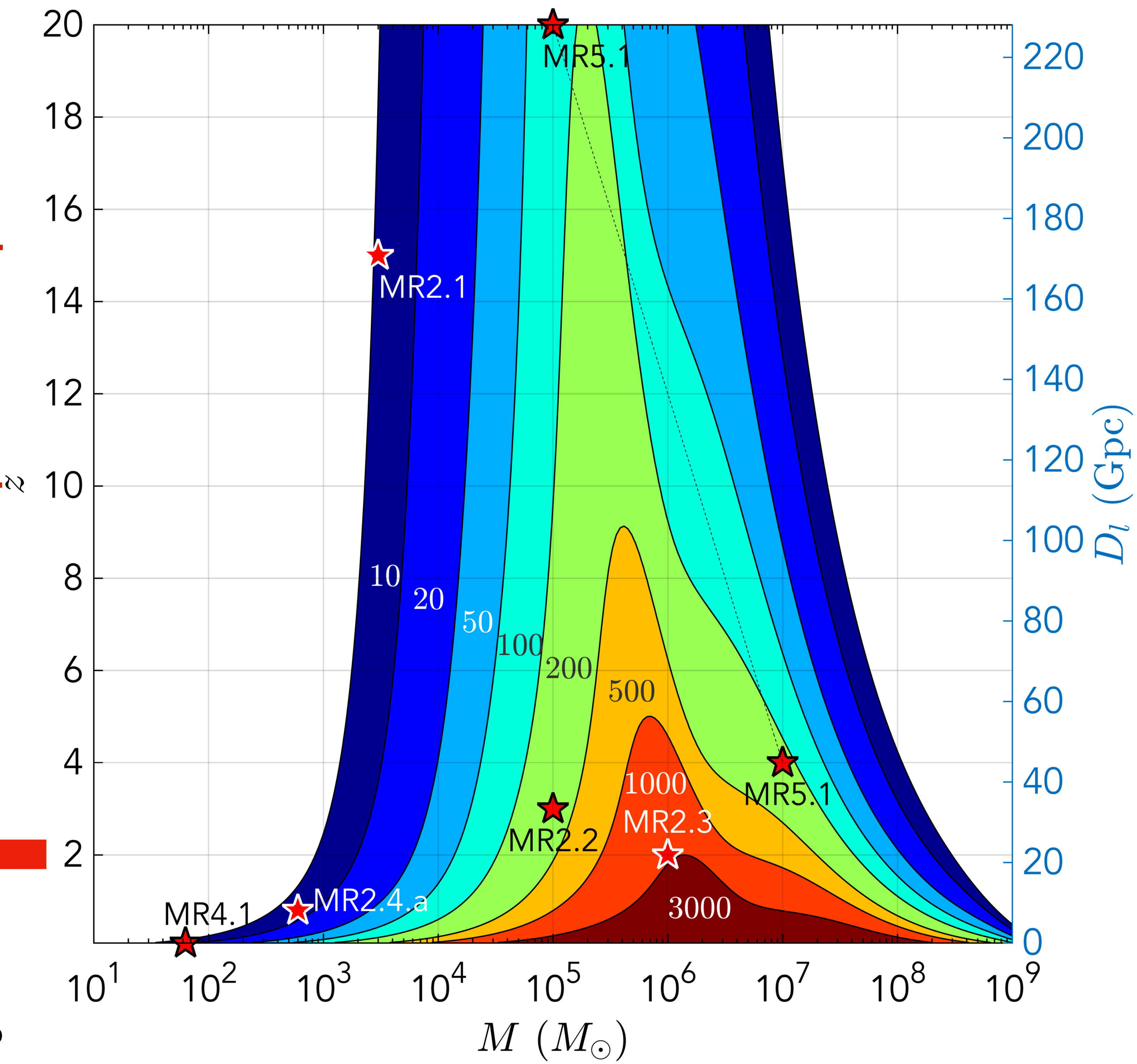

z < 9

peak of
star formation
⇒ EM counterpart?

Wealth of source information from GWs alone

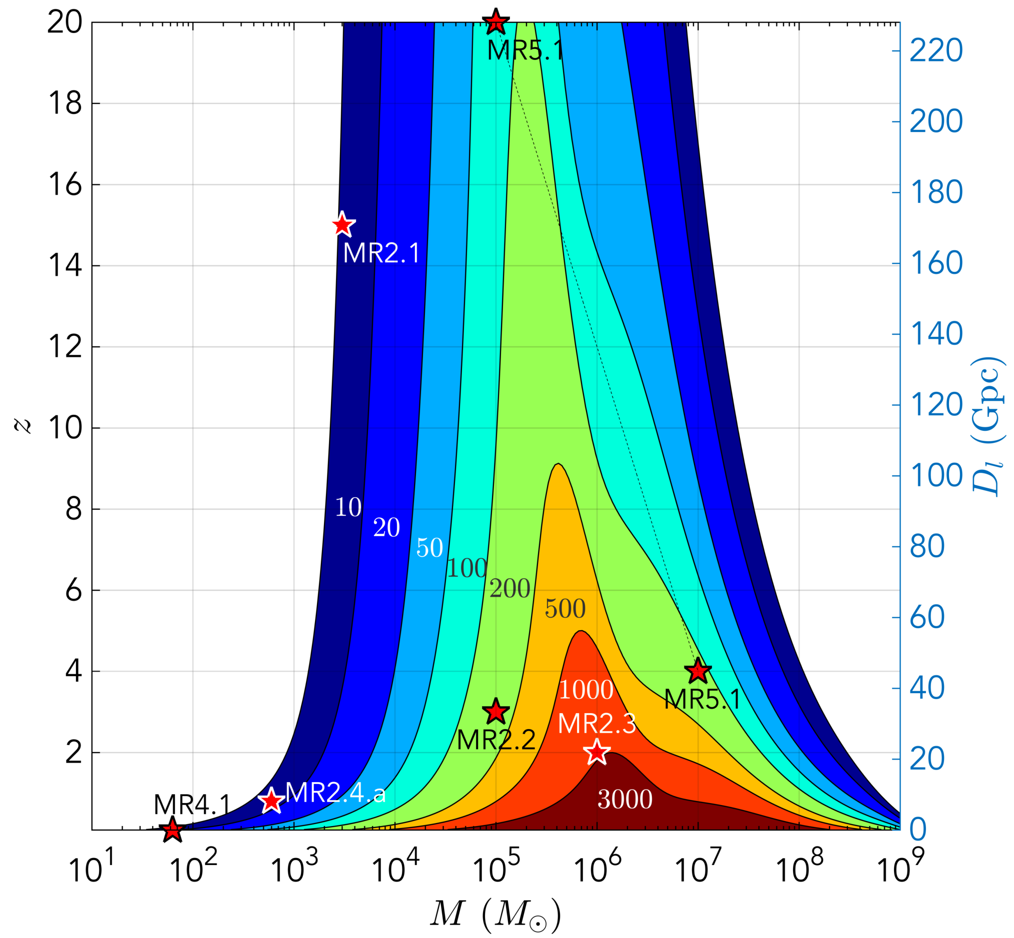

- 100+ detections with sky localization to 10 deg.[2] and individual masses to 1%
- 50 systems with primary and secondary spins determined to 0.01 and 0.1.
- 50 systems with spin direction determined to within 10 deg.

[Klein et al., Phys. Rev. D 93, 024003 (2016)]

Insights into MBH formation:

MBH seeding mechanism (heavy vs. light)
Metallicity feedback
Accretion efficiency (Eddington?)
Accretion geometry

Wealth of source information from GWs alone

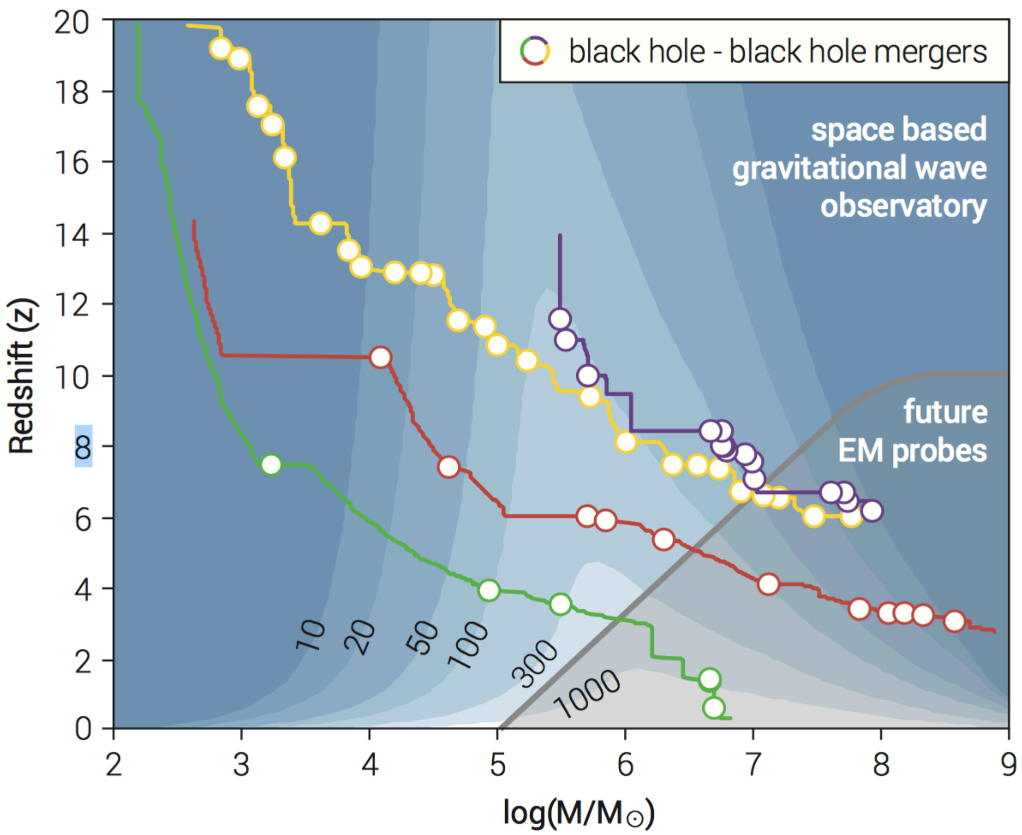

[eLISA consortium, arXiv:1305.5720]

- 100+ detections with sky localization to 10 deg.^{2} and individual masses to 1%
- 50 systems with primary and secondary spins determined to 0.01 and 0.1.
- 50 systems with spin direction determined within 10 deg.

[Klein et al., Phys. Rev. D 93, 024003 (2016)]

<u>Associated EM signature ?:</u>

Simulations (MHD, hydro) show significant mass inflow of the binary + cavity in a circumbinary disk.

2. A hundred resolvable stellar-mass BBHs by space-based GW detectors before they enter LIGO- Virgo band

[Sesana 2016; see also Brevik et al. 2016, Klein et al. 2016, Vitale 2016]

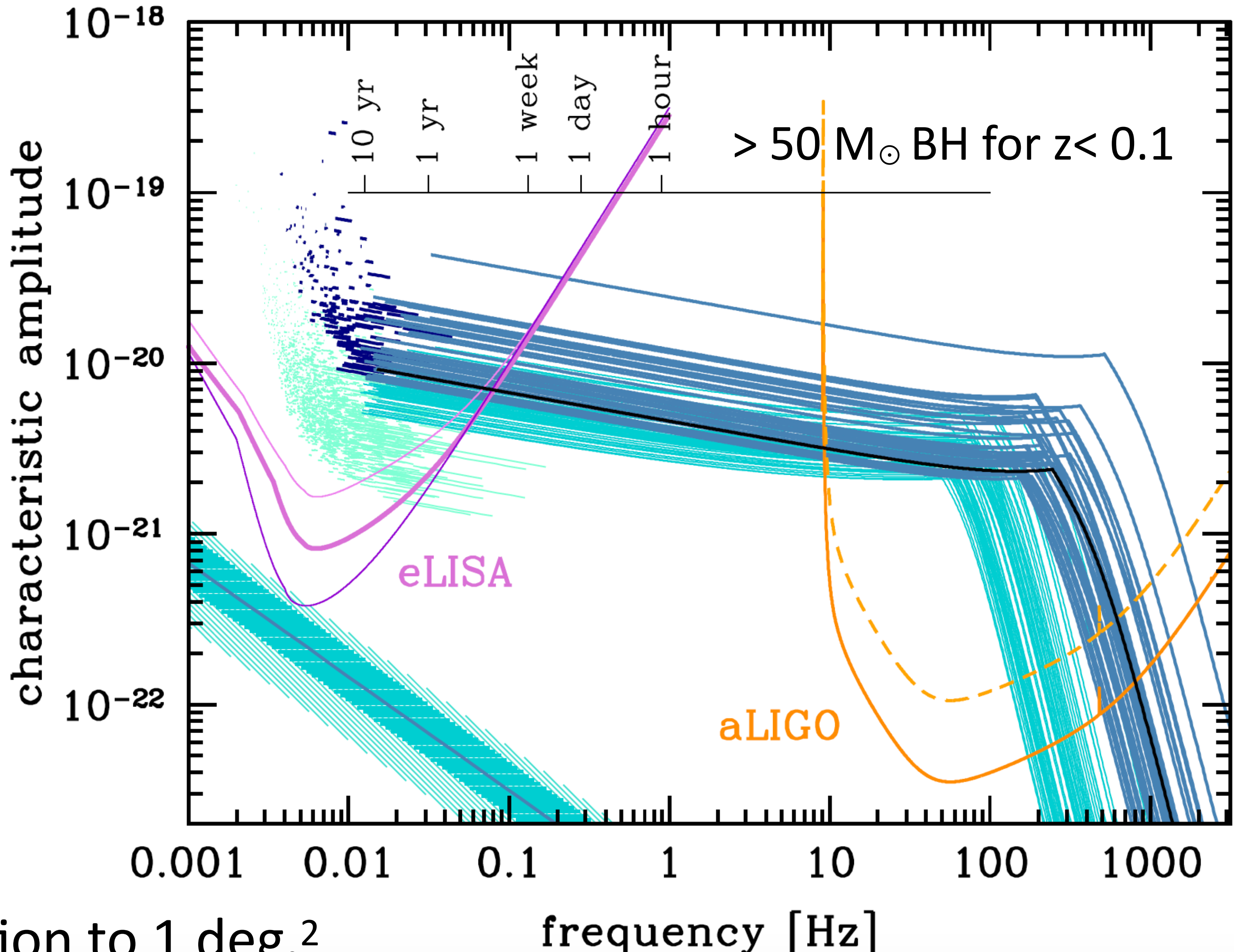

- sky localization to 1 deg.^{2}
- time of coalescence to 1 min
- mass and eccentricity to better than 0.01 and 0.001

3. Extreme-mass ratio inspirals for fundamental physics and astrophysics

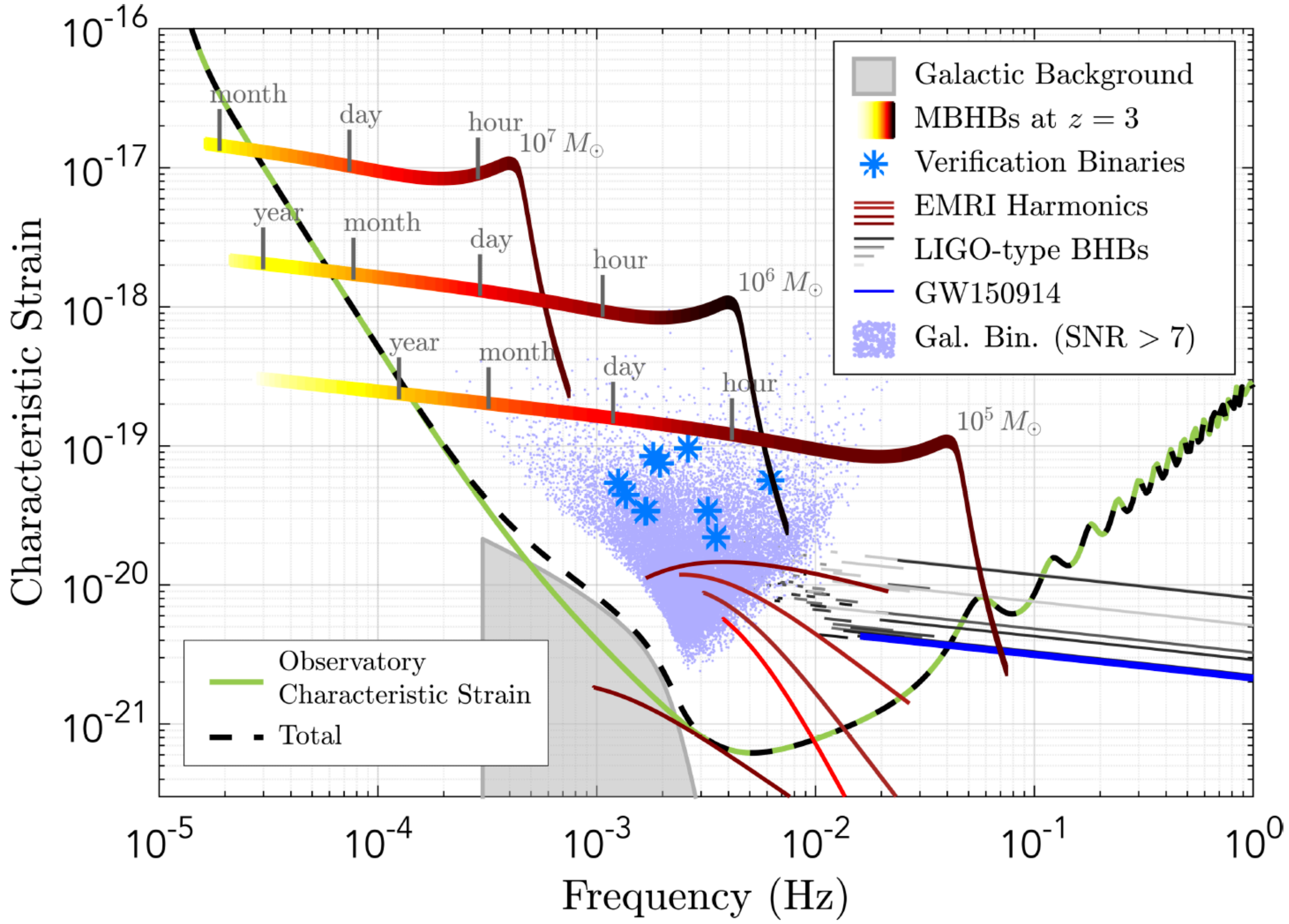

10 - 60 $M_\odot$ BHs into 10^5 - 10^6 $M_\odot$ BH out to z ~ 4 with SNR ≥ 20.

1-1000 detections yr^{-1}.

Sky localization and distance to 10 deg.^{2} and better than 10%.

MBH and compact object masses to 0.01 and 0.001%.

MBH spin to better than 0.001.

Eccentricity and deviation from Kerr Quadruple moment to better than 0.0001 and 0.001.

[Babak et al. Phys. Rev. D 95, 103012 (2017)]

Mass distn. of stellar remnants at galactic centers.
Mass segregation & relaxation for stellar populations.
Extreme Kerr Spacetimes: 10^3-10^5 cycles.

4. Galactic compact object binaries

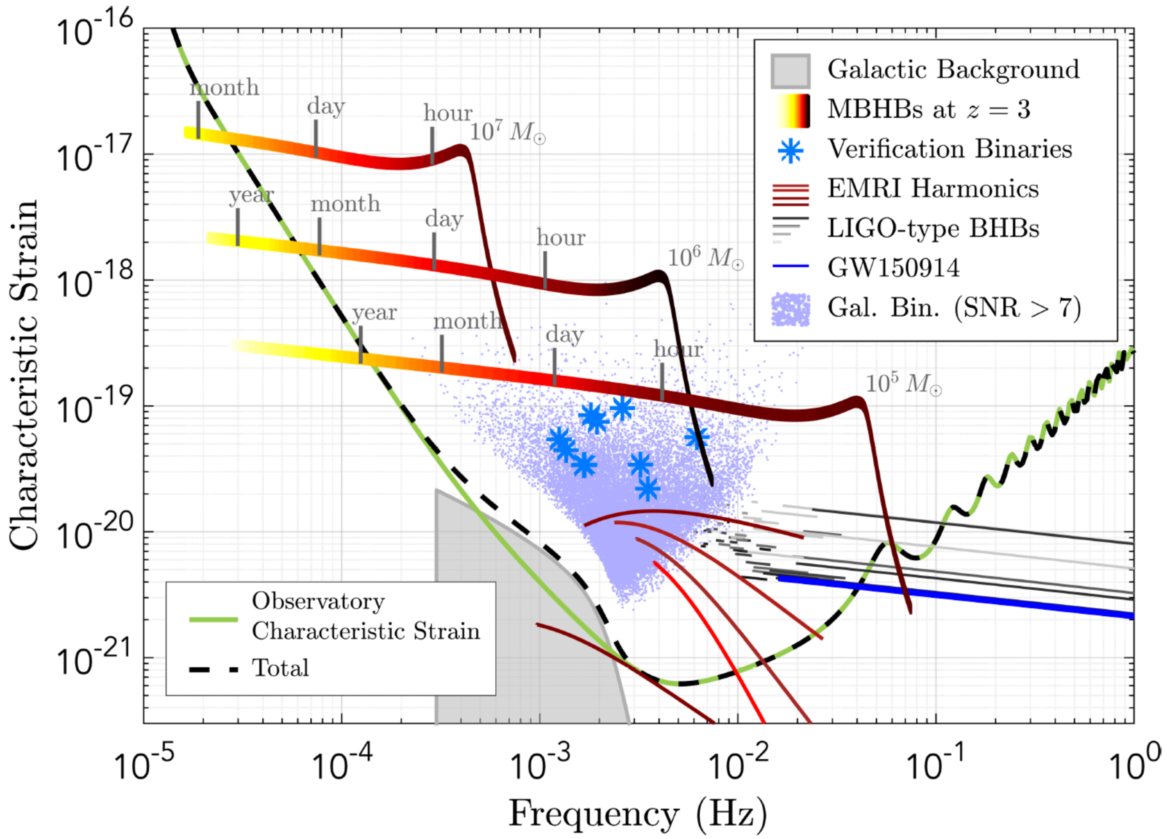

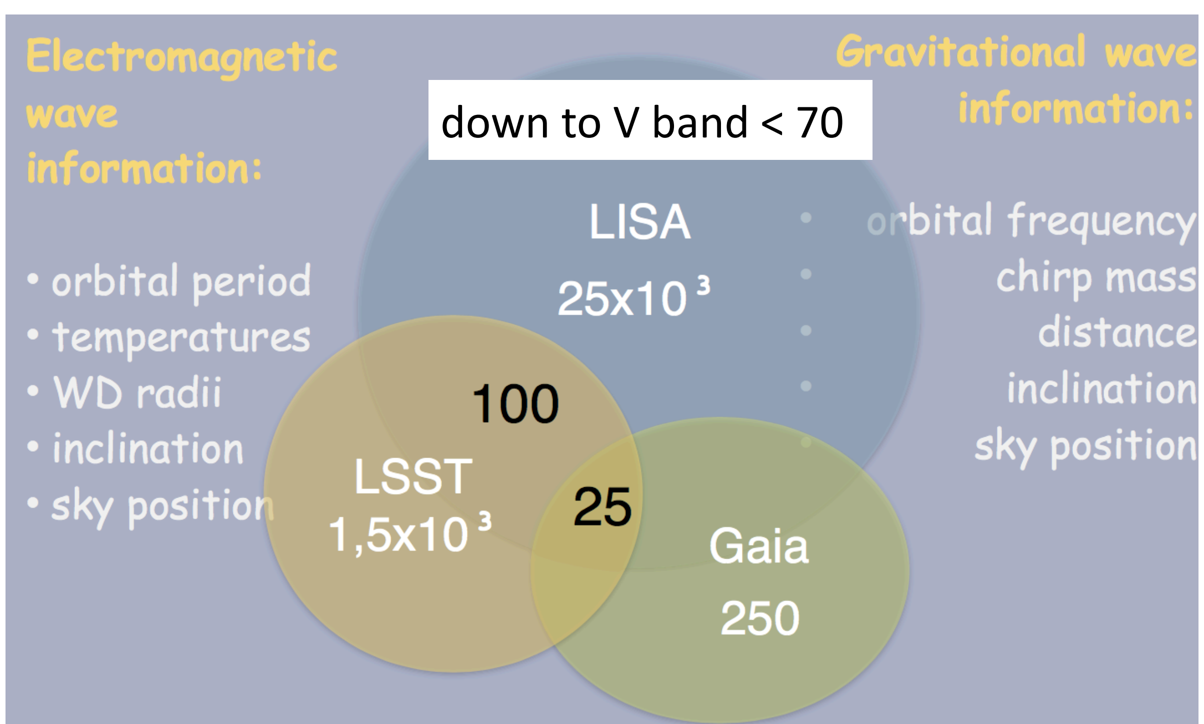

[figure courtesy of E. Rossi, Korol et al. 2017]

~25 000 resolvable Galactic binaries (detached white dwarfs and AM CVns, NS-NS, NS-WD, NS-BH)

For ~5000 systems, measure mass, distance, sky location with $dP/P < 10^{-5}$ within 15 kpc

For ~500 systems, measure sky location to 1 deg.^{2}

For ~100 systems, measure sky location to 1 deg.^{2} with Pdot to better than 10%.

Part I: Stellar Evolution 101 (a compact object's perspective!)

Stellar Remnants from Massive Stars

Table 16.4. *End products of stellar evolution as a function of initial mass*

		Final product
Initial mass	He-core mass	Single star
$< 2.3\,M_\odot$	$< 0.45\,M_\odot$	CO white dwarf
$2.3 - 6\,M_\odot$	$0.5 - 1.9\,M_\odot$	CO white dwarf
$6 - 8\,M_\odot$	$1.9 - 2.1\,M_\odot$	O-Ne-Mg white dwarf or C-deflagration SN?
$8 - 12\,M_\odot$	$2.1 - 2.8\,M_\odot$	neutron star
$12 - 25\,M_\odot$	$2.8 - 8\,M_\odot$	neutron star
$> 25\,M_\odot$	$> 8\,M_\odot$	black hole

[Tauris and van der Heuvel 2006]

Evolution: self-gravitating gas in hydrostatic equilibrium (virial theorem) — radiative loss of energy causes it to contract and hence, due to release of gravitational potential energy, T ↑ .

Negative heat capacity: while the star tries to cool itself by radiating away energy from its surface, it gets hotter instead of cooler.

Unstable virial theorem: the more it radiates to cool itself, contract ↑, T ↑ and the more it is forced to go on radiating.

Massive Star Evolution: three timescales

Dynamical timescale:

when the hydrostatic equilibrium of a star is disturbed

$$\tau_{\rm dyn} = \sqrt{R^3/GM} \simeq 50 \text{ min } (R/R_\odot)^{3/2}(M/M_\odot)^{-1/2}$$

Kelvin-Helmholtz timescale:

when the thermal equilibrium of a star is disturbed, time taken to emit all of its thermal energy content at its present luminosity

$$\tau_{\rm th} = GM^2/RL \simeq 30 \text{ Myr } (M/M_\odot)^{-2}$$

Nuclear timescale

time needed for the star to exhaust its nuclear fuel reserve ($\propto$ M), at its present fuel consumption rate ($\propto$ L)

$$\tau_{\rm nuc} \simeq 10 \text{ Gyr } (M/M_\odot)^{-2.5}$$

$$R \propto M^{0.5}$$

$$L \propto M^{3.5}$$

Massive Stellar Evolution: Hertzsprung Russell Diagram

Example	t_{dyn}	t_{KH}	t_{nuc}
main-sequence stars			
a) $M = 0.1\,M_\odot$, $L = 10^{-3}\,L_\odot$, $R = 0.15\,R_\odot$	4 min	10^9 yr	10^{12} yr
b) $M = 1\,M_\odot$, $L = 1\,L_\odot$, $R = 1\,R_\odot$	30 min	15×10^6 yr	10^{10} yr
c) $M = 30\,M_\odot$, $L = 2 \times 10^5\,L_\odot$, $R = 20\,R_\odot$	400 min	3×10^3 yr	2×10^6 yr
red giant ($M = 1\,M_\odot$, $L = 10^3\,L_\odot$, $R = 200\,R_\odot$)	50 d	75 yr	
white dwarf ($M = 1\,M_\odot$, $L = 5 \times 10^{-3}\,L_\odot$, $R = 2.6 \times 10^{-3}\,R_\odot$)	7 s	10^{11} yr	
neutron star ($M = 1.4\,M_\odot$, $L = 0.2\,L_\odot$, $R = 10\,\mathrm{km}$, $T_{eff} = 10^6\,\mathrm{K}$)	0.1 ms	10^{13} yr	

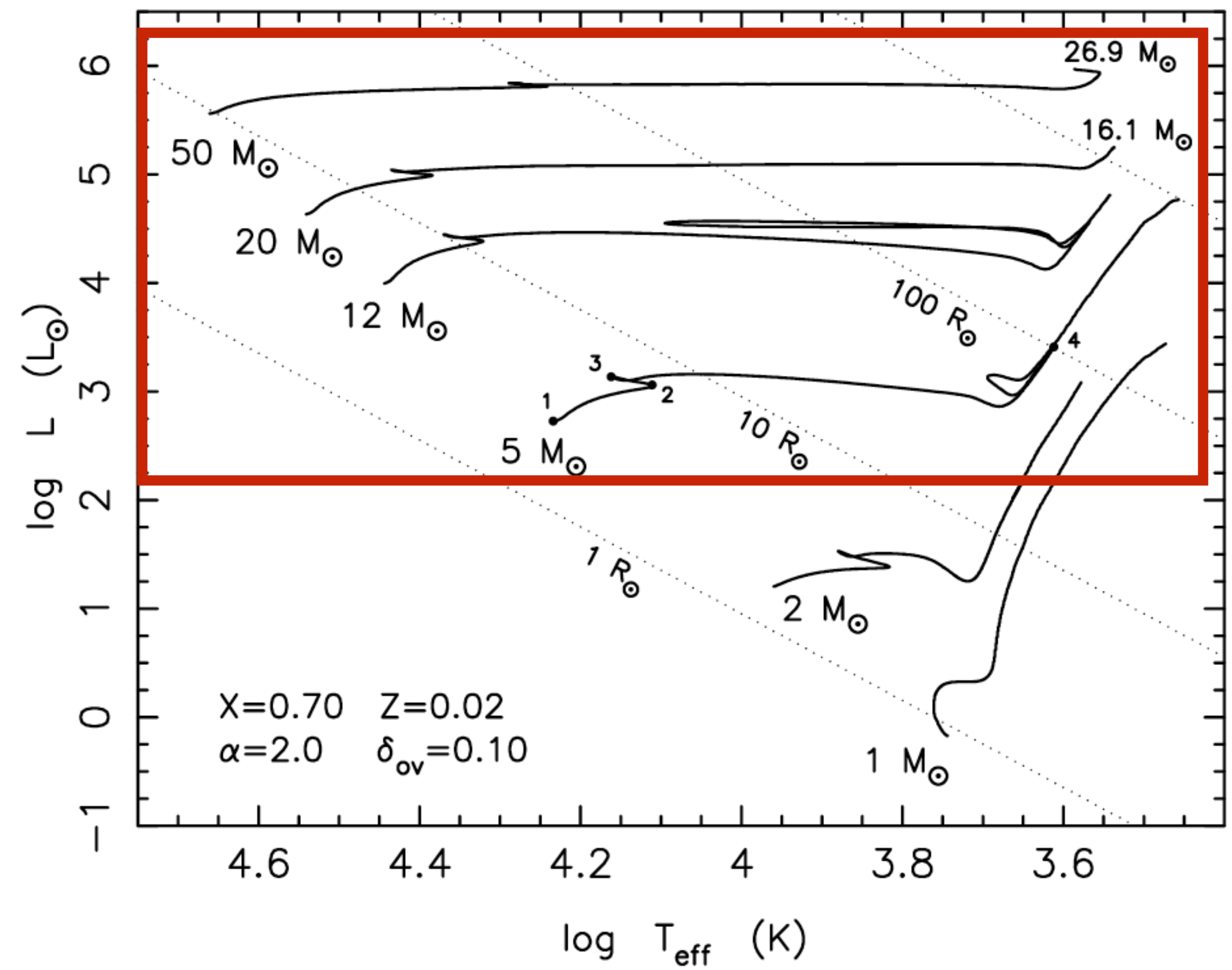

$$L = 4\pi R^2 \sigma T_{\mathrm{eff}}^4$$

Important Evolutionary Stages

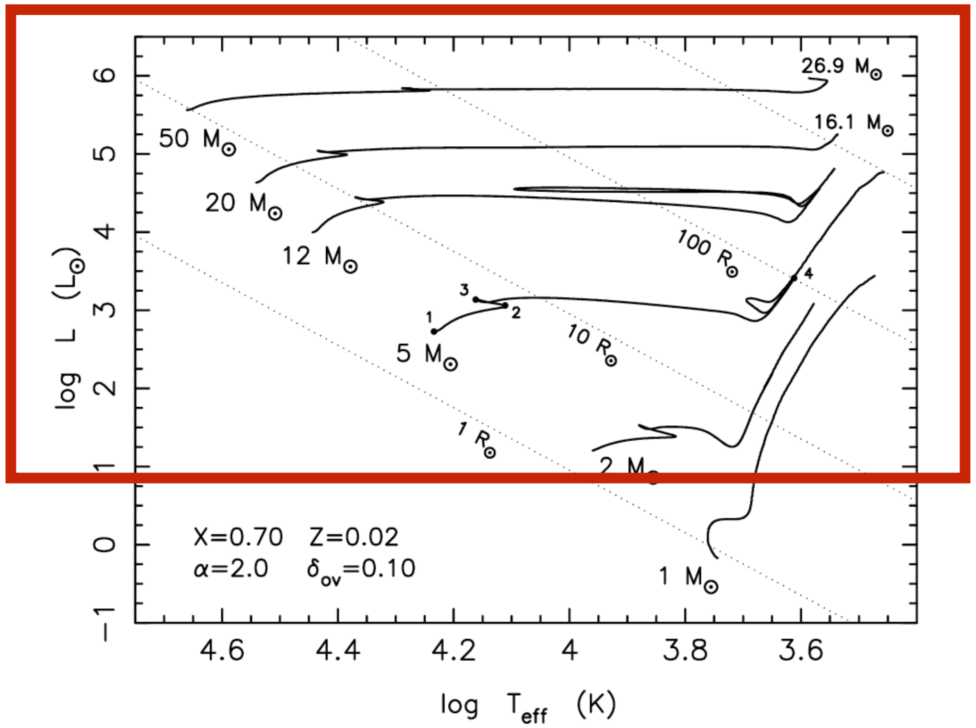

5 M ☉ ZAMS

1->2. long-lasting phase of core H burning (nuclear timescale).

3. H ignites in a shell around the He core. For massive stars, the entire star briefly contracts causing its central temperature to rise.

4. When the central temperature reaches ~ 10^8 K, core He ignites -> red giant, with a dense core and a very large radius. During He burning, we have a loop in the H-R diagram.

2->4. thermal timescale; helium-burning loop on a (helium) nuclear timescale.

5. During He shell burning, the outer radius expands again and at C ignition the star has become a red supergiant on the asymptotic giant branch (AGB) ⇒ e^- degenerate C core.

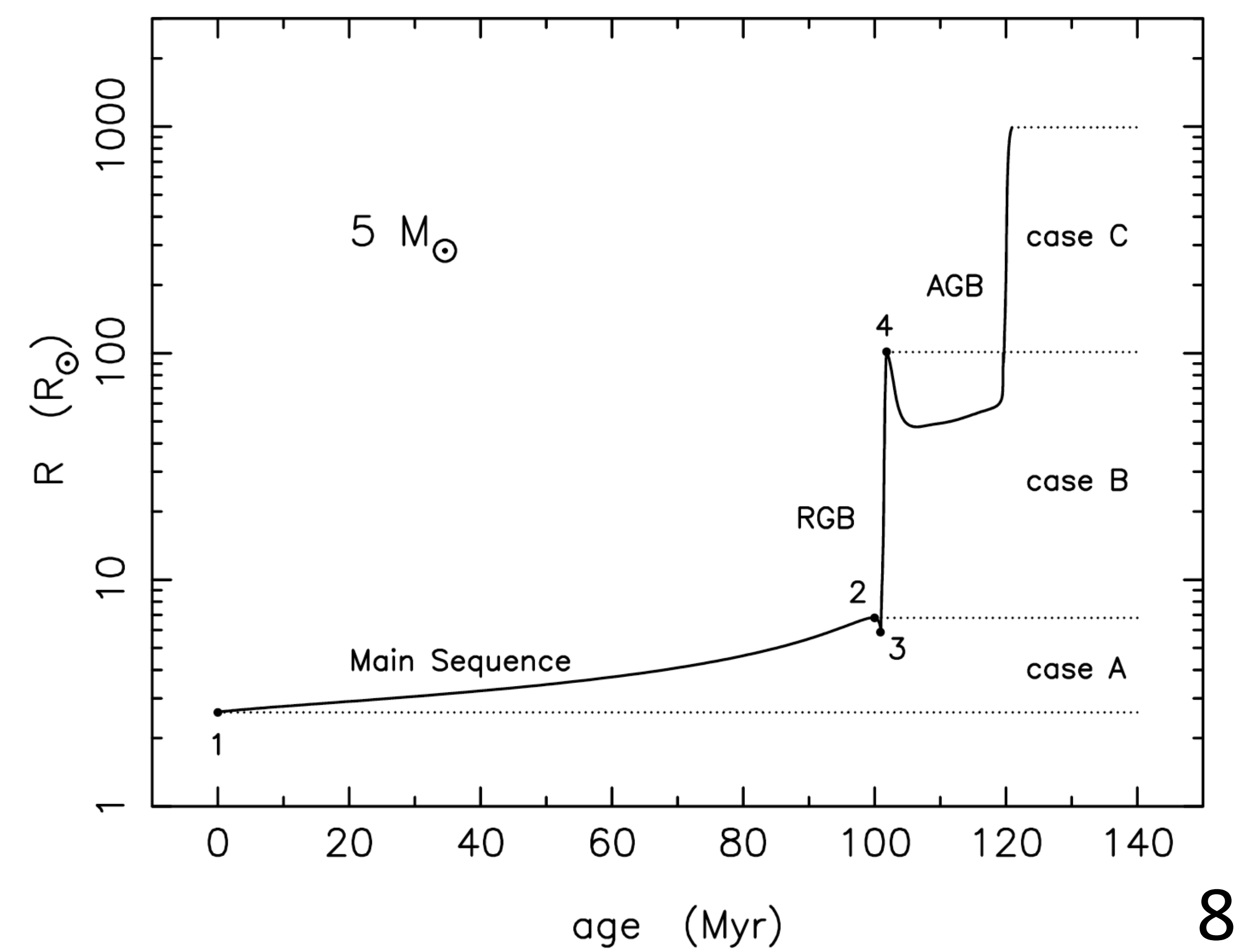

Important Evolutionary Stages

<u>> 10 $_{\odot}$ ZAMS</u>

- Massive stars continue to burn nuclear fuel beyond H and He burning and ultimately form an Fe core.

- Alternation of nuclear burning and contraction phases.

  carbon burning ($T \sim 6 \times 10^8$ K)
  oxygen burning ($T \sim 10^9$ K)
  silicon burning: photodisintegration of complex nuclei, hundreds of reactions ⇒ iron

- form iron core

- iron is the most tightly bound nucleus ⇒ no further energy from nuclear fusion

- iron core surrounded by onion-like shell structure

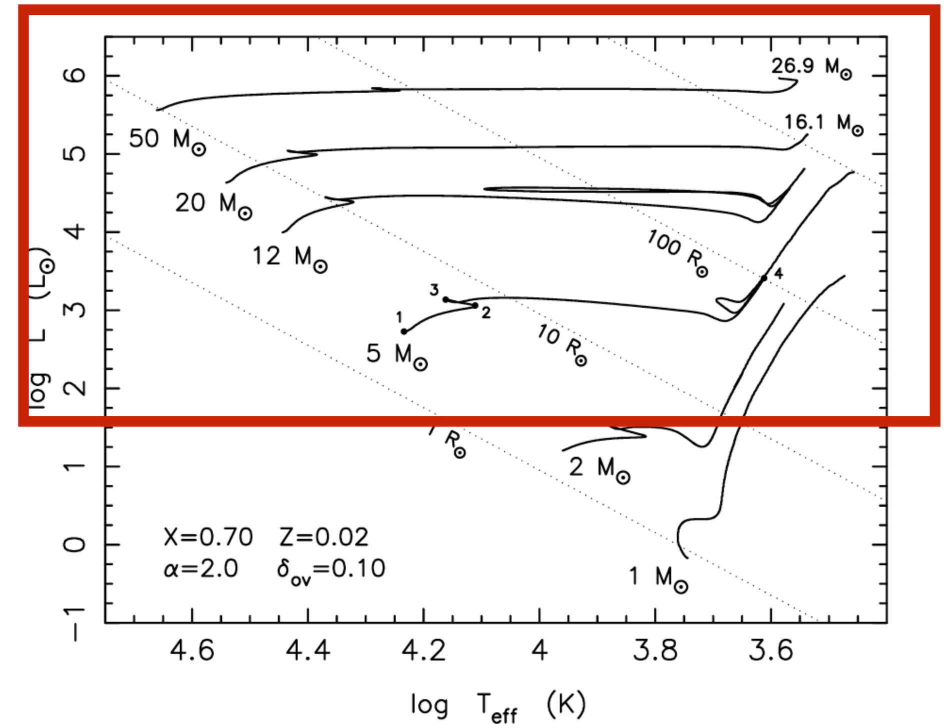

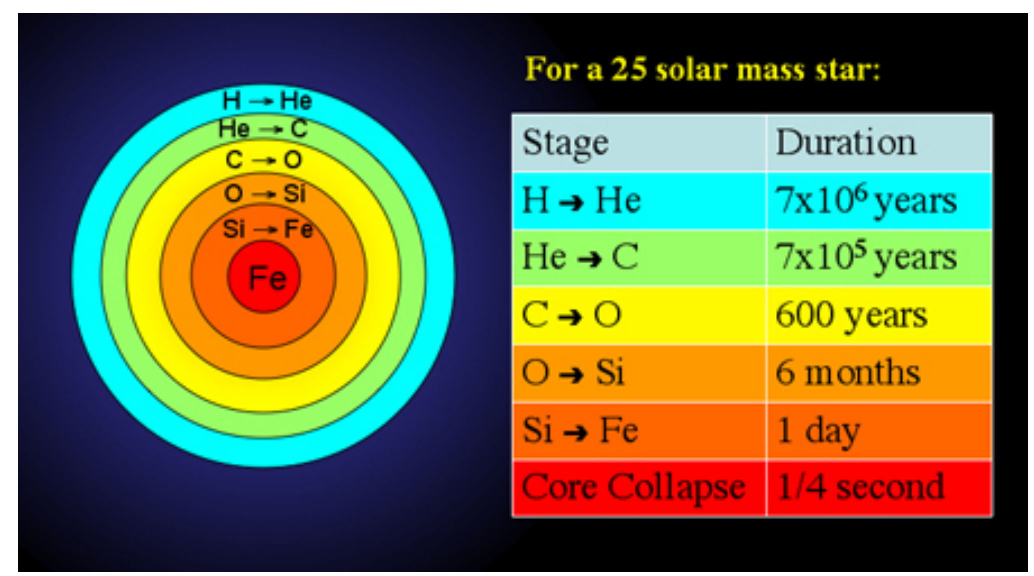

Stage	Duration
H → He	7×10^6 years
He → C	7×10^5 years
C → O	600 years
O → Si	6 months
Si → Fe	1 day
Core Collapse	1/4 second

$$
\begin{aligned}
{}^{12}\mathrm{C} + {}^{12}\mathrm{C} &\rightarrow {}^{20}\mathrm{Ne} + {}^{4}\mathrm{He} \\
&\rightarrow {}^{23}\mathrm{Na} + {}^{1}\mathrm{H} \\
&\rightarrow {}^{23}\mathrm{Mg} + \mathrm{n}
\end{aligned}
$$

$$
\begin{aligned}
{}^{16}\mathrm{O} + {}^{16}\mathrm{O} &\rightarrow {}^{28}\mathrm{Si} + {}^{4}\mathrm{He} \\
&\rightarrow {}^{31}\mathrm{P} + {}^{1}\mathrm{H} \\
&\rightarrow {}^{31}\mathrm{S} + \mathrm{n} \\
&\rightarrow {}^{30}\mathrm{S} + 2\,{}^{1}\mathrm{H} \\
&\rightarrow {}^{24}\mathrm{Mg} + {}^{4}\mathrm{He} + {}^{4}\mathrm{He}
\end{aligned}
$$

How to make a stellar-mass BH?

Stellar core collapse at end of lives of massive stars:
direct formation or fallback? first stars?

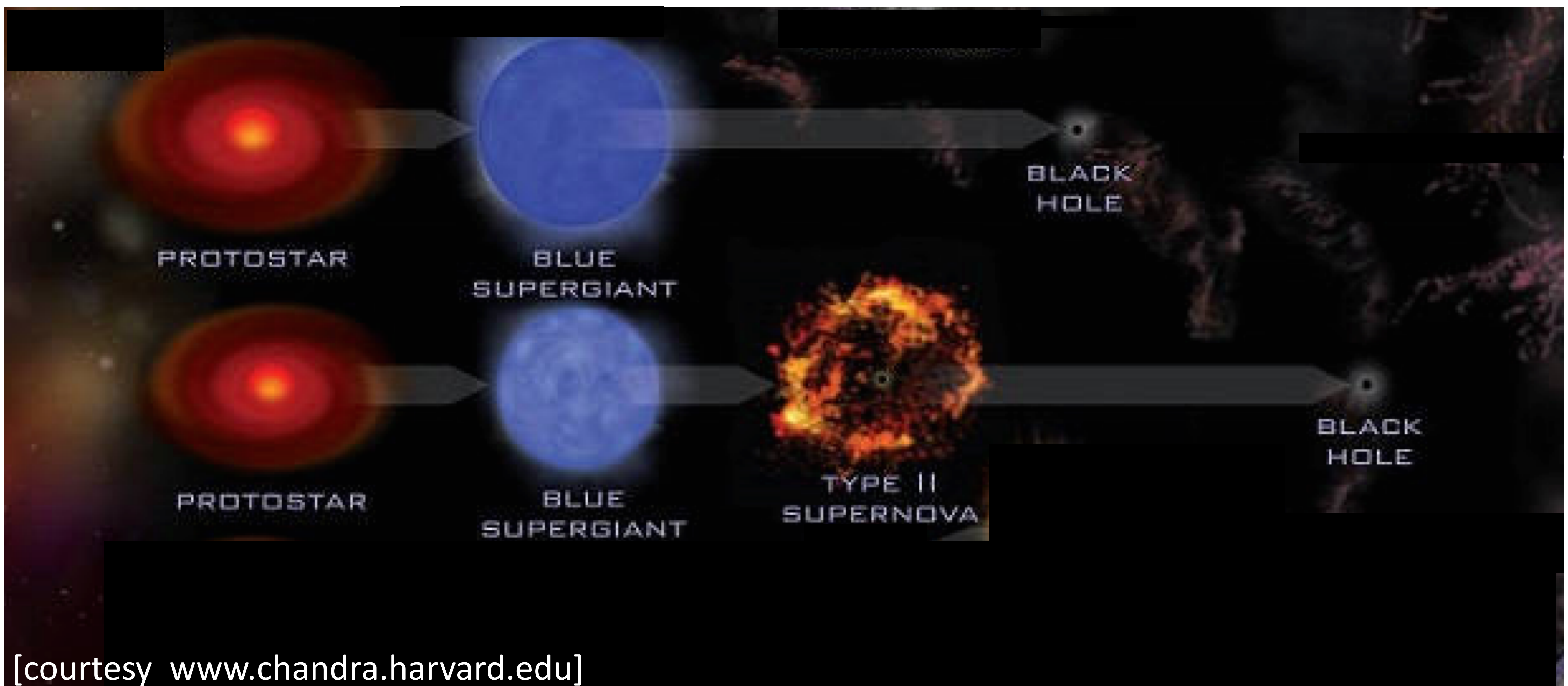

[courtesy www.chandra.harvard.edu]

Recipe for making heavy BHs

[LVC, ApJL 818, L22, 2016; adapted from Belczynski et al. 2010]

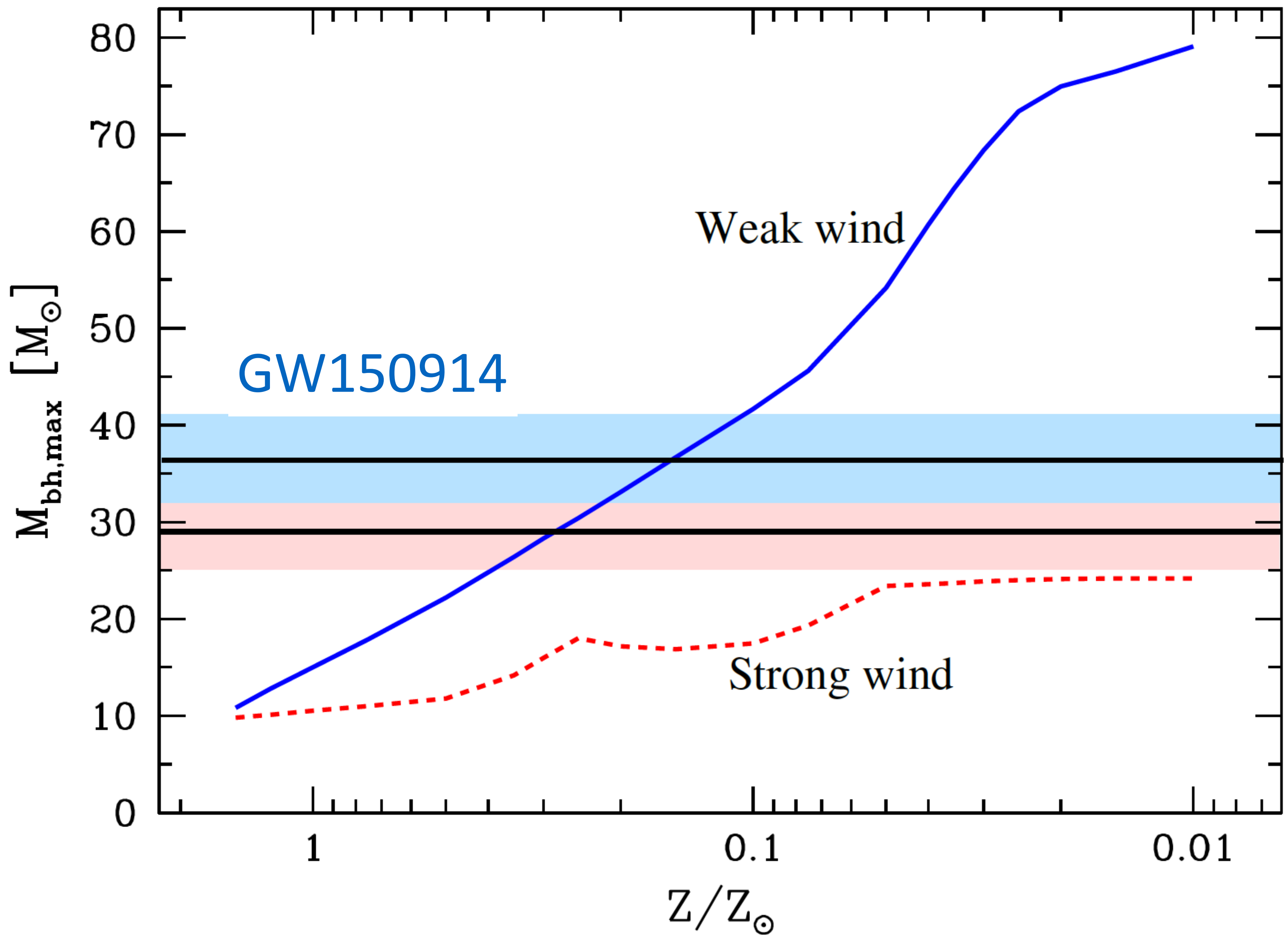

Low metallicity with $Z < 0.5\ Z_\odot$ (solar) and weak massive stellar winds